

**Best  
Available  
Copy**

AD-763 758

ELECTROMAGNETIC PULSE SOUNDING  
FOR GEOLOGICAL SURVEYING WITH APPLI-  
CATION IN ROCK MECHANICS AND THE  
RAPID EXCAVATION PROGRAM

D. L. Moffatt, et al

Ohio State University

Prepared for:

Advanced Research Projects Agency  
Bureau of Mines

April 1973

DISTRIBUTED BY:

**NTIS**

National Technical Information Service  
U. S. DEPARTMENT OF COMMERCE  
5285 Port Royal Road, Springfield Va. 22151

AD 763750

ELECTROMAGNETIC PULSE SOUNDING FOR GEOLOGICAL SURVEYING  
WITH APPLICATION IN ROCK MECHANICS AND THE  
RAPID EXCAVATION PROGRAM

D. L. Moffatt  
R. J. Pusker  
L. Peters, Jr.

The Ohio State University

**ElectroScience Laboratory**

Department of Electrical Engineering  
Columbus, Ohio 43212

Semiannual Technical Report 3408-1

April 1972

Contract Number: H023009  
Principal Investigator: D. L. Moffatt  
Phone: 614-422-5749  
Contract Officer: Frank Pavlic  
Phone: 303-234-4421  
Effective Date of Contract: 24 February 1972  
Contract Expiration Date: 6 August 1973  
Amount of Contract: \$46,762

Sponsored by  
Advanced Research Projects Agency  
ARPA Order No. 1579, Amend. 3  
Program Code 2F10

The views and conclusions contained in this document are those  
of the authors and should not be interpreted as necessarily  
representing the official policies, either expressed or implied,  
of the Advanced Research Projects Agency or the U.S. Government.

U. S. Dept. of Interior  
Bureau of Mines  
Advanced Research Projects Agency  
Denver, Colorado 80225

Reproduced by  
**NATIONAL TECHNICAL  
INFORMATION SERVICE**  
U. S. Department of Commerce  
Springfield VA 22151

DISTRIBUTION STATEMENT A  
Approved for public release  
Distribution Unlimited

RECEIVED  
JUL 27 1972  
RESEARCH

CLASSIFICATION	GROUP
EXEMPT	GROUP 1
GROUP 2	GROUP 3
GROUP 4	GROUP 5
GROUP 6	GROUP 7
GROUP 8	GROUP 9
GROUP 10	GROUP 11
GROUP 12	GROUP 13
GROUP 14	GROUP 15
GROUP 16	GROUP 17
GROUP 18	GROUP 19
GROUP 20	GROUP 21
GROUP 22	GROUP 23
GROUP 24	GROUP 25
GROUP 26	GROUP 27
GROUP 28	GROUP 29
GROUP 30	GROUP 31
GROUP 32	GROUP 33
GROUP 34	GROUP 35
GROUP 36	GROUP 37
GROUP 38	GROUP 39
GROUP 40	GROUP 41
GROUP 42	GROUP 43
GROUP 44	GROUP 45
GROUP 46	GROUP 47
GROUP 48	GROUP 49
GROUP 50	GROUP 51
GROUP 52	GROUP 53
GROUP 54	GROUP 55
GROUP 56	GROUP 57
GROUP 58	GROUP 59
GROUP 60	GROUP 61
GROUP 62	GROUP 63
GROUP 64	GROUP 65
GROUP 66	GROUP 67
GROUP 68	GROUP 69
GROUP 70	GROUP 71
GROUP 72	GROUP 73
GROUP 74	GROUP 75
GROUP 76	GROUP 77
GROUP 78	GROUP 79
GROUP 80	GROUP 81
GROUP 82	GROUP 83
GROUP 84	GROUP 85
GROUP 86	GROUP 87
GROUP 88	GROUP 89
GROUP 90	GROUP 91
GROUP 92	GROUP 93
GROUP 94	GROUP 95
GROUP 96	GROUP 97
GROUP 98	GROUP 99
GROUP 100	GROUP 101

NOTICES

When Government drawings, specifications, or other data are used for any purpose other than in connection with a definitely related Government procurement operation, the United States Government thereby incurs no responsibility nor any obligation whatsoever, and the fact that the Government may have formulated, furnished, or in any way supplied the said drawings, specifications, or other data, is not to be regarded by implication or otherwise as in any manner licensing the holder or any other person or corporation, or conveying any rights or permission to manufacture, use, or sell any patented invention that may in any way be related thereto.

A

9

ELECTROMAGNETIC PULSE SOUNDING FOR GEOLOGICAL SURVEYING  
WITH APPLICATION IN ROCK MECHANICS AND THE  
RAPID EXCAVATION PROGRAM

Semiannual Technical Report 3408-1

ElectroScience Laboratory  
The Ohio State University

This research was supported by the Advanced Research Projects  
Agency of the Department of Defense and was monitored by  
Bureau of Mines under Contract No. H0230009



*ite*



## ABSTRACT

Research on Contract H0230009 for the period 1 September 1972 to 28 February 1973 is summarized. A full scale version of an electromagnetic pulse sounding probe is described with attendant experimental data. Propagation and scattering measurements in limestone and dolomite media are presented. The scattering measurements are for targets consisting of faults, joints and lithologic contrasts in a dolomite medium. Measured frequency-dependent constitutive parameters for the limestone and dolomite media are given and realistic pulse propagation calculations using these data are shown. The basic problem of probe calibration is discussed and progress toward solution of this problem described.

## TABLE OF CONTENTS

	Page
I. TECHNICAL REPORT SUMMARY	1
II. PURPOSE	3
III. INTRODUCTION	4
IV. ELECTROMAGNETIC PULSE SOUNDING SYSTEM	6
V. PROPAGATION MEASUREMENTS AND CONSTITUTIVE PARAMETER ESTIMATES	19
VI. SCATTERING MEASUREMENTS IN DOLOMITE	31
VII. PULSE PROPAGATION CALCULATIONS	51
VIII. PROBE CALIBRATION	63
IX. CONCLUSIONS	71
X. FUTURE PLANS	72
ACKNOWLEDGMENT	73
REFERENCES	74

UNCLASSIFIED

Security Classification

DOCUMENT CONTROL DATA - R & D

(Security Classification of title, body of abstract and indexing annotation must be entered when the overall report is classified)

1. ORIGINATING ACTIVITY (Corporate method) ElectroScience Laboratory Department of Electrical Engineering, The Ohio State University, Columbus, Ohio 43212	2a. REPORT SECURITY CLASSIFICATION Unclassified 2b. GROUP
---	---

3. REPORT TITLE ELECTROMAGNETIC PULSE SOUNDING FOR GEOLOGICAL SURVEYING WITH APPLICATION IN ROCK MECHANICS AND THE RAPID EXCAVATION PROGRAM
--

4. DESCRIPTIVE NOTES (Type of report and inclusive dates) Semiannual Technical Report - 1 September 1972 to 28 February 1973
---

5. AUTHOR(S) (First name, middle initial, last name) Moffatt, D.L., Puskar, R.J., Peters, L., Jr.
--

6. REPORT DATE	7a. TOTAL NO. OF PAGES 75 81	7b. NO. OF FIGS. 12
----------------	---------------------------------	------------------------

8a. CONTRACT OR GRANT NO. H0230009 b. PROJECT NO. c. d.	9a. ORIGINATOR'S REPORT NUMBER(S) ElectroScience Laboratory 3408-1 9b. OTHER REPORT NO(S) (Any other numbers that may be assigned this report)
---	--

10. DISTRIBUTION STATEMENT
----------------------------

11. SUPPLEMENTARY NOTES	12. SPONSORING MILITARY ACTIVITY U.S. Dept. of Interior, Bureau of Mines Advanced Research Projects Agency Denver, Colorado 80225
-------------------------	--

13. ABSTRACT <p>Research on Contract H0230009 for the period 1 September 1972 to 28 February 1973 is summarized. A full scale version of an electromagnetic pulse sounding probe is described with attendant experimental data. Propagation and scattering measurements in limestone and dolomite media are presented. The scattering measurements are for targets consisting of faults, joints and lithologic contrasts in a dolomite medium. Measured frequency-dependent constitutive parameters for the limestone and dolomite media are given and realistic pulse propagation calculations using these data are shown. The basic problem of probe calibration is discussed and progress toward solution of this problem described.</p>
--

14

KEY WORDS

LINK A		LINK B		LINK C	
ROLE	WT	ROLE	WT	ROLE	WT

Electromagnetic  
Video pulse  
Hard rock  
Fault  
Contrast

*ia*

## I. TECHNICAL REPORT SUMMARY

A unique electromagnetic pulse sounding probe for the detection, diagnosis and identification of geological and man-made anomalies within the earth is being developed. The immediate application of the probe is as a hazard detection device in advance of hard rock rapid tunneling operations. Numerous other applications in geophysical exploration, geophysical prospecting, mining, agriculture, civil engineering, earthquake engineering and archeology can be envisioned. While applications in geophysical prospecting and mining are apparent, many other more subtle applications appear to be feasible. Location of archaeological features in soil prior to digging would save the archaeologist a great deal of labor. Evaluating the effectiveness of grouting procedures the construction of dams would save much time and money. Detection of and the monitoring of sub surface fault structures would present new information to the earthquake engineer. The probe is basically an active remote sensor capable of interrogating a material medium from the surface of the medium. Within limits imposed by the electrical properties of the medium in question, the probe has both a detection and identification capability and this capability suggests an ever-widening range of applications. The identification capability of the system stems from the use of a periodic video-type pulse as the interrogating signal. This basically means that the spectrum of the returned signal from the target spans a sufficient frequency range to permit classification. The system can also be operated in two modes, one of which does not "see" symmetrical targets such as the air-rock interface. Thus the horrendous difficulties caused by layering in seismic or acoustical work can be avoided. At the same time, the layering can be "seen" using the system in its other mode.

The main goals of the program during this contract period are; 1) to obtain full scale field measurements of the type of geological hazards likely to be encountered in deep tunneling such as faults, joints and lithologic contrasts, 2) to devise techniques for estimating in situ the frequency-dependent electrical properties of a rock medium and 3) to complete theoretical analyses and computer programs which will permit realistic calculations of pulse propagation and pulse scattering by geological-type targets. During the first 6 month interim, effort has been concentrated on the first two items above.

In this Semiannual Technical Report the purpose of our research is described in Section II, where the specific objectives of the program are detailed. In Section III, the operation of the electromagnetic pulse system is briefly reviewed and the status of the system, as of the initiation date of the present contract, is given. The full scale electromagnetic pulse sounding system is described in Section IV together with measured data illustrating the performance of system components. It is also demonstrated that the system effectively couples video pulse

signals into a rock medium\* and that the location of large metallic objects on the rock surface quite near the probe (the drilling machine) does not affect the coupling.

Section V of the report describes and illustrates video pulse propagation data taken in limestone and dolomite media. This section also presents and demonstrates a technique for obtaining the frequency-dependent electrical properties of a medium from pulse propagation data.

Successful electromagnetic pulse soundings of faults, joints and lithologic contrasts in a dolomite medium are shown in Section VI. It is to be noted that these targets are clearly evident in the raw temporal and spectral data - thus for these targets a sophisticated processing is not necessary.

Analytical pulse propagation calculations are reported in Section VII. These results illustrate the attenuation and dispersion effects of the medium on video pulse signals. It is also shown that using the medium properties deduced experimentally (Section V) and a state-of-the-art analysis for wire antennas in an arbitrary medium, excellent agreement between measured and calculated video pulse propagation is achieved.

The problem of probe calibration, and the necessity for this calibration, if processing to obtain target impulse response waveforms is required, is discussed in Section VIII. It is also shown here that the transfer function of the probe geometry in situ on the rock surface can be obtained experimentally if the rock medium offers a particular geometry. This section also discusses analytical methods for modifying the wire antenna programs to include an air-rock interface.

Conclusions regarding the electromagnetic pulse sounding system are summarized in Section IX, and research plans for the remaining contract period are given in Section X.

---

\*All of the field measurements have been made in limestone or dolomite quarries. Dolomite and limestone are not igneous-type rocks but their electrical properties are quite similar to those of an igneous rock such as granite. To make the measurements in igneous rock would have required prohibitive travel from our Ohio site. It is felt however that at this stage the system is fully ready for demonstration in a true igneous-rock tunnel and that the experimental results reported herein fully justify this conclusion.

In summary, significant progress in the development of an electromagnetic pulse sounding system has been made. Measurements have been made, in the field, of those geological targets defined to be of interest for a hazard detection device. It remains to further measure these same targets from more difficult positions to explore the system's full capabilities and to add a final modification to a theoretical analysis which will then permit impulse response-type processing. These should be accomplished by the end of the current program. At that time, as stated earlier, it is felt that the documented successful measurements reported herein fully justify a testing program for the electromagnetic pulse sounder in an actual igneous rock tunnel.

## II. PURPOSE

A unique electromagnetic pulse sounding system using periodic video pulse signals for the detection and diagnosis of hazards in advance of rapid tunneling operations is being developed. The tunneling is assumed to be in hard igneous-type rock and the hazards considered are planar and include faults, joints and lithologic boundaries of infinite extent. The research program during this contract period has the following objectives:

- 1) Obtain full scale electromagnetic pulse soundings of faults, gouge-filled faults, joints and lithologic contrasts in a rock medium with electromagnetic properties similar to hard rock. These measurements were made in Plum Run Quarry near Peebles, Ohio approximately 120 miles from the ElectroScience Laboratory. The quarry rock is basically dolomite and the above mentioned geological features exist in abundance. The quarry rock is a soft rock medium but because of the abundance of the desired geological features has been studied for economic reasons. The essential difference between hard and soft rock media is the difference in the conductivity which in essence implies that the operating range in hard rock will be increased.
- 2) Construct a smaller and lighter version of the full scale probe (antennas) geometry which can be easily supported against a vertical rock face. The smaller probe will greatly facilitate certain of the measurements in 1 and at the same time permit some experimentation with end terminations and synthetic aperture-type signal processing.

- 3) Obtain estimates of the frequency-dependent relative dielectric constant and conductivity of the dolomite quarry rock via in situ video pulse propagation measurements. Certain measurements of this type are useful in interpretation of measured time and spectral target signatures.
- 4) Complete the theoretical analysis and computer programs for adding an air-rock interface correction to a previously developed computer program for an arbitrary wire antenna (bare, insulated or partially insulated) in an infinite, lossy, homogeneous medium. This result will add a system calibration and theoretical probe design capability to an existing capacity for realistic (frequency-dependent constitutive parameters) pulse propagation calculations.
- 5) Devise new signal processing schemes for electromagnetic pulse sounding data to enhance the detection and identification capabilities of the system. Basically, improved estimates of the target's impulse response waveform are to be obtained. Given the calibration capability listed in objective 4, it will then be possible to calculate the transfer function of the probe from measurements of a known target geometry. Improved impulse response waveforms will then be possible.

### III. INTRODUCTION

The basic electromagnetic pulse sounding system has been described in previous reports[1,2]. Briefly, periodic video pulse signals with spectral content spanning the Hz to (Hz or Hz to MHz range are used as interrogating signals. The interrogating signal is coupled to and from the medium by two orthogonally oriented dipoles flush with the medium surface with a sampling oscilloscope acting as a receiver. The system operates in two modes; direct, with transmission and reception on the same dipole and orthogonal with transmission on one dipole and reception on the other. In the orthogonal mode, the system is "blind" to targets which are symmetric to an axis perpendicular to the dipoles and centered at their feed points. Thus in the orthogonal mode the system does not "see" the air-medium interface or similarly oriented layering within an isotropic medium. The system is automated, i.e., control and processing of the scattered signal waveforms is via an instrumentation computer. Extensive programs have been developed for processing of the temporal or spectral data[2].

In operation as a hazard detection device in rapid tunneling operations, the probe will be mounted flush with the tunnel working face and measurements taken in both operational modes. For tunnels of sufficient size (diameters 20 to 30 feet) a synthetic aperture-type processing will also be used by making measurements at discrete points on horizontal and vertical diameters of the face.

On the previous contract[1,2] it was demonstrated experimentally that interrogating video pulse signals could be effectively coupled to the overburden using properly designed and terminated dipoles and that these probes were very insensitive to obstructions on the air-medium interface. A detection and identification capability was also demonstrated for a particular class of man-made targets buried in both soil and limestone media. These measurements were made with low power and scaled-down versions of the probe because components for full power operation were not yet completed.

In this report, a full scale version of the electromagnetic pulse sounding probe is described in Section IV. Temporal and spectral data illustrating the performance of system components are given. Finally it is demonstrated that with proper design of the dipoles, video pulse signals can be effectively coupled to a rock medium (limestone) and that the probe is insensitive to large scatterers on the rock surface near the probe.

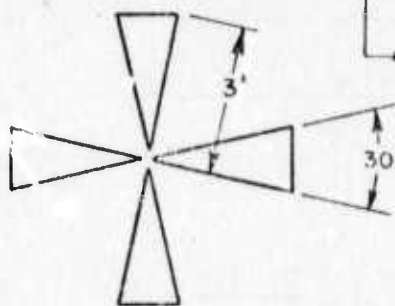
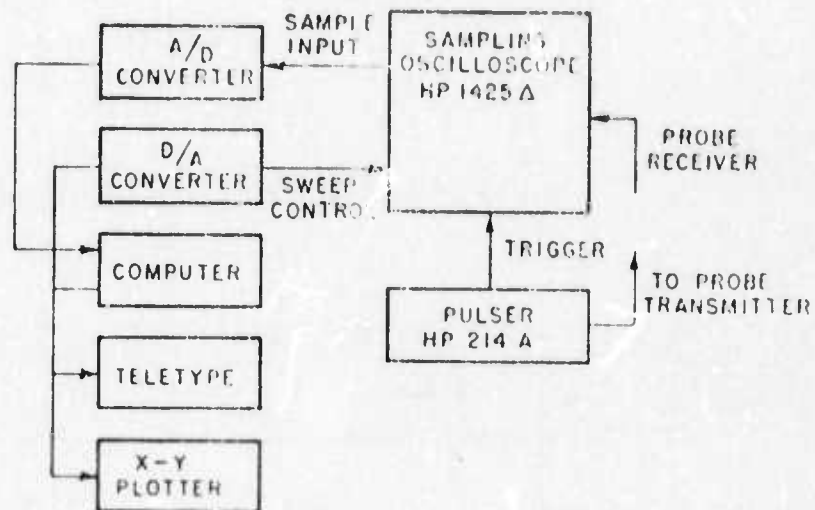
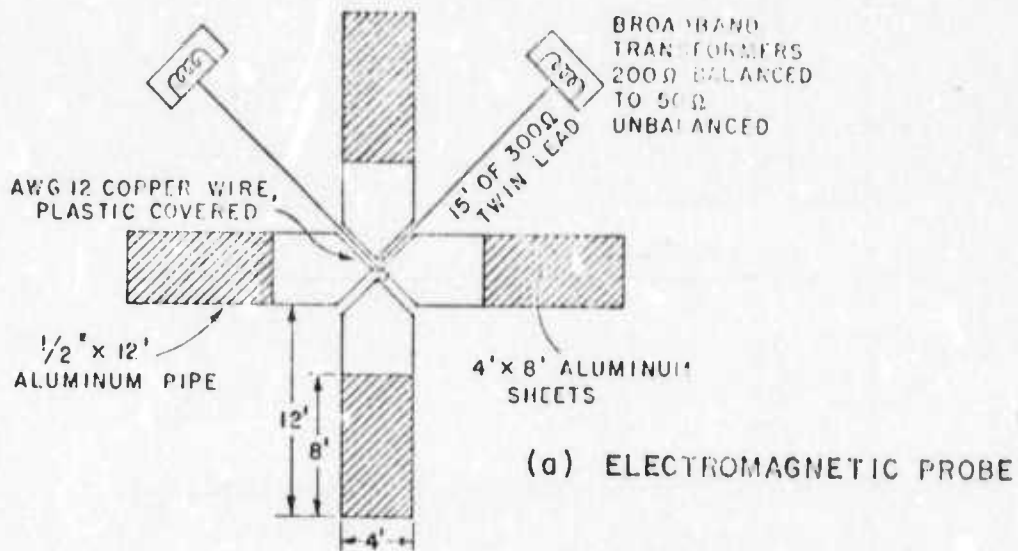
Section V of this report describes and illustrates video pulse propagation data taken in limestone and dolomite media. Also in Section V, frequency-dependent attenuation and constitutive parameter data obtained via the propagation measurements are given. Alternative schemes for deducing these latter parameters are also discussed. Section VI presents results of measurements on specific faults, joint and lithologic contrast targets defined to be of interest on the current contract.

In Section VII, theoretical pulse propagation calculations in rock media are given. The effect of frequency-dependent relative dielectric constant and conductivity is illustrated. Section VIII describes the problem of probe calibration - a necessary result if scattered field data are to be processed to obtain the impulse response waveform of a given target. Our conclusions with respect to electromagnetic pulse sounding in rock media are discussed in Section IX and plans for the remaining contract period are given in Section X.

#### IV. ELECTROMAGNETIC PULSE SOUNDING SYSTEM

A sketch of the dipole probe geometry and block diagram of the sounding system with the computer on-line is shown in Figs. 1a and 1b respectively. In Fig. 1a, the transition from coaxial cable to 300 ohm twin lead is via special high power broadband baluns (50 ohm unbalanced to 200 ohm balanced) specifically built to handle the two video pulse generators used with the system. The purpose of the line whose dominant mode is balanced, to physically separate the baluns for the two dipoles thus preventing coupling across the baluns and to remove the balun response from the time region of interest. A second probe used with the system is shown in Fig. 1c. This much smaller probe in Fig. 1c is fed in exactly the same way, i.e., cable, balun and twin-lead line. With the small probe, a 2 inch layer of hairflex absorber is inserted between the probe and the air-ground interface. Of course, different baluns and shorter lengths of twin lead are used. The probe shown in Fig. 1c was developed on another program for use with a very narrow video pulse generator (Ikor generator - see below) in shallow overburden measurements. Its small size proved convenient for certain propagation tests and later for fault delineation, and it was made available for our use. However, design data and tests of the probe performance are proprietary with that program sponsor pending patent applications.

Two video pulse generators are used with the pulse sounding system, a Hewlett Packard (HP) model 214A and an Ikor model R-100. The nominal output of these generators is respectively a 50 volt peak 45 ns base width, 10 KHz repetition rate (HP) and a 1000 volt peak, 250 ps 3 dB width, 250 Hz repetition rate (Ikor). The output pulses of the HP and Ikor generators are shown in Figs. 2a and 3a respectively with the noted attenuation inserted to protect the sampling head. In the case of the Ikor generator (Fig. 3) the waveform in Fig. 3a includes the effects of the feed cables (400 feet of RG-9 coaxial cable). This is necessary in order to obtain sufficient delay - the trigger signal for the Ikor generator (which cannot be triggered externally) is obtained via a tee at the generator output. In Figs. 2b and 3b the effect of both feed cables, both baluns and both sections of twin lead are shown, i.e., the probe is removed and the sections of twin lead are shorted together. The corresponding amplitude (note that the amplitude spectra are normalized by setting the largest spectral amplitude to unity) and phase spectra for the waveforms in Figs. 2 and 3 are shown in Figs. 4 and 5, respectively. For the results shown, the twin lead was lying on a limestone medium. The severe attenuation of the high frequency content of the Ikor pulser (Fig. 5) is the result of the long length of twin lead transmission line (30 feet) used. At high frequencies, roughly above 100 MHz, the 300 ohm twin lead lying on a surface is extremely lossy. For example, if the twin lead is shortened to a total length of 6 feet, the improved amplitude



(c) SMALLER VERSION OF ELECTROMAGNETIC PROBE

Fig. 1. Electromagnetic pulse sounding probe.  
 (a) probe geometry  
 (b) block diagram  
 (c) small probe geometry

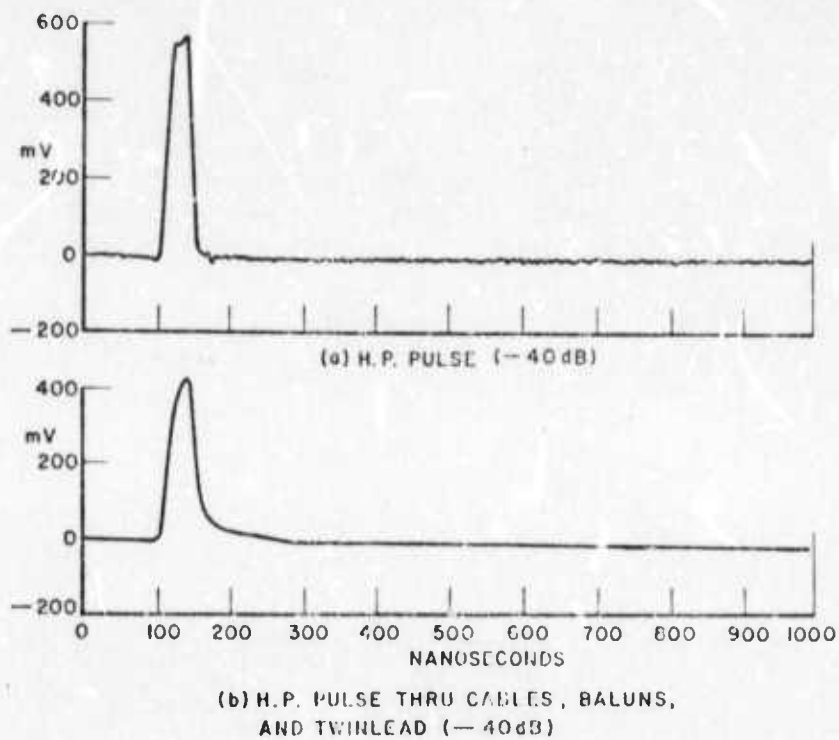


Fig. 2. Hewlett Packard 214-A pulse generator.

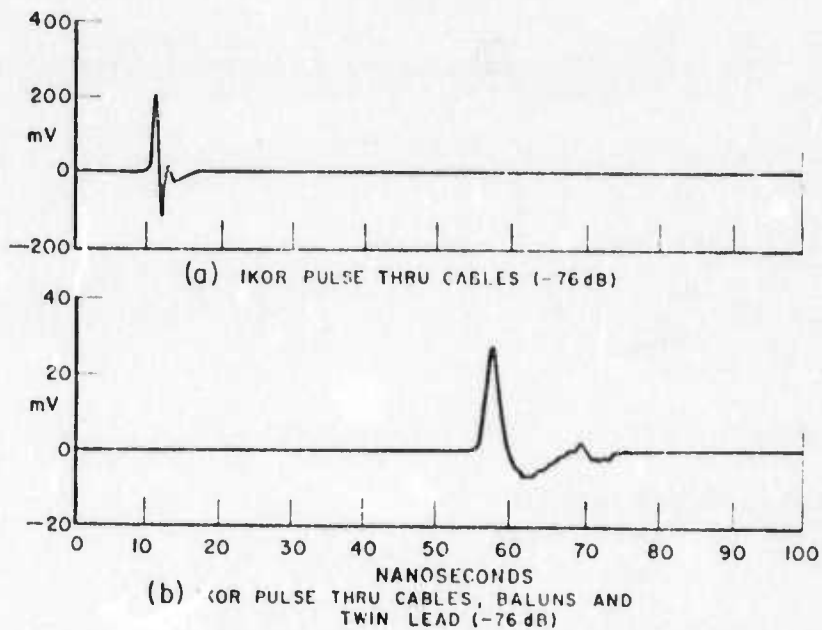


Fig. 3. Ikor R-100 pulse generator.

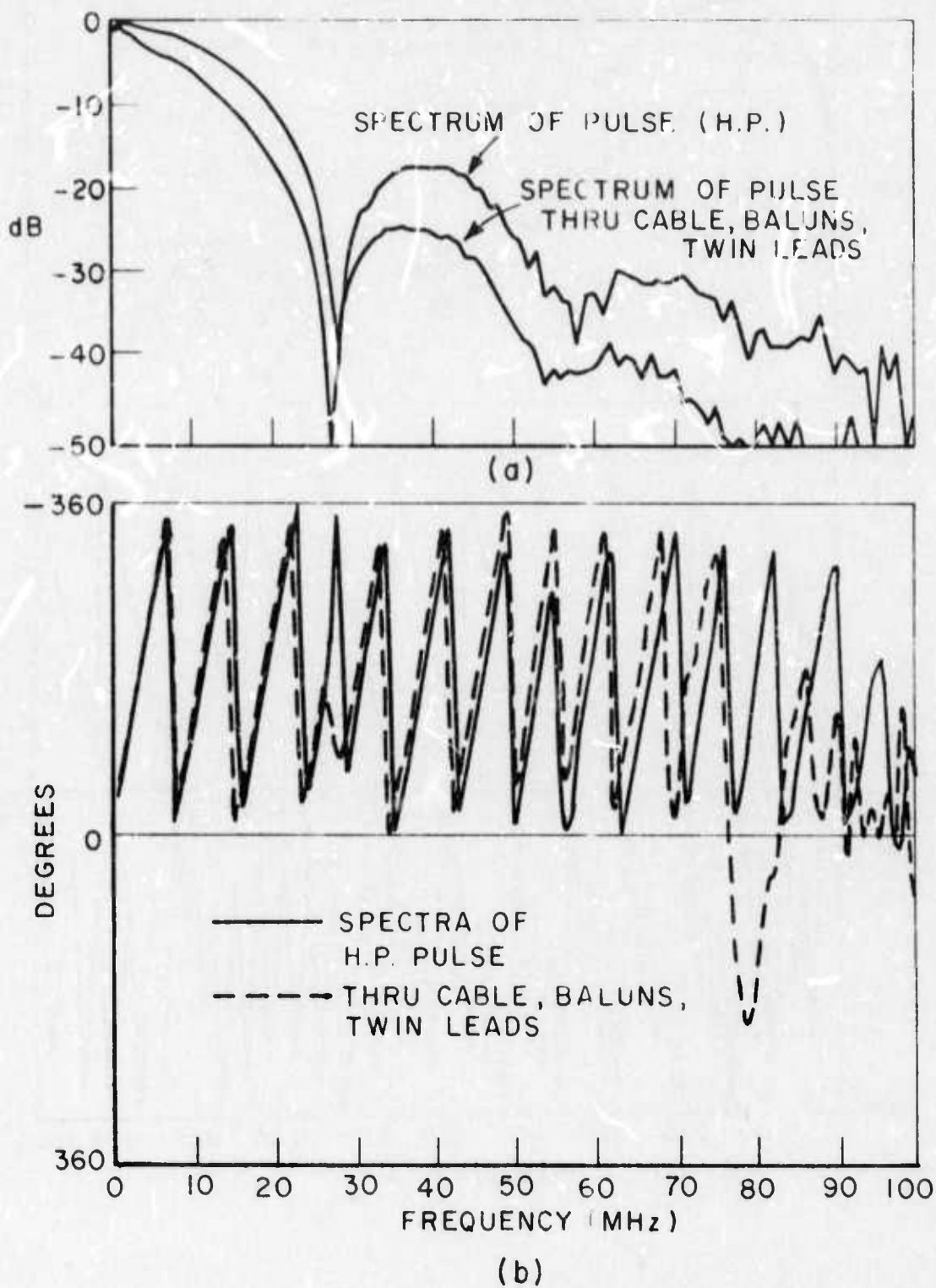
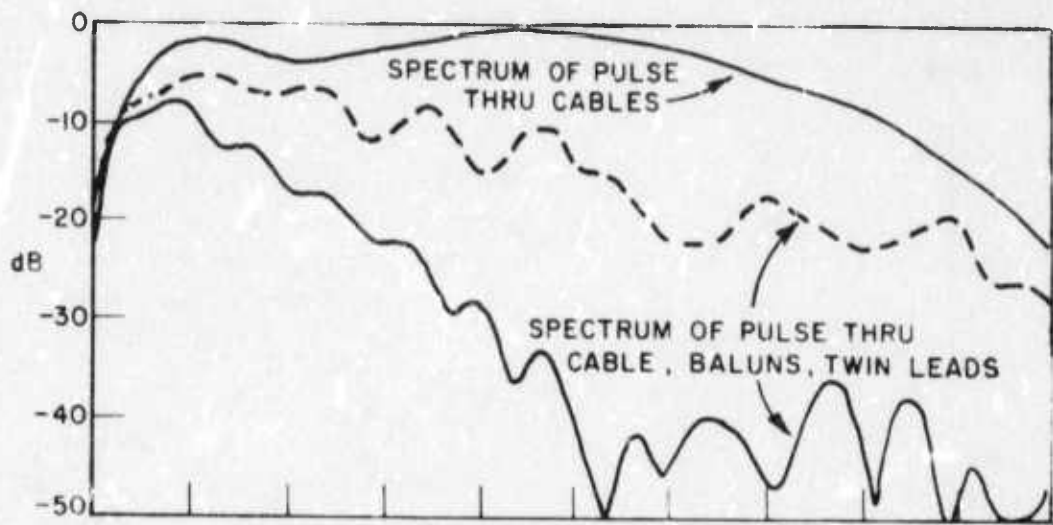
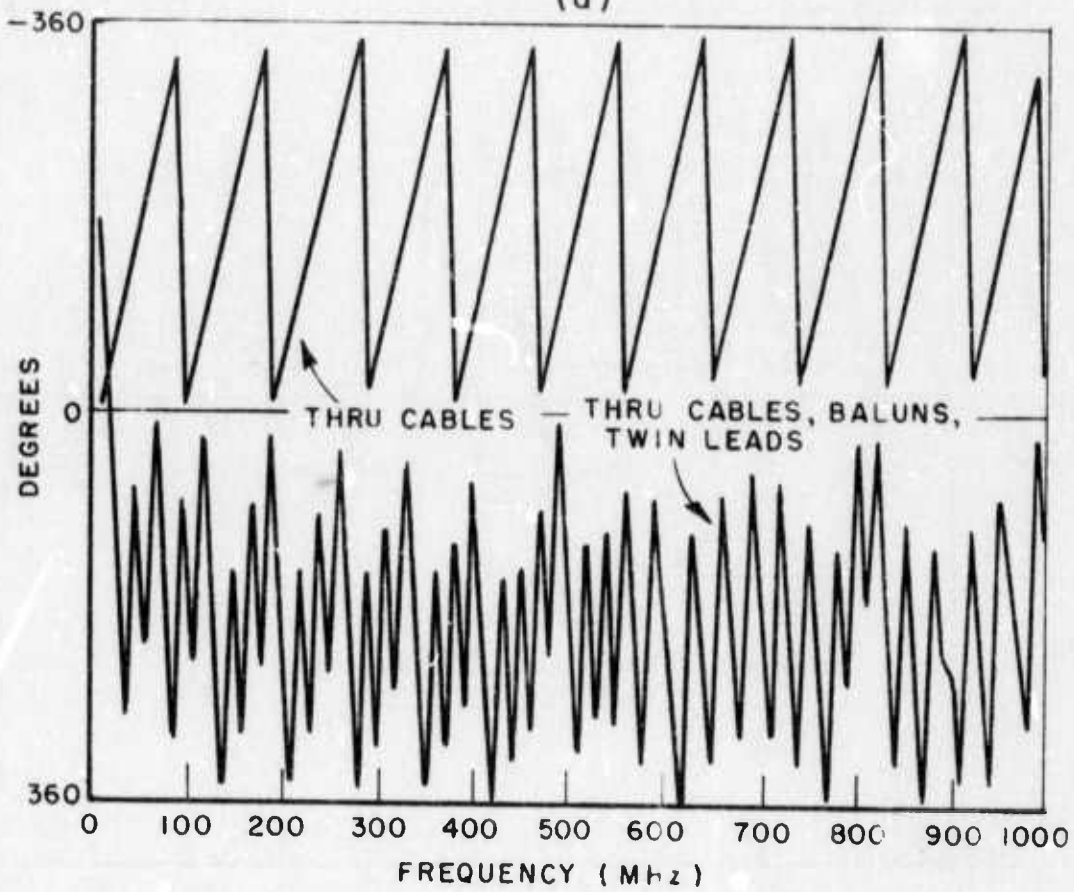


Fig. 4. Spectra of Hewlett Packard pulse.  
 (a) amplitude  
 (b) phase



(a)



(b)

Fig. 5. Spectra of Ikor pulse.  
 (a) amplitude  
 (b) phase

spectrum shown dashed in Fig. 5a results. With the Ikor pulse generator, a physical separation of the baluns (at least 2 feet) is necessary to prevent coupling across the baluns. It is also desirable, with either pulser, to remove the balun response from the time region of interest. A slight improvement in the attenuation shown in Fig. 4 could be obtained by reducing the 15 foot lengths of twin lead. This length however permits the balun holder to be firmly supported by polypropelene lines which are used across the quadrants of the dipoles to rigidize the large probe in Fig. 1 when it is oriented in a vertical position against a rock face. For this reason no attempt to reduce the twin lead lengths was made. Much the same comment applies to the length of feed (coaxial) cables. The nominal length of the transmit and receive cables is 200 feet. In many field situations it would be possible to reduce these lengths to 10 feet or less, thereby again decreasing the attenuation. In other situations however the full length of the cables is needed. It is not practical to continually alter the cable lengths, therefore the lengths were fixed in all measurements. Over the period when active measurements were in progress in the limestone quarry, the changes seen in monitoring response waveforms similar to Figs. 4 and 5 were insufficient to warrant recording. This is not to say that seasonal variations would not occur. Note however that the only component susceptible to changes in the electrical properties of the medium is the short length of twin lead - and indirectly the characteristic impedance seen by the baluns. This type of measurement will be repeated and monitored during the summer measurement period. Some changes are anticipated, particularly since both pulse generators have been returned to the manufacturer for repairs since our last series of measurements.

The actual pulse transmitted into the medium is, of course, an entirely different matter. It is not possible to measure this waveform and a system calibration is required in order to obtain it. This point will be discussed later. The two pulse generators whose characteristics are shown in Figs. 2 and 3 provide different capabilities. The very narrow pulse in Fig. 3 affords a fine resolution for close-in targets and yields a wide spectral coverage but the power at any given frequency is actually quite small ( $<20\text{mW/MHz}$ ). The broader pulse (Fig. 2) has much less resolution and a narrower spectral coverage, but does yield significantly greater power within its spectrum ( $>110\text{mW/MHz}$ ). Roughly, the broad pulse has a resolution capability of  $6.75/n$  meters and the narrow pulse a capability of  $0.075/n$  meters, where  $n$  is the effective refractive index for the medium. The above numbers are lower bounds which neglect any dispersive effects of the medium.

Operation of the sounder can be described qualitatively as follows: Periodically, a wave is launched on the transmit arm of the dipole at the feed point which penetrates into the medium. As the wave propagates along the dipole its fringe fields penetrate deeper into the medium. For shallow targets, the dipole is not currently being employed

as a radiating structure in the normal sense since it is the near-fields which are being used. For the deeper targets, the dipole is acting as a radiator. Reflected signals from the medium via the same or orthogonal dipole are observed on a sampling oscilloscope acting as a receiver. The measurements are automated, i.e., the computer controls the oscilloscope sweep and records the response waveform.

#### A. Dipole Design

The design of the dipole structure for soundings of a specific medium has two primary objectives; to couple as much of the available electromagnetic energy into the medium as possible, and to provide the clearest "time window" possible by minimizing the reflections from the balun, the dipole feed point, the ends of the dipole, the medium surface and obstructions on or above the surface. The objective is to isolate in time the scattered pulse associated with a subsurface target from the above noted clutter mechanisms.

The time domain design of antennas requires somewhat different considerations than conventional frequency domain approaches. It is convenient to view the structure (include feed cables, baluns etc.) as a transmission line with changing characteristic impedances along the line. Each discontinuity in characteristic impedance is examined individually, and minimized, without regard to any other point along the line. If an experimental approach is taken, as in this case, then a very long pulse ( $\mu$ secs) rather than a video pulse is used, since reflections from the leading and trailing edges of the pulse tend to become confusing. With the long pulse, the trailing edge of the pulse is far beyond the time region of interest. Thus the antenna structure is interrogated in the direct reflection mode by a step function with a finite rise time. The rise time is determined by the resolution required, i.e., the size of the antenna structure and spacing between discontinuities. A typical measurement is shown in Fig. 6, where the interrogating step has a 15 ns rise time and the dipole is that shown in Fig. 1a. Dashed lines at plus and minus 600 mV correspond to open and short circuits, respectively at the input port of the balun, i.e., at the end of the coaxial cable. Reflections at the balun, the feed point and the end of the dipole are clearly seen. Fig. 6 also illustrates the control of the end reflections affected by varying amounts of conducting sheet (foil) across the ends of the dipole arms. In Fig. 7, control on the feed point reflection effected by changing the shape of the dipole arm (and therefore the characteristic impedance at the feed point) is shown. In this case the medium is the overburden and the linear antenna elements are plastic coated AWG12 solid copper wire. Again the incident pulse has a 15 ns rise time which is evident from the open and short circuit reflections. For the measurements shown in Fig. 7, the section of twin lead was removed, i.e., the baluns were connected directly to the feed terminals. It is evident in Fig. 7 that

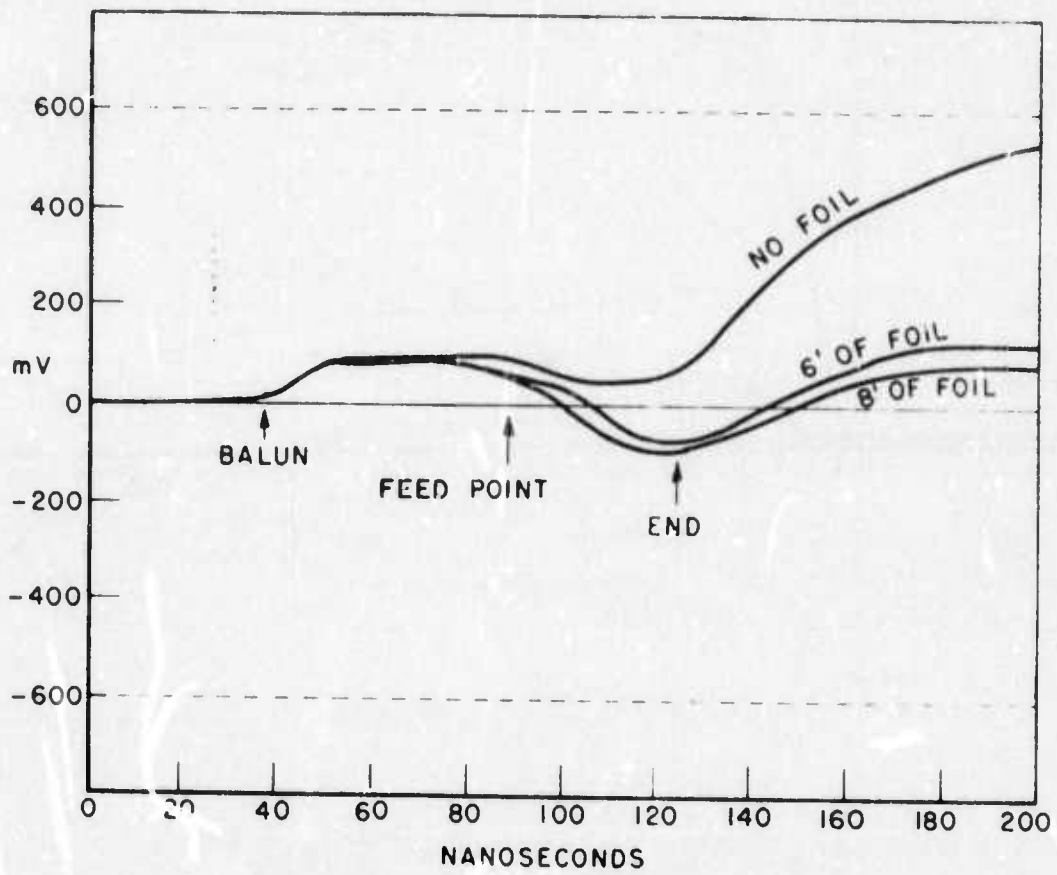


Fig. 6. Step reflection (direct) measurements of large probe on limestone medium.

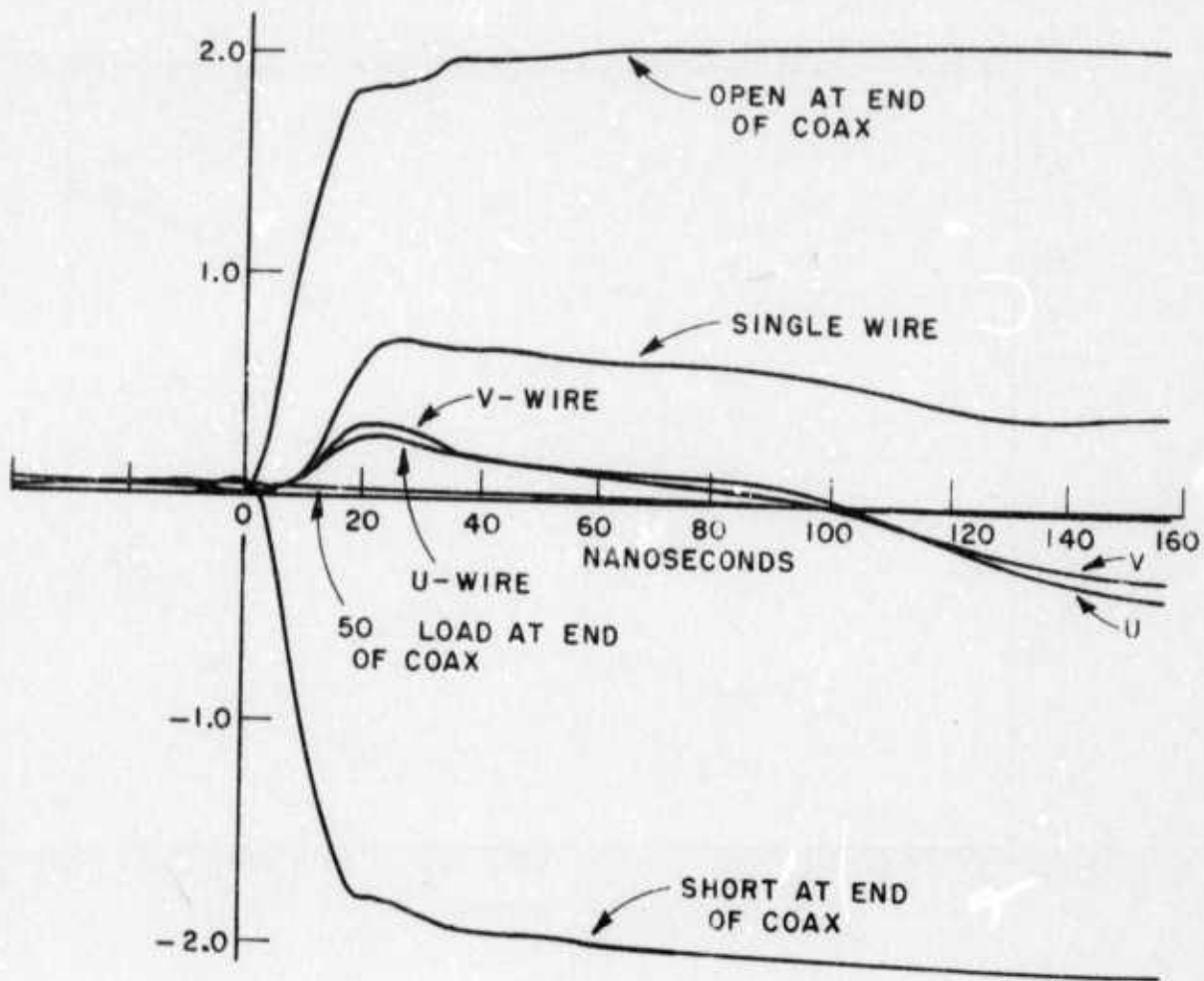


Fig. 7. Direct reflection measurements (step) of one dipole (wire) on the overburden. Various probe arm shapes.

a dipole arm in either a U or V configuration is considerably better than a single wire arm for the balun used here. The waveform shown for a matched load at the feed point is the ideal clear "time window" one seeks to approximate. Fig. 7 is repeated from an earlier report[2]. Our experience to date indicates that the designs in Figs. 1a and 1c are adequate for a wide variety of media. For example, the same configurations have been used successfully on the overburden, on limestone and on dolomite. Clearly, larger changes in the electrical properties of the medium will require alterations of the angular taper from the feed point. This adjustment is easily made, and the necessity for the adjustment is easily discerned from a direct reflection measurement.

Note that from Fig. 7 one can, by estimating the reflection coefficient at the feed point, obtain the characteristic impedance of the various dipole arm configurations at the feed point. The characteristic impedances are 250, 262 and 400 ohms respectively for the U,V and single wire configurations. For the antenna of Fig. 1a with the 300 ohm twin lead in place it is necessary to obtain short and open circuit waveforms at both the balun output and dipole feed point. From these results, the characteristic impedance of the 300 ohm twin lead lying on a limestone medium is 268 ohms and that of the dipole on limestone is 161 ohms. Some improvement could be obtained by designing components specifically for this task rather than using "on the shelf" units. Results for a dolomite medium were approximately the same, indicating that the electromagnetic properties of limestone and dolomite are quite similar.

Note that in Figs. 6 and 7 (using the direct reflection mode) the input signal was quite low to protect the sampling head which has a  $\pm 2$  volt limitation. A voltage limiter designed to protect the oscilloscope sampling head from harmful high voltage pulses has now been designed and built which permits direct reflection mode operation of the underground probe system. A block diagram of the layout is shown in Fig. 8a. In the direct reflection mode of operation, a single antenna is used as both transmitter and receiver, so that the sampling head must obviously be exposed to the high voltage input pulse. A pair of step recovery diodes (SRD's), which are used as charge controlled switches, provide the limiting action necessary to protect the sampling head. When charge is inserted into an SRD by forward bias, the diode appears as a very low impedance ( $<1\Omega$ ). When this charge is being removed, the diode continues to appear as a low impedance until all the stored charge is removed, at which point it quickly switches to a high impedance.\*

In this application, the oncoming high voltage pulse provides the forward bias to an SRD shunted across a small section of 50 ohm microstrip transmission line (Fig. 8b). When the voltage of the input pulse becomes greater than roughly 800 mV, the diode switches to a low impedance, causing the limiter to appear as a short circuit, thereby reflecting the incident pulse back down the line. After the trailing edge of the pulse has been reflected, the diode remains a low impedance until all of the stored charge is removed, at which point it switches back to a high impedance, which is unnoticeable in parallel with the 50 $\Omega$  transmission line. Any signal that is less than 800 mV in magnitude as most target returns happen to be, passes through the

\*Hewlett-Packard Application Note 918.

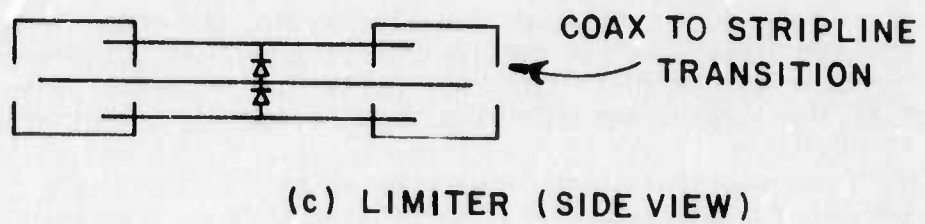
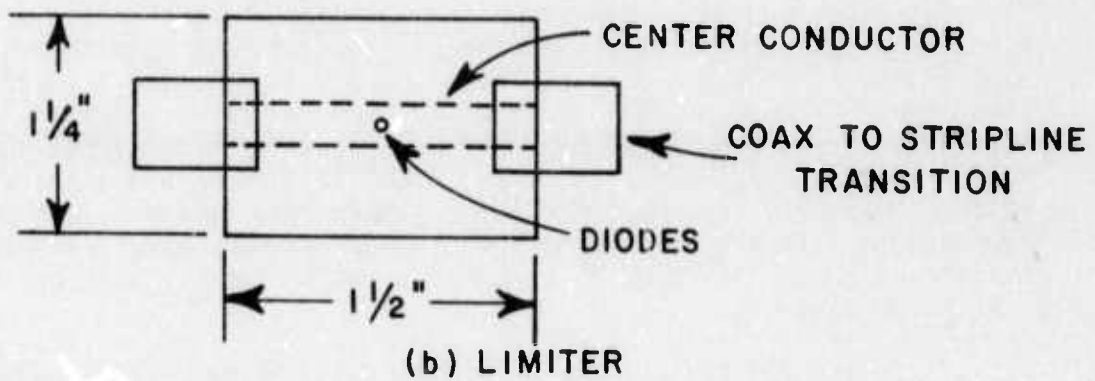
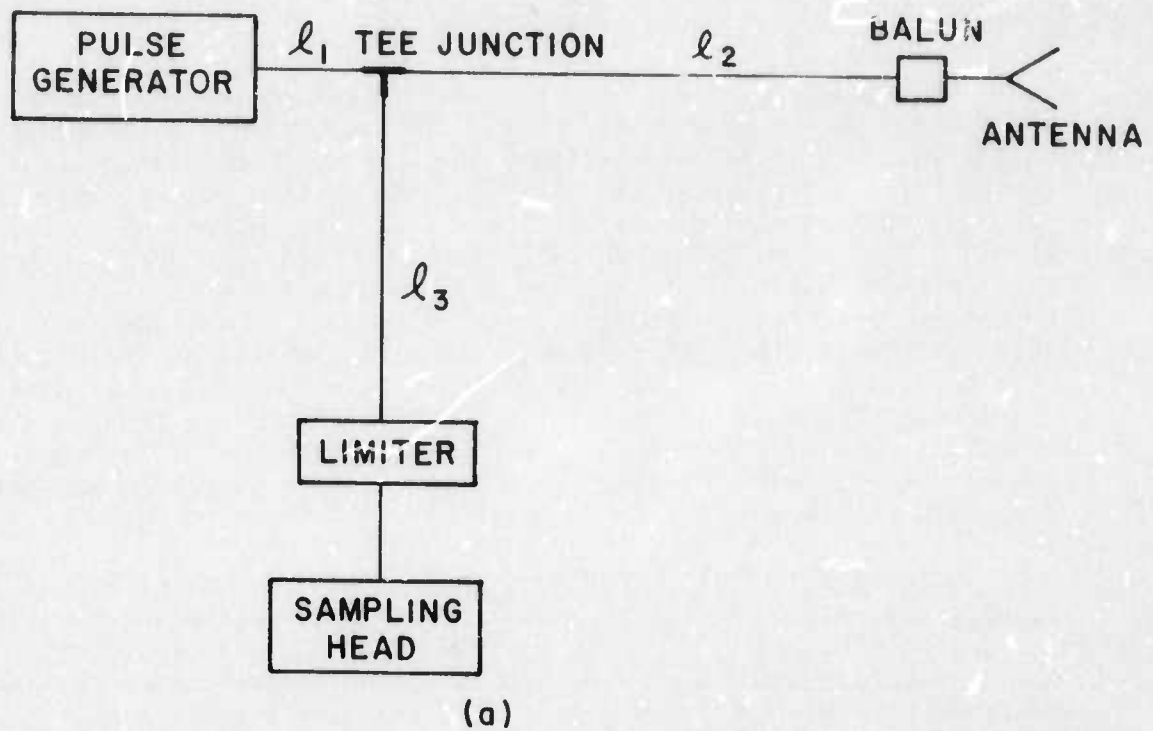


Fig. 8. Limiter for sampling head protection.  
 (a) block diagram with limiter  
 (b) detail of limiter  
 (c) detail of limiter

limiter undistorted. Actually, only one SRD is required to protect the sampling head from the input pulse, however, for added protection from reflections from accidental short circuits or large magnitude target returns, a second diode was inserted.

Figure 8a shows the direct reflection mode system with the limiter. The length  $l_1$  can be made as short as possible, but  $l_2$  and  $l_3$  must be long enough (have sufficient time delay) so that reflections from the tee junction do not clutter the time window of interest. The stripline limiter simply consists of two parallel plates with a center conductor sandwiched in a dielectric between them (Fig. 8b). The SRD's are shunted between the center conductor and the parallel plates as shown in Fig. 8c. The diodes are Hewlett-Packard Type 5082-0300 with a maximum breakdown voltage of 100 volts and a maximum transition time of 360 psec. These specifications make the diodes ideal for use with the 50 volt, 45 nsec HP pulse generator.

The waveform shown in Fig. 9 clearly shows the relationship between the time delays involved and the lengths  $l_2$  and  $l_3$ . The operation proceeds as follows: A pulse is generated and propagates down the line  $l_1$  to the tee junction. The impedance looking into the junction is  $25\Omega$ , (two  $50\Omega$  cables in parallel), so a portion ( $\rho = -1/3$ ) of the voltage is reflected back to the pulse generator where it is dissipated in the matched  $50\Omega$  output impedance of the pulse generator. The remaining portion of the incident pulse is split equally between the two  $50\Omega$  cables  $l_2$  and  $l_3$ . Assuming a 50 volt input pulse (HP) and neglecting attenuation of the cables, a voltage reflection coefficient of  $\rho = \frac{25-50}{25+50} = -\frac{1}{3}$  at the tee implies that about 24 volts is being applied to the antenna and limiter. The first pulse shown in Fig. 9 is this 24 volt input pulse limited to approximately 800 mV. The second and third pulses are the reflections from the balun and from the antenna and ground, respectively. The antenna was not located near a target at this time, so there is no target signal. The time delay ( $2\tau_2$ ) from the input pulse to the balun reflection corresponds to twice the time delay of line  $l_2$ . The remaining pulses in Fig. 9 are multiple reflections. The second balun reflection and the second antenna reflection result from the first balun and antenna reflections having been reflected back down  $l_2$  to the antenna from the mismatch at the tee junction and then back to the tee and down ( $l_3$ ) to the sampling head. The last pulse is a second reflection of the first pulse which had been reflected back along line  $l_3$  by the short-circuited limiter to the tee junction which in turn partially ( $\rho = -1/3$ ) reflects a pulse back to the sampling head. This method admittedly can be more confusing than the orthogonal mode because of the multiple reflections, and slightly inefficient because of the signal power lost in the reflections at the tee junction, but the clutter problem caused by the reflections can be overcome by proper choice of the lengths  $l_2$  and  $l_3$ .

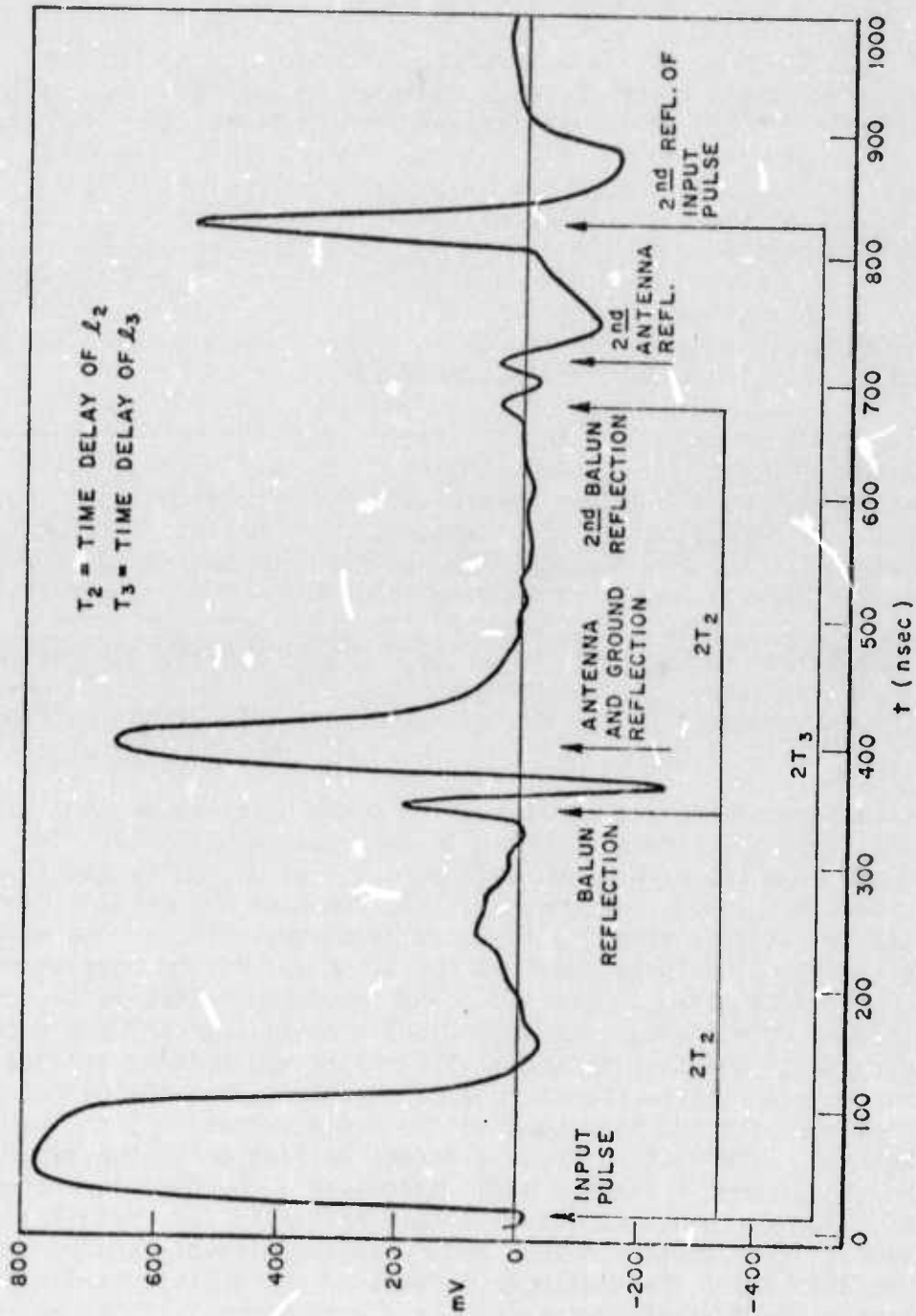


Fig. 9. Direct reflection mode measurement using limiter.

alternatively, the multiple reflections could be eliminated by matching the system with respect to the reflected signal port. A 25 ohm series resistor placed in the  $\rho_2$  port would provide such a match. The reflection losses are overshadowed by the advantages of working with only one antenna and the elimination of the direct coupling between two antennas in the orthogonal mode. It is interesting to note that a limiter capable of handling both pulse generators is now available commercially. This limiter has been purchased on another program but should be available part time for our use during the summer measurement period. Thus it will be possible to make both direct and orthogonal mode measurements of various targets. The limiter described here was not completed in time to be used when earlier measurements were made.

It was noted earlier that the probe configuration was very insensitive in the orthogonal mode to large scatterers lying on the surface when on the overburden. Similar observations can be made with regard to the large probe on a limestone or dolomite surface, and this is with full power, with and without a station wagon parked within one of the quadrants of the dipole arms for both pulse generators (see Fig. 31). No discernable change in the response waveform is seen. We conclude therefore that the dipole geometries can be well matched to rock or soil media (without ground rods for the case of rock), and are insensitive to targets on the surface. Thus in a tunnel, the presence of large equipment immediately behind the working face should not interfere with probe operation. One might infer from this that the sides of the tunnel will also not interfere. This has not been tested as yet, but will be during the summer measurement period.

#### V. PROPAGATION MEASUREMENTS AND CONSTITUTIVE PARAMETER ESTIMATES

In order to interpret pulse sounding data for a particular medium and to gate the response waveform to interrogate particular depths, it is necessary to obtain the effective refractive index for that medium and for the particular pulse generator being used. Clearly, the effective refractive index for the medium depends upon both the spectral content of the pulse and the propagation path length. Assume that pulse propagation measurements are made for path lengths  $\ell$  and  $\ell + \Delta\ell$ , where  $\Delta\ell$  is sufficiently small that the change in path length is the only change in the experiment. Taking the Fourier transform of both received pulses and normalizing the longer path by the shorter one obtains

$$(1) \quad \frac{H_{(j\omega)}^{\ell+\Delta\ell}}{H_{(j\omega)}^{\ell}} = e^{-jk\Delta\ell} ,$$

where  $k$  is the propagation factor for the medium. From this result, estimates of the frequency-dependent attenuation and the relative dielectric constant and conductivity of the medium are obtained. If the time delay is also monitored then the effective refractive index (ratio of speed of light in vacuum times the time delay to path length) is obtained. In deducing the relative dielectric constant and conductivity, there is obviously an ambiguity of a multiple of  $2\pi$  in the phase of Eq. (1). However, if it is assumed that both parameters display relatively smooth changes with frequency then consistent results can usually be obtained with a few trials. This approach is admittedly crude, but no really good method for *in situ* measurements of constitutive parameters over a wide spectral range exists. Unfortunately, nature may not be kind enough to provide convenient propagation geometries where the propagation path length and only the propagation path length can be changed. In this case it may be necessary to resort to laboratory measurements of samples or to fixed frequency measurements at selected spot frequencies spanning the desired spectral range using a transmission line approach[3]. It may be possible to apply time domain reflectometry techniques to the transmission line method, but this has not been attempted as yet. There are a number of practical limitations on using pulse propagation data over 2 different path lengths to deduce the frequency-dependent relative dielectric constant and conductivity of a medium. In order to retain significant high spectral content in the received pulse, the propagation path length must be reasonably short. However, if the path length is too short, then at lower frequencies the near zone fields of the antennas will cause problems. The size of the transmitting and receiving antennas also must be considered. The change in path length  $\Delta\ell$  also presents conflicting needs. If  $\Delta\ell$  is very small, then it is reasonable to assume approximate cancellation of even the near zone terms. But if  $\Delta\ell$  is small then the quantity  $\gamma\Delta\ell$  is quite small and this can cause accuracy problems. It will be noted in the data to be presented that for the propagation path lengths used in the experimental measurements, the calculated relative dielectric constant and conductivity appear to be incorrect for frequencies below approximately 15 MHz. This occurs for both pulse generators. At 15 MHz, the conductivity is beginning to dominate the propagation effects and consequently the effect of the dielectric constant on the experimental quantities is small. It was demonstrated in an earlier report[2] that for constitutive parameters typical of a soil medium, nearly an order of magnitude change in the relative dielectric constant had no effect on the signal propagated between two dipole antennas at frequencies below 1 MHz. It is demonstrated in this section using analytical calculations that valid relative dielectric constants can be obtained below 15 MHz if the conductivity is reduced. These same calculations also show however that for very low conductivities ( $10^{-4}$ - $10^{-5}$ ) calculations of the conductivity via pulse propagation data become inaccurate since the conductivity is not the significant parameter in the experiment. Certainly if experimental data are used, one can anticipate inaccurate

results for the smaller term in the expression for the complex propagation factor. At the same time, however, if at low frequencies the relative dielectric constant has little or no effect on the pulse propagation then it is really of no interest for our purpose. The same is true of very low conductivities, where propagation path lengths would be quite long before the conductivity effects became noticeable. Therefore, the number of practical limitations on obtaining relative dielectric constant and conductivity data from pulse propagation measurements would not appear to preclude use of the method for our purpose.

Fig. 10 shows a sketch of a tunnel geometry in a limestone quarry\*

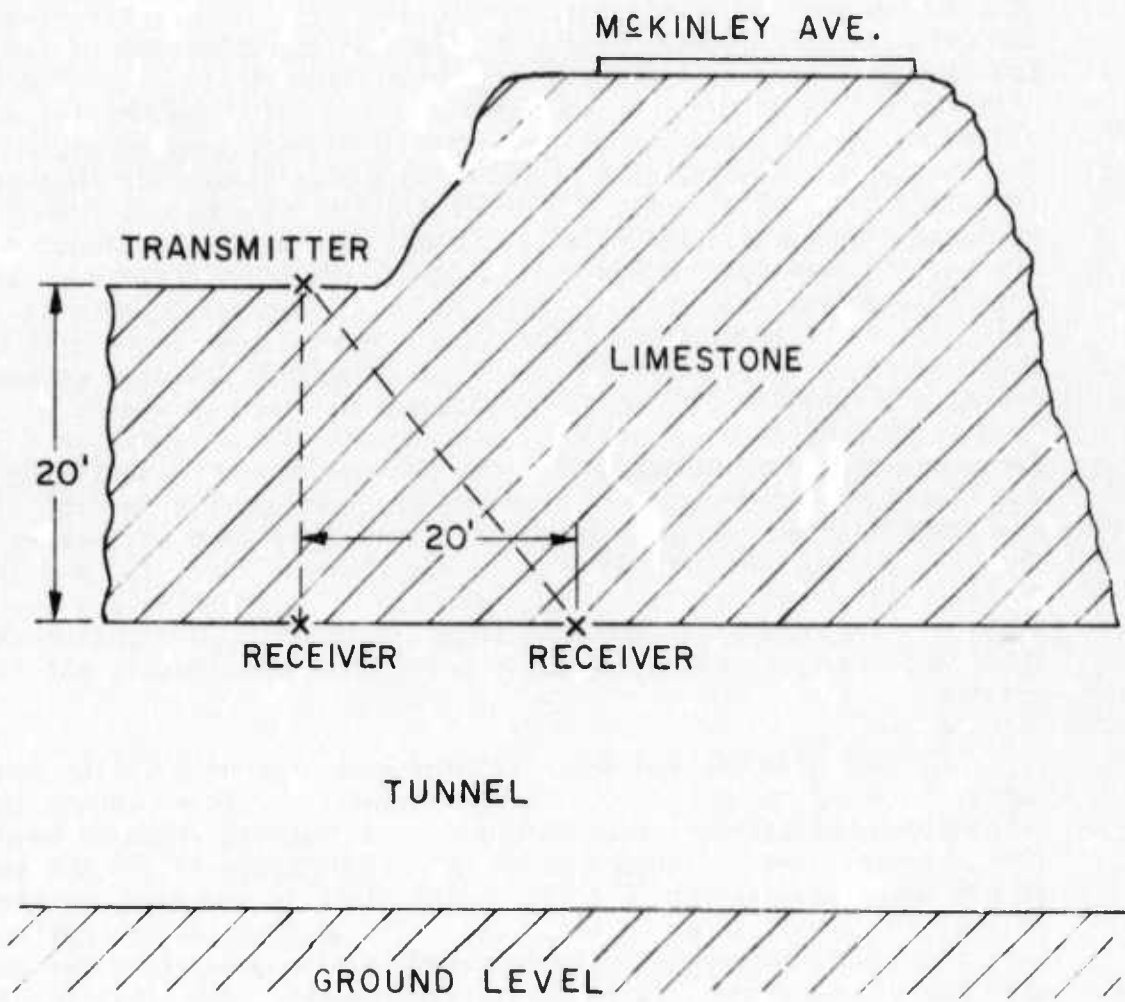


Fig. 10. Sketch of tunnel geometry.

\*Marble Cliff Quarries, 3135 Trabue Road, Columbus, Ohio.

where propagation measurements were made by transmitting from one of the large dipoles of Fig. 1a on the ledge to a small dipole (Fig. 1c) held against the roof of the tunnel. In Fig. 11a, the received pulses for 20 and 30 foot transmission paths are shown for the 45 ns pulse of Fig. 2a. The amplitude and phase spectra of the received pulses are shown in Figs. 11b and c. Corresponding measurements for the narrow pulses (Fig. 3) are shown in Fig. 12. The effective refractive indices obtained were 3.66 and 3.48 respectively for the 20 and 30 foot path lengths for the pulses in Fig. 11a and 3.47 and 3.22 for those in Fig. 12a. Note that the effective index changes with both pulse frequency content and path length. It is apparent from the spectra in Fig. 11b that the processed results at frequencies greater than 50 MHz will be meaningless, as is also true for the spectrum of the original pulse given by Fig. 4. Much of the character of the spectrum of Fig. 4 is preserved in the spectrum of Fig. 11. The major difference lies in the lobe centered about 30 MHz. The smaller antenna placed on the rock media would be resonant in this general region of the spectrum. Thus it would probably be a better radiator in this frequency band. Similarly, a 250 MHz limit seems apparent from Fig. 12b. Frequency-dependent attenuation and phase data in dB/foot deduced via Eq. (1) are shown in Fig. 13. Figures 13a and b correspond to Fig. 11 and Figs. 13c and d to Fig. 12. The propagation data in Figs. 11 and 12 were taken in the summer about a week apart with intervening rains. It is not surprising therefore that the attenuation levels are slightly different. No attempt was made to obtain a quantitative estimate of the moisture content of the limestone. The frequency-dependent relative dielectric constant and conductivity of the limestone medium obtained from the propagation data in Fig. 11 are shown in Figs. 14a and 14b respectively. The same parameters from the propagation data in Fig. 12 are shown in Figs. 15a and 15b. In Figs. 14 and 15, available data from the literature[4] are shown as crosses. The moisture content is known to have a strong influence on the electrical parameters and consequently the variation is not surprising.

For the dolomite medium\*, dipole-dipole type propagation measurements could not be made at convenient ranges. For this medium, the propagation measurements were made using an inverted grounded monopole (18" diameter circular ground plane and 1 foot antenna) and the small dipole described earlier (Fig. 1c) lying flush on the rock. A sketch of the geometry is shown in Fig. 16b. This geometry is not optimum for this study but represents a simple expedient for generating the data with the accuracy required for these experiments. Note that for the grounded monopole-dipole geometry,  $k$  in Eq. (1) does not have the same simple interpretation as for the dipole-dipole experiment, i.e.,

\*Plum Run Stone Division, Route 32, Peebles, Ohio.

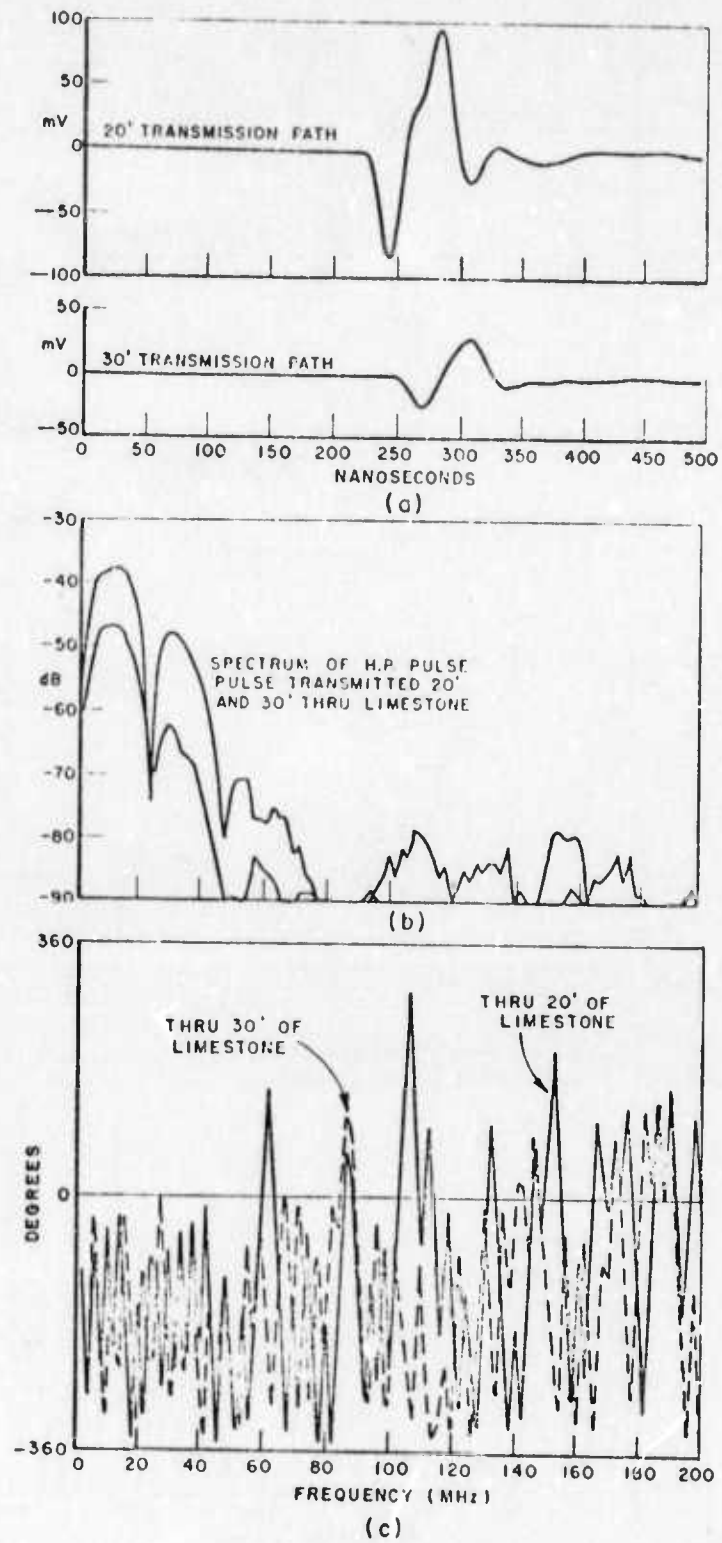


Fig. 11. Propagation data for limestone medium using Hewlett Packard generator.  
 (a) time domain pulses  
 (b) amplitude spectra  
 (c) phase spectra

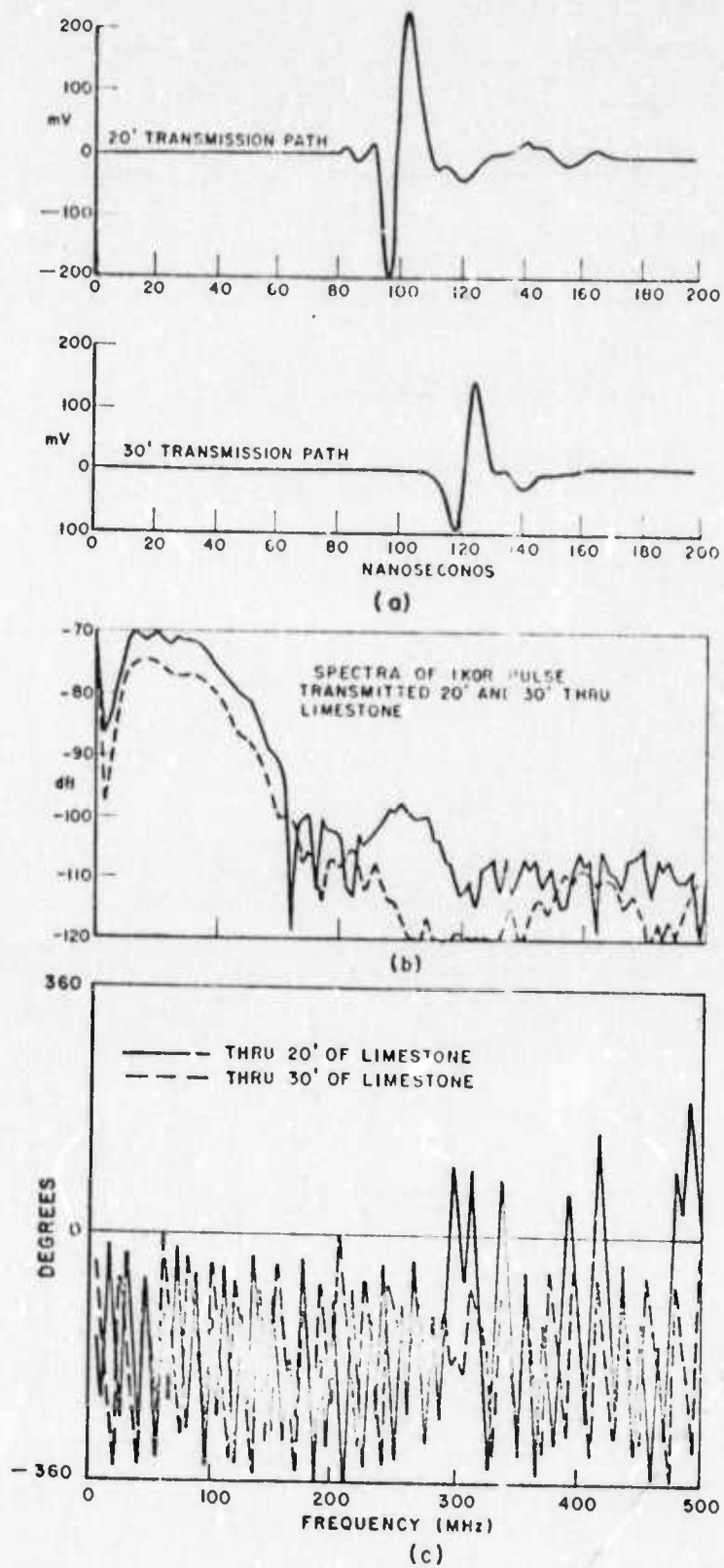


Fig. 12. Propagation data for limestone medium using Ikor generator.  
 (a) time domain pulses  
 (b) amplitude spectra  
 (c) phase spectra

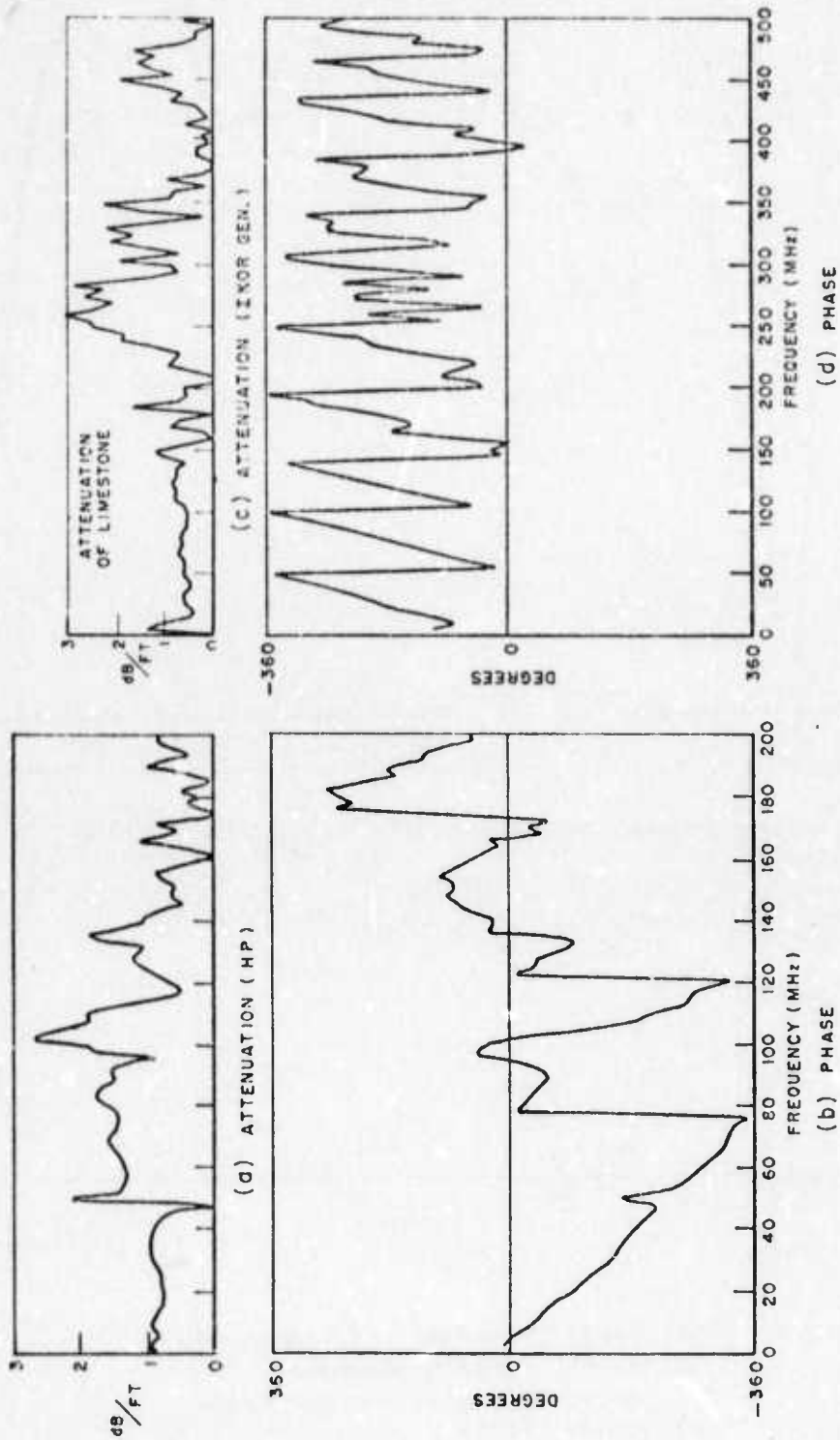


Fig. 13. Attenuation of limestone medium.  
 (a) via Hewlett Packard generator  
 (b) phase  
 (c) via Ikor generator  
 (d) phase

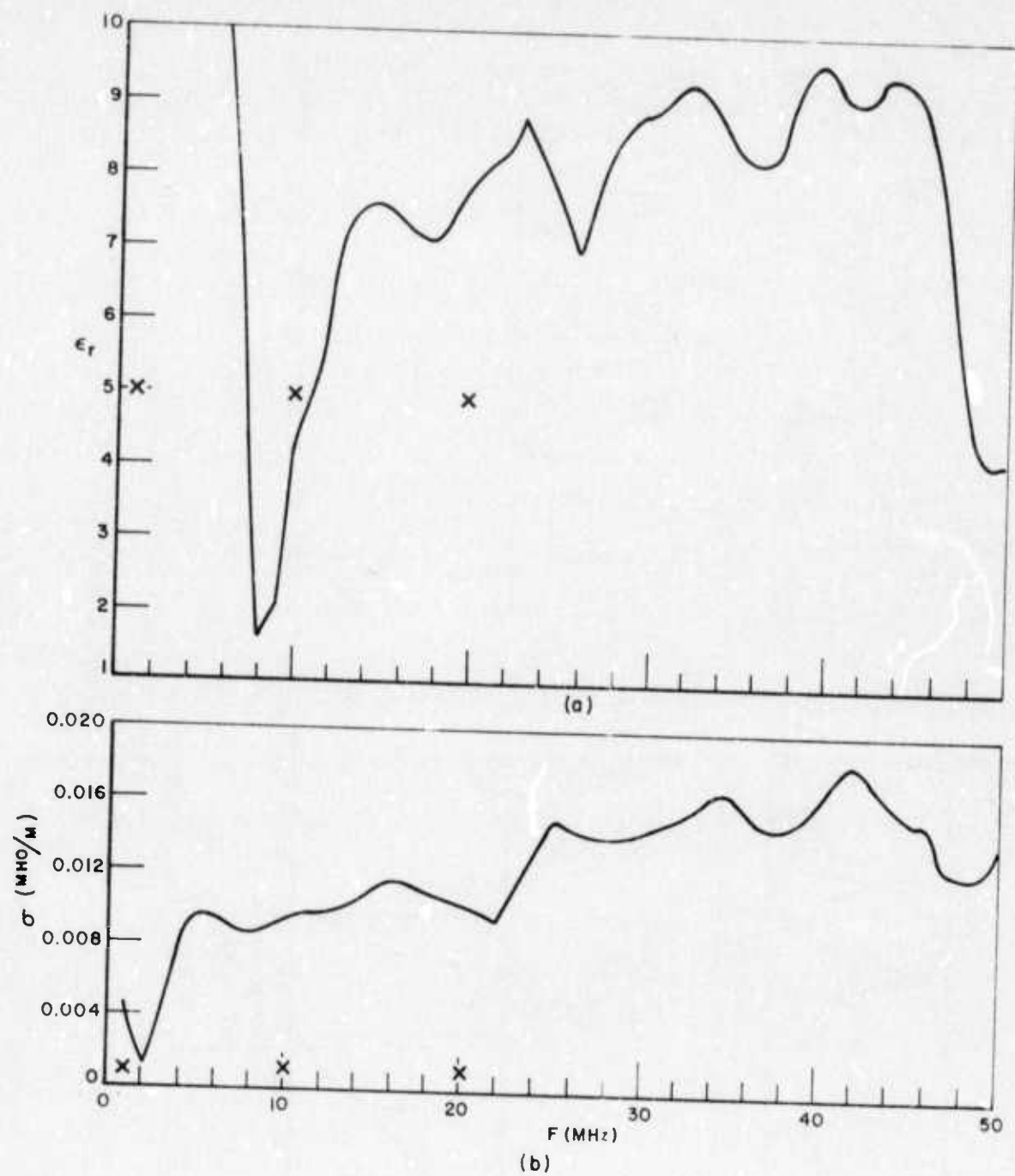


Fig. 14. Electrical properties of limestone via Hewlett Packard generator.  
 (a) relative dielectric constant  
 (b) conductivity

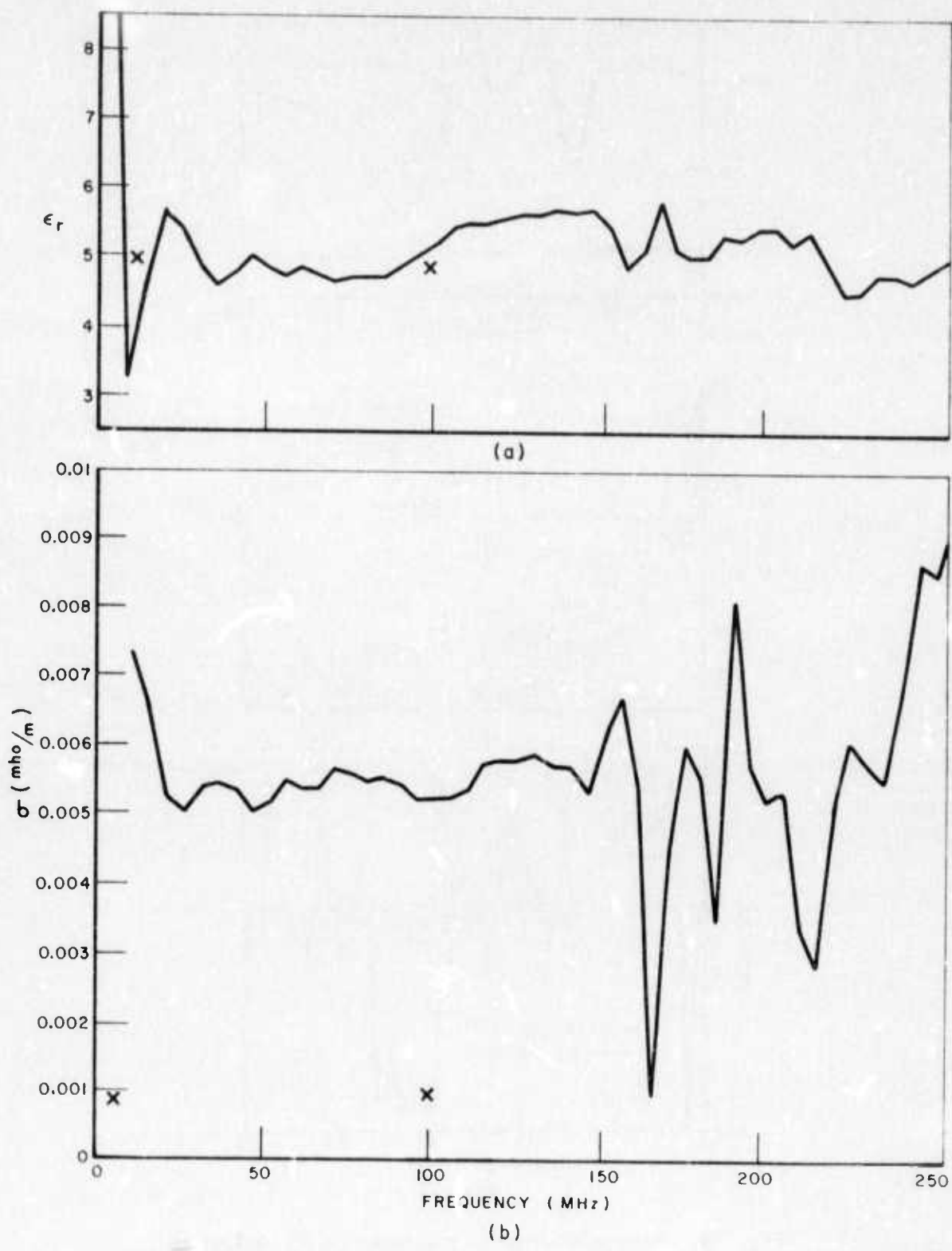
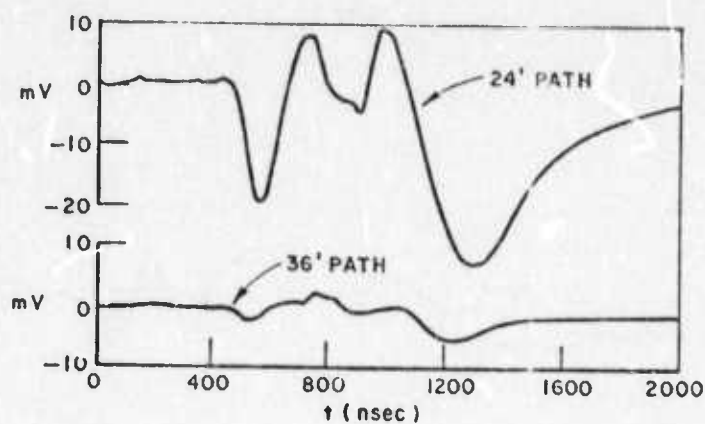
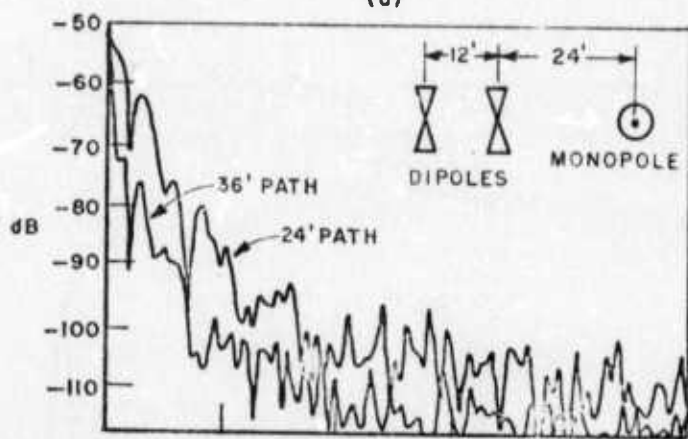


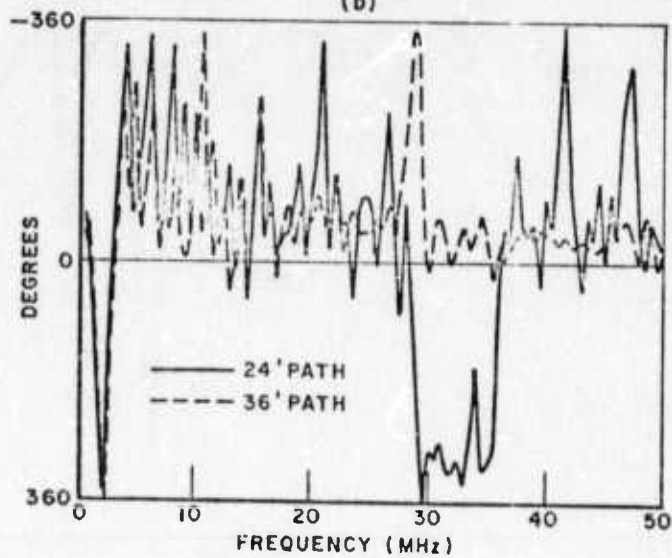
Fig. 15. Electrical properties of limestone via Ikor generator.  
 (a) relative dielectric constant  
 (b) conductivity



(a)



(b)



(c)

Fig. 16. Monopole-dipole propagation in dolomite  
Hewlett Packard generator.  
(a) time domain waveform  
(b) amplitude spectrum  
(c) phase spectra

$$(2) \quad k^2 \neq \left(\frac{\omega}{c}\right)^2 \left[\epsilon_r - j\frac{\sigma}{\omega\epsilon_0}\right],$$

where  $\epsilon_r$  is the relative dielectric constant of the medium,  $\sigma$  is the conductivity of the medium,  $\omega$  is the angular frequency and  $\epsilon_0$  is the permittivity of free space. We have processed measured data for the dolomite medium as if Eq. (2) contained an equal sign, but know that this is a very gross approximation. During the summer measurement period, dipole-dipole propagation data will be taken using the small dipoles flush with adjacent cliff faces.

Development of a good technique for measuring, in situ, the constitutive parameters of a medium over a broad range of frequencies is a research problem of some magnitude in its own right. Wait[5] has suggested a fixed frequency two-loop method where the loops are located in a borehole. If the rapid excavation machinery uses a pilot bore of sufficient size - the two-loop method extended to consideration of pulse signals via fast Fourier transform methods might offer an attractive method for monitoring the constitutive parameters of the rock medium. Wait has also suggested a method for measuring the constitutive parameters of a medium using two small loops on the surface of the medium[6]. This technique could also be extended to pulse signals and would appear to be applicable within limits to a tunnel working face. These techniques need to be tested (as was noted by Wait). If time and funds permit, a two surface loop pulse measurement will be made in the dolomite medium during the summer measurement period. It should be noted however that basic application of the electromagnetic pulse sounder does not require "*a priori*" knowledge of the constitutive parameters of the medium. The fundamental requirement is an estimate of the effective refractive index of the medium for a particular pulse signal. With this information, gating to provide temporal and spectral signatures at particular depths can be effected. As discussed in Section IX, a sophisticated processing would proceed to remove the attenuation and dispersion effects of the medium via theoretical calculations (for which the frequency-dependent constitutive parameters would be needed) and thus obtain an impulse response waveform for the target in question. Note particularly that these are not plane wave attenuation and dispersion calculations nor are they for infinitesimal elements.

The time and frequency domain waveforms of the transmitted pulses of the HP and Ikor pulse generators for the monopole-dipole configuration in dolomite are shown in Figs. 16 and 17, respectively. Note that over a path length of 24', the received HP pulse (Fig. 16) endures for well over 1  $\mu$ sec while the received Ikor pulse (Fig. 17) endures for over 2.5  $\mu$ sec. The excessive dispersion is believed to be due primarily to the moisture content of the rock - it had been raining for at least 24 hours immediately prior to the recording of these

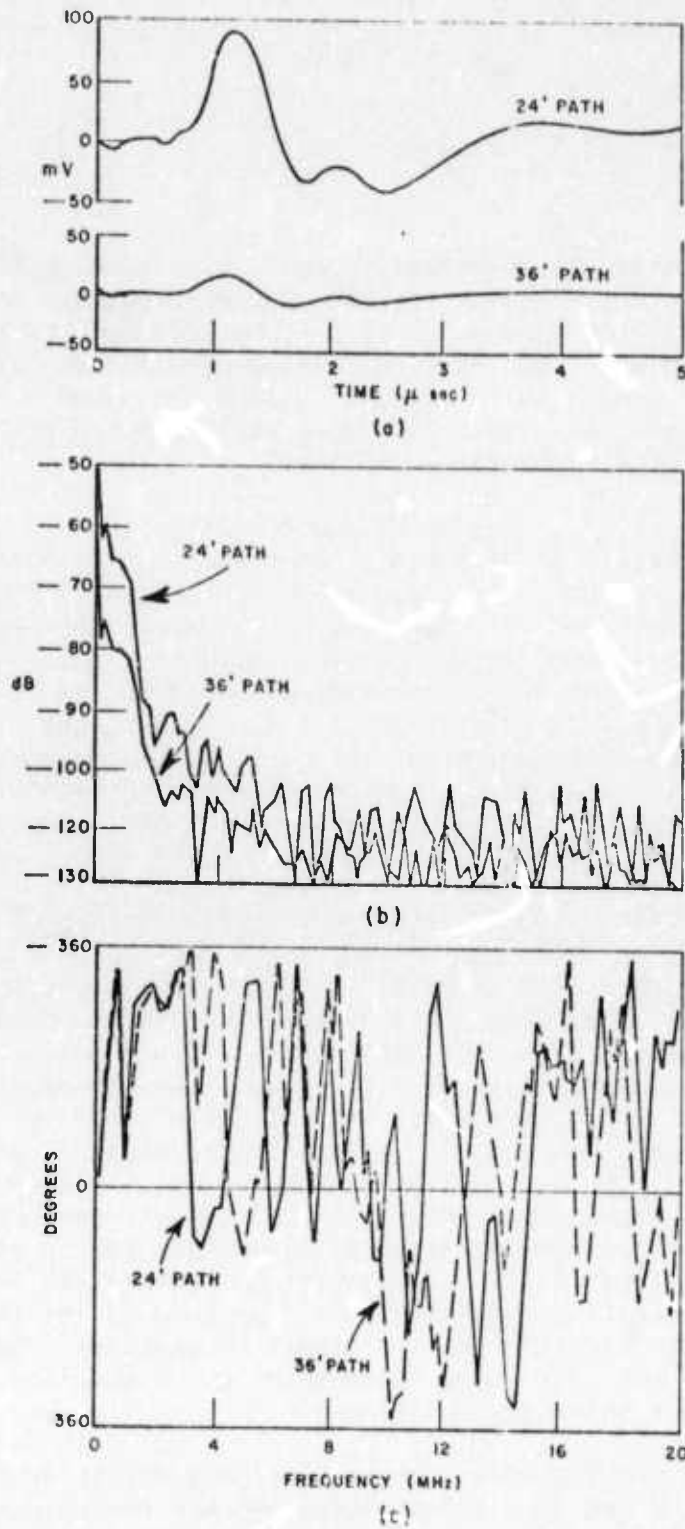


Fig. 17. Monopole-dipole propagation in dolomite Ikor pulser.  
 (a) time domain waveform  
 (b) amplitude spectra  
 (c) phase spectra

measurements. Poor coupling to the rock medium may also be a factor in that the surface (2"-3") of the rock was actually a loose gravel and dirt mixture.

The time domain waveforms of Fig. 16 (HP) were Fourier transformed to obtain the amplitude and phase spectra shown in Figs. 16b and c which upon subtraction and normalization by path length yield the attenuation in dB/ft and phase constants of the rock medium as a function of frequency (Figs. 18a,b). This process was repeated for the Ikor (1  $\mu$ sec) pulse waveforms of Fig. 17a to obtain the amplitude and phase spectra (Figs. 17b,c) and attenuation (Figs. 18c,d). From the Ikor data, it is apparent that frequencies above 6 MHz were lost in the noise over a propagation distance of 24 feet, while from the HP data, frequencies above 20 MHz were lost over the same distance. It is important to note that the attenuation vs frequency data in Fig. 18 mean absolutely nothing above these limiting frequencies.

Using the Eq. (1) assumptions, the transmission data were processed to obtain a frequency dependent relative dielectric constant and conductivity for the medium (Fig. 19). Again these data should be considered only over the frequency range determined by the significant spectral content of the transmitted pulses. Due to the excessive attenuation and dispersion and the fact of Eq. (2), these data are admittedly very gross estimates, but even so, they are still within an order of magnitude of published results[4].

## VI. SCATTERING MEASUREMENTS IN DOLOMITE

An initial series of orthogonal mode measurements have been made in a dolomite quarry (Plum Run Stone Division) near Peebles, Ohio. Unfortunately, the quarry is approximately 120 miles from the Electro-Science Laboratory - thus measurements at this site involve significant travel costs. This quarry is the closest location known where faults, joints and lithologic contrasts exist without an intervening overburden cover. A geological description of the quarry was given in the Research Plan dated 7 September, 1972, and can also be found in Reference [7].

To accommodate measurements at the Plum Run site, the electro-magnetic pulse sounding system was modified to permit operation from a small 1250 watt generator. The modification consisted primarily of the construction of a small waveform generator to supply the ramp and gate waveforms necessary for remote site operation. The entire system can now be transported in a station wagon or similar-type vehicle. Thus the large truck described and shown in a previous report[1] is no longer required. This also means, however, that the boom on the truck is not available. As will be seen, the boom would be particularly advantageous for certain of the proposed measurements. A second probe

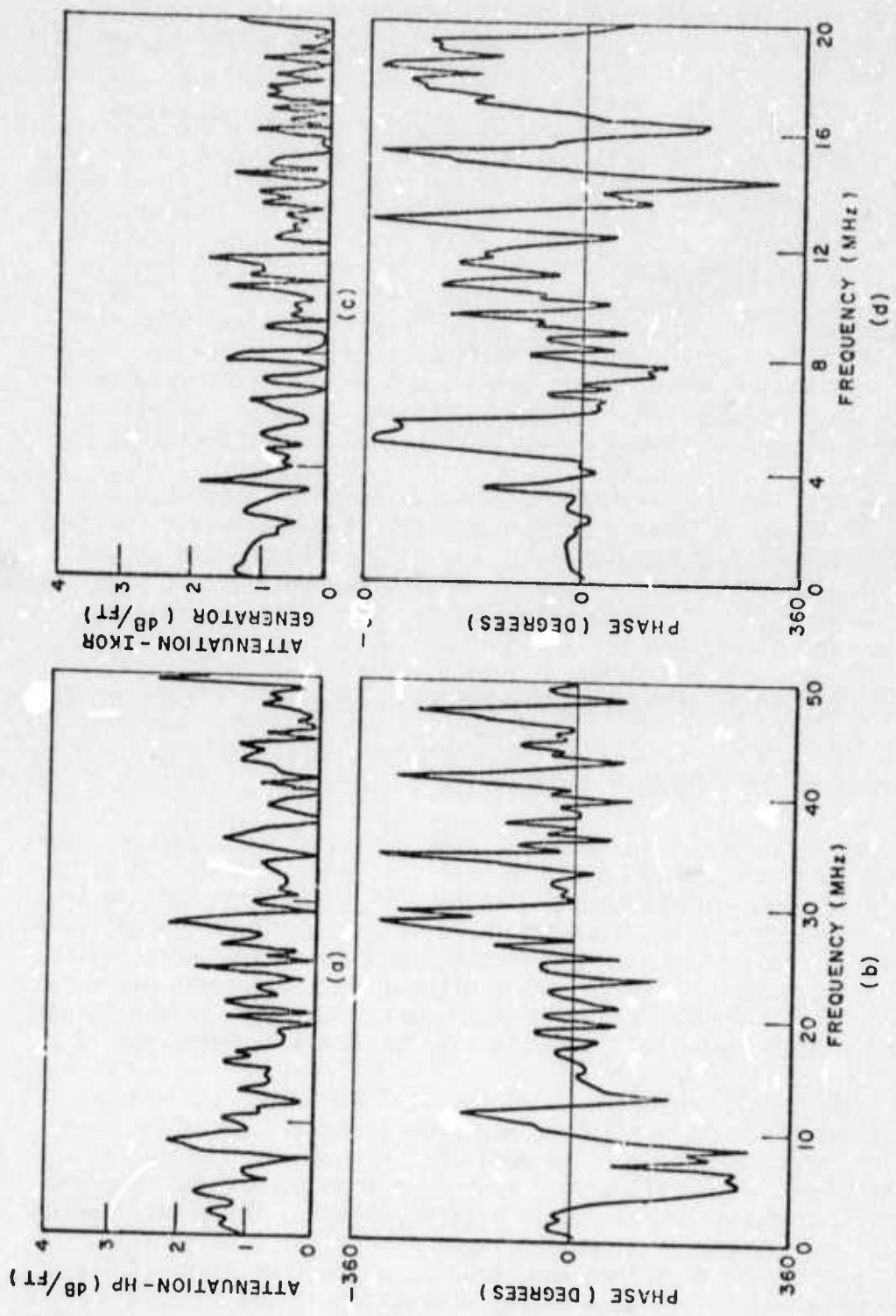
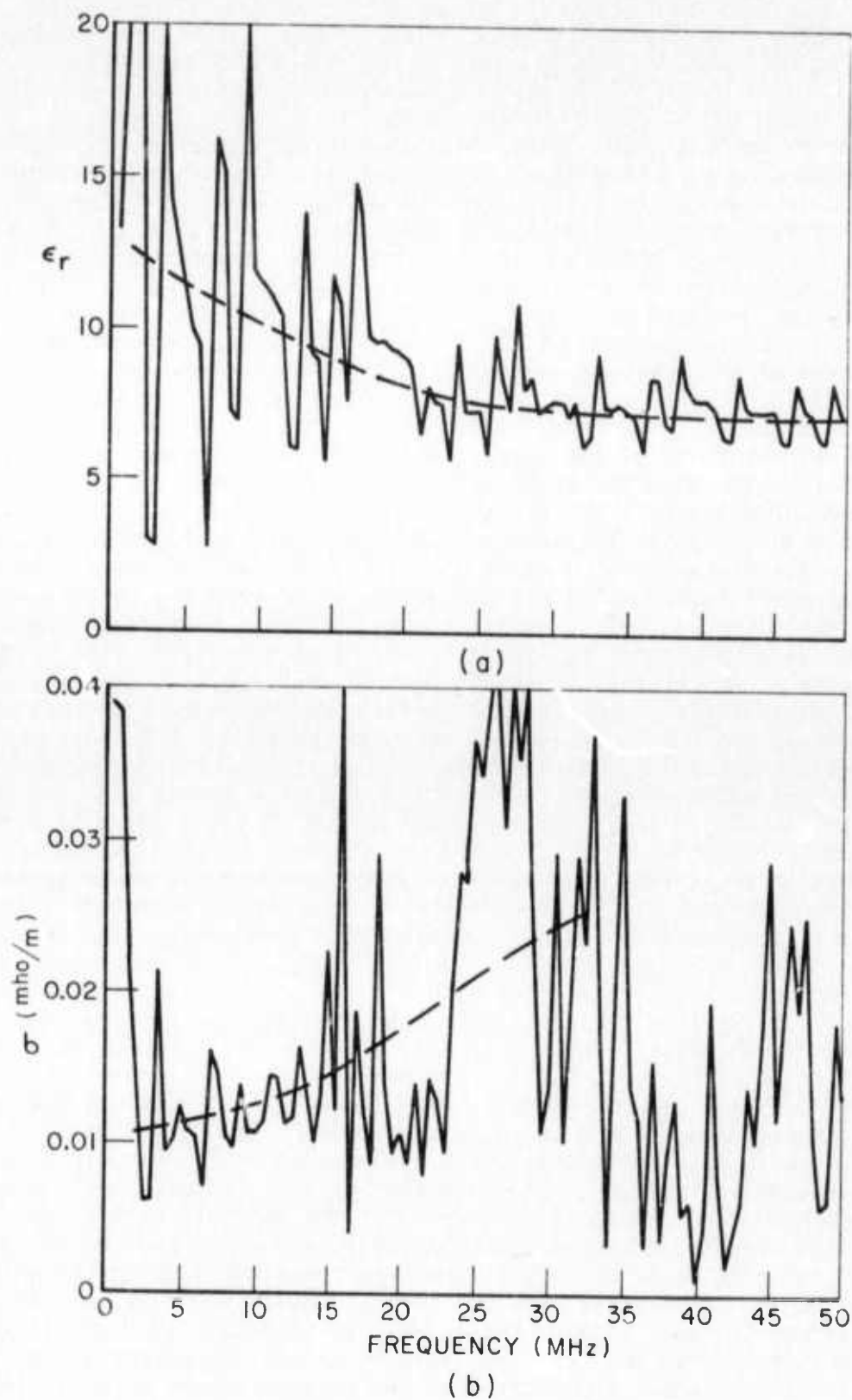


Fig. 18. Attenuation of dolomite.  
 (a) Hewlett Packard generator  
 (b) phase  
 (c) Ikor generator  
 (d) phase



geometry was also made available. This probe (shown in Fig. 1c) was developed on another program and is designed for remote probing in the overburden at relatively shallow depths. Basically, the end reflections from the dipole arms are controlled in this case by placing absorber between the probe and the medium to attenuate most of the high frequency energy before it reaches the ends of the dipole. The small probe was designed for operation with the narrow (Ikor) pulse of Fig. 3. It was used for certain of the dolomite quarry measurements primarily because of the ease with which it could be set up and moved.

Figure 20 shows the results of 4 orthogonal mode measurements made on the floor of the quarry, which is also referred to as the Lilley-formation. The probe was that in Fig. 1c and the Ikor pulse generator was used. The top waveform is a control or no target waveform with the probe located near the center of the floor and no known contrasts beneath the probe to a depth of at least 35 feet. The next three waveforms show the effects as the probe geometry is displaced laterally from a fault occurring along the floor. The fault has a vertical displacement of approximately 13 feet and the probe is on the up side of the fault. The fault was reasonably clean. One can clearly see the correlation between the position of the probe with respect to the fault and the corresponding response waveform. Note that this is using the unprocessed time waveforms. In each of the 4 waveforms shown, the first negative spike is the direct coupling across the feed points of the dipoles. Note that the shape of this leading spike is a replica of the pulse shown in Fig. 3b. In particular, the base width is roughly 8 to 10 ns. The direct coupling magnitude is quite sensitive to the levelness of the probe. One can anticipate therefore variations in this magnitude throughout a series of measurements. The direct coupling is of no consequence since it can always be gated out, but it does serve as a convenient time reference - that is it explicitly references in time the arrival of the interrogating pulse at the feed point of the probe. The propagation measurements taken on this day yielded an effective delay for the Ikor pulser in dolomite of 2.17 nsec/ft. When the measurements were taken a light rain was falling and it had been raining steadily for at least 24 hours. It is difficult with this configuration to estimate when the response from the fault actually started. In the normal case, i.e., with the target below the probe plane, it is clear that the shortest path is via feed point - target-feed point with the response via the ends of the dipole arms arriving somewhat later. Consider first the first positive peak and the second negative peak in the fault waveforms. For all three measurements these remain almost constant at delays of 9 and 15 ns, respectively from the start of the direct coupling except at the 5 foot distance where something else has obviously been added to the response. Since these characteristics do not move as the probe is moved, it is contended that they are due to another target beneath the rock whose nature is unknown. On the other hand the second positive

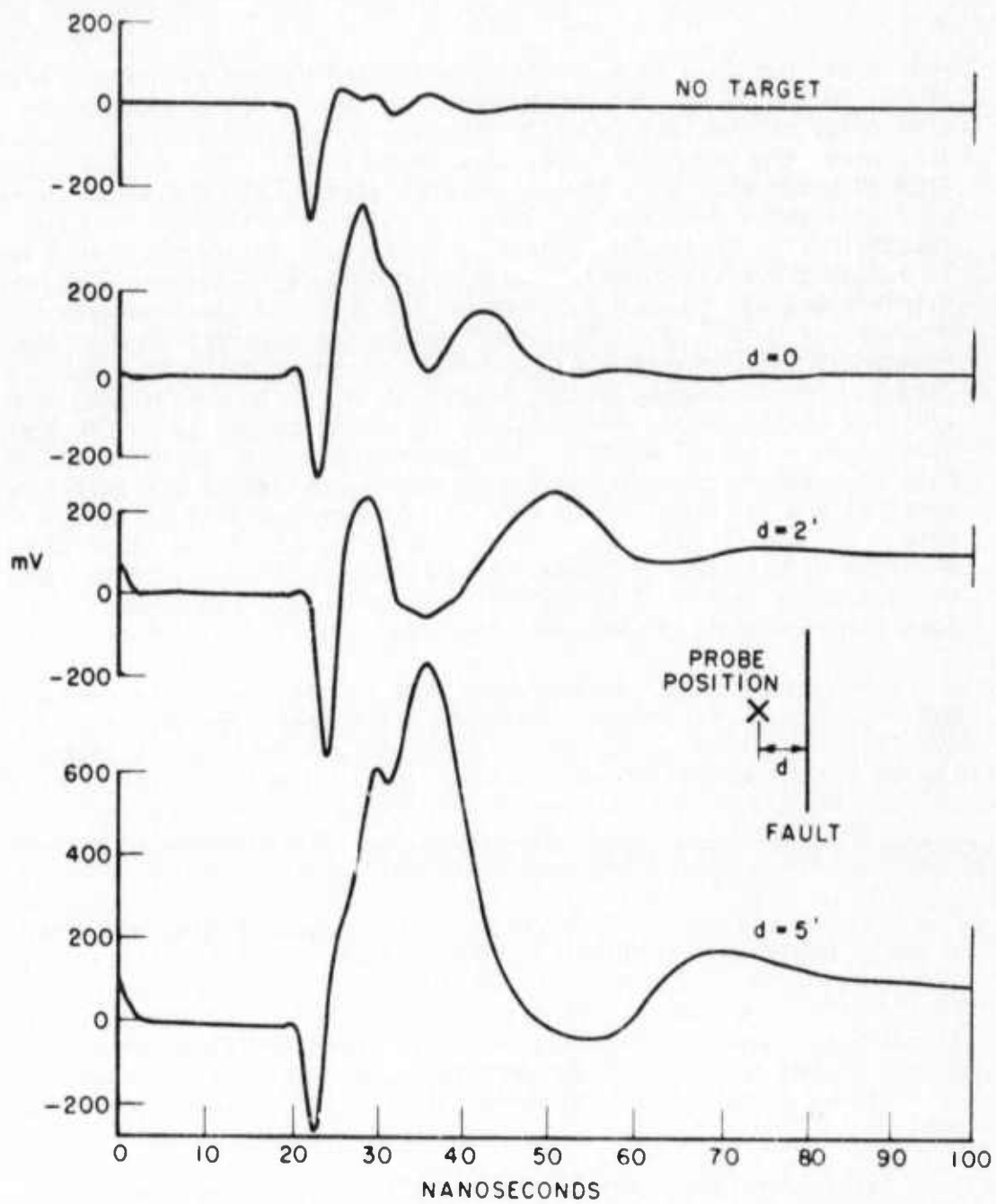


Fig. 20. Orthogonal mode measurements of fault and no target geometries. Small probe and Ikor pulse generator.

peak moves out in time from the direct coupling and occurs respectively at 21, 30 and 49 ns from the direct coupling. With the estimated time delay of the Ikor pulse in dolomite and considering a 2-way path, this means the probe has been moved respectively 2.07 and 6.2 feet away from this target. This agrees reasonably well with the known movement of 2 feet and 5 feet for the last 2 measurements in Fig. 20. The sketch in Fig. 20 may be somewhat misleading. The fault line shown is actually the start of fracturing in the rock - the actual vertical displacement was roughly 2.5 feet to the right of the line shown. However, it is unlikely that the response can be attributed to the fault. Apparently the probe had been moved within range of another subsurface target. The amplitude spectra in Fig. 21 also clearly display the presence of the fault when compared to the no target amplitude spectra (dashed curve in all three). The phase spectra are shown in Fig. 22. Note the similarities in the low frequency content of the target amplitude spectra, and the peculiar absence of frequency content at (above) approximately 140 MHz in Fig. 21c, which is the spectra of the unexplained target waveform of Fig. 20. Although it is rather difficult to interpret the phase spectral data, it is evident from the phase spectrum of the d=5 foot waveform that the unknown target has affected the phase.

The above set of measurements were repeated with the same probe and the HP pulse generator. These response waveforms are shown in Fig. 23. Note in Fig. 23 that while there are differences in the target and no target responses, they are not simply interpreted. This vividly illustrates the advantages of a very narrow interrogating pulse for close in targets. Note also that the addition of a new target in the 5 foot waveform is also evident.

It was originally intended to make orthogonal mode measurements with the probe on a vertical cliff face such that the vertical displacement of the fault and also certain joint configurations would be in the same direction as the plane of the probe. These measurements were not possible because heavy rains caused standing water in the quarry making the base of the vertical rock faces inaccessible. It is intended to make these measurements during the summer measurement period.

Because of the success of the initial fault measurements using the Ikor generator, further fault measurements were conducted in an attempt to locate a minor fault line in a section of the quarry that had not been accurately mapped. With the indispensable help of the quarry geologist\*, the fault location was narrowed down to roughly a 75 foot wide strip. Figure 24 shows a sketch of the site with the

\*Dr. Richard Bowman, Head Geologist, Plum Run Stone Division.

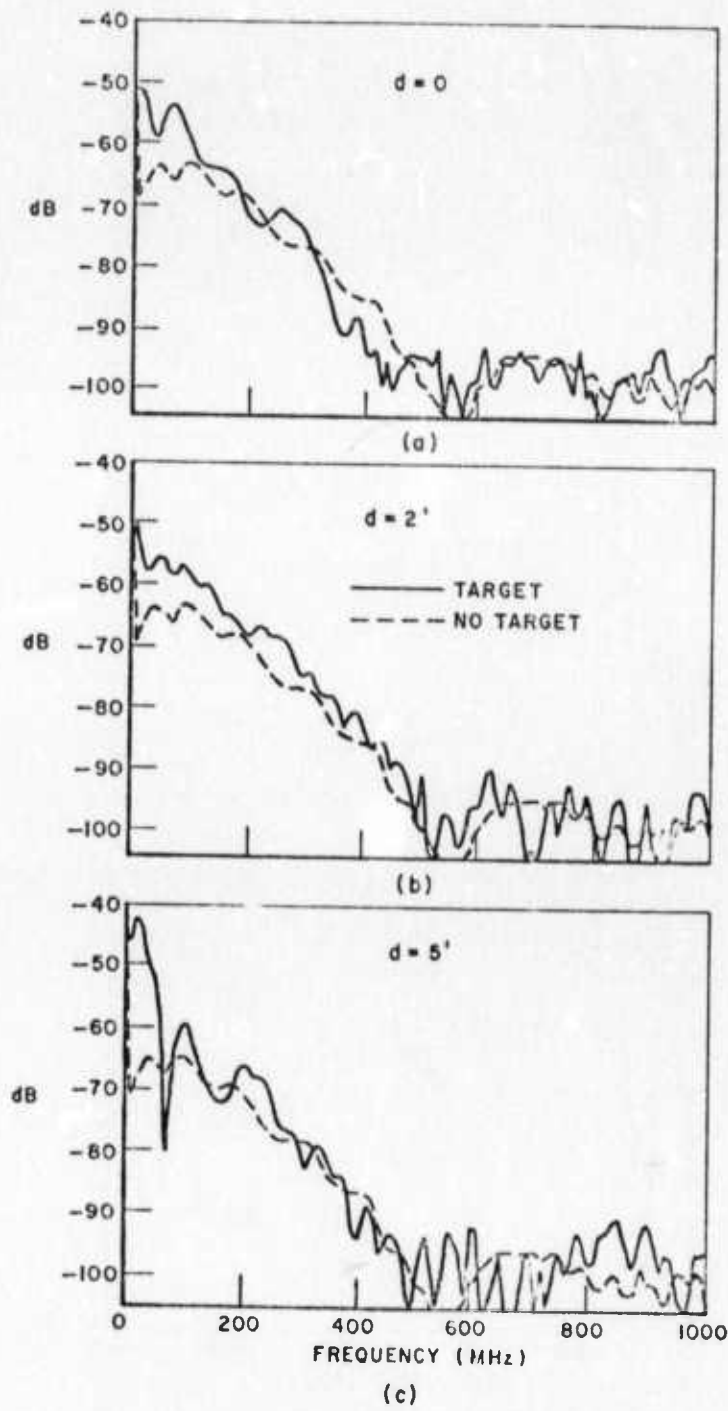


Fig. 21. Amplitude spectra of fault measurements.

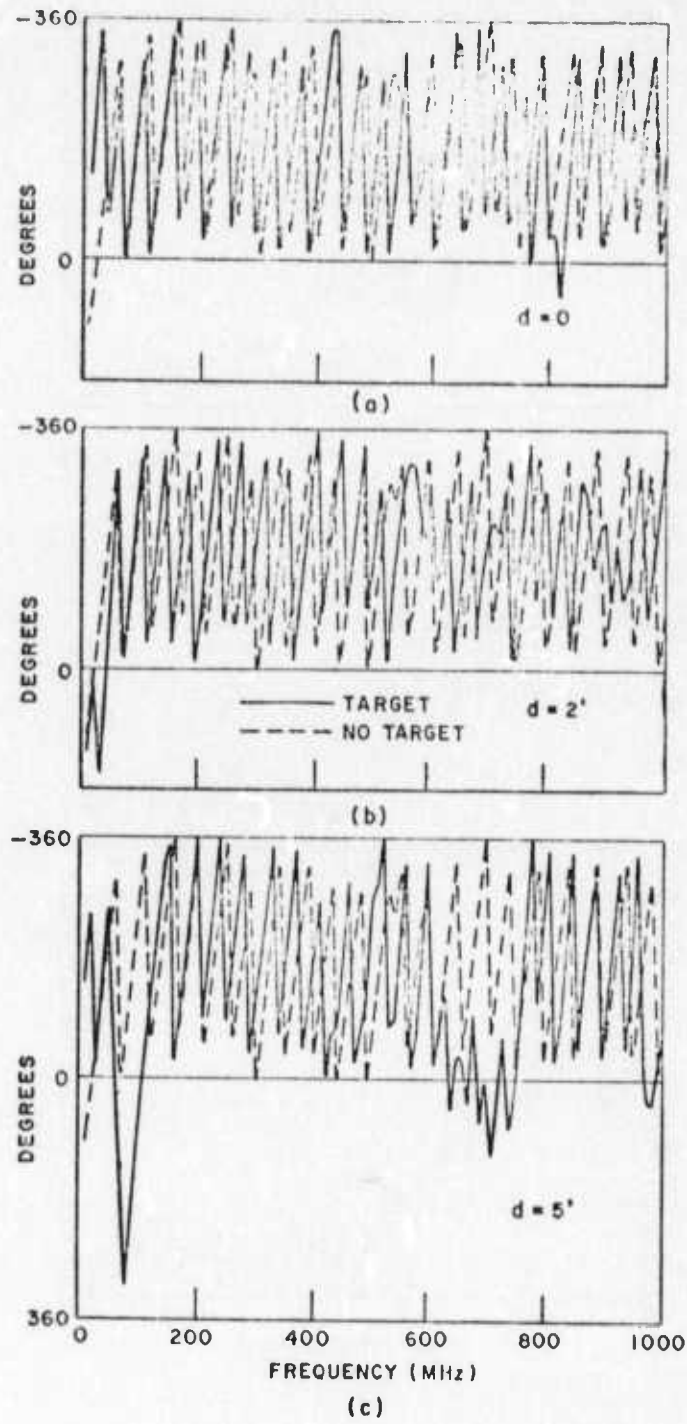


Fig. 22. Phase spectra of fault measurements.

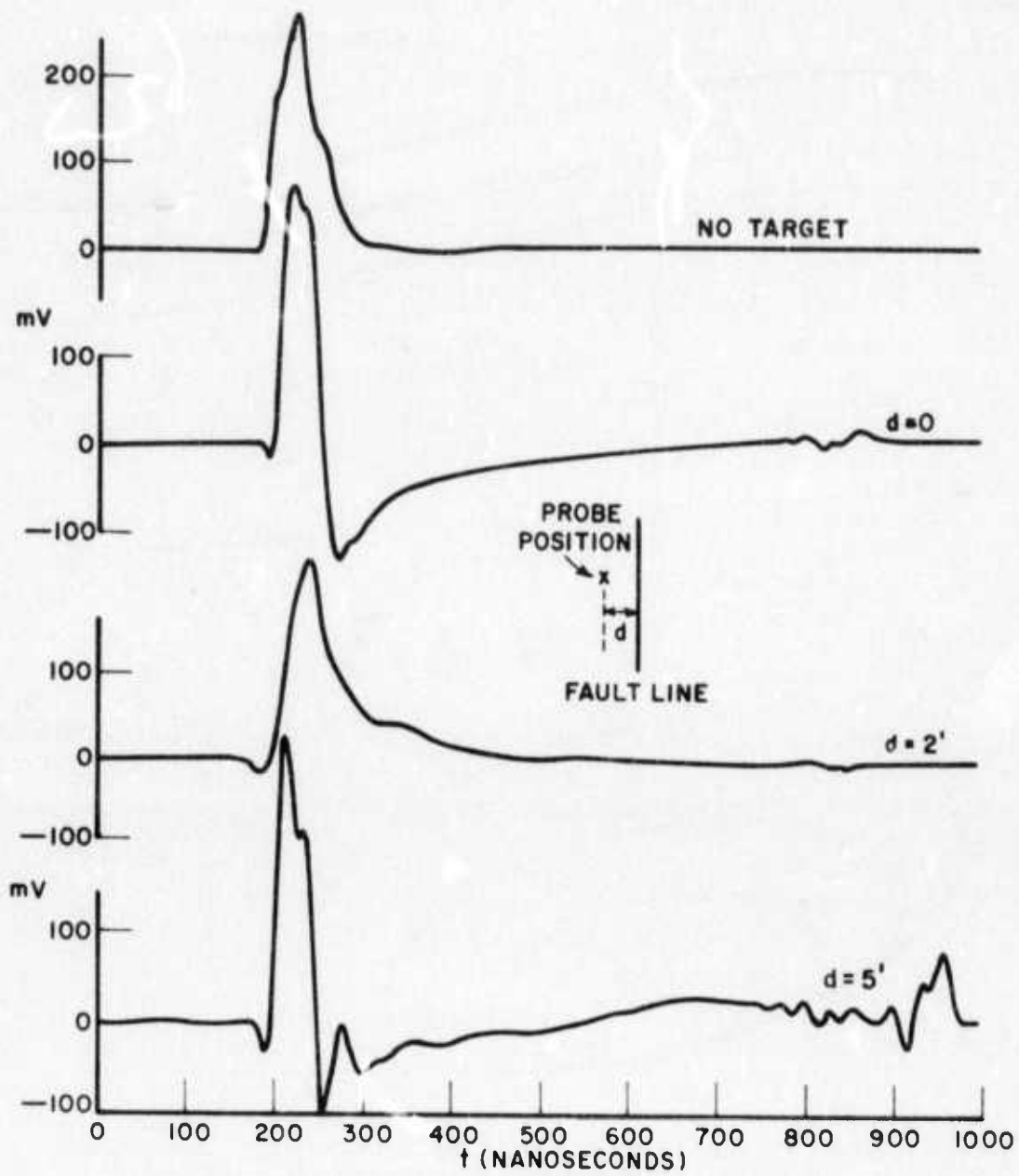


Fig. 23. Orthogonal mode measurements of fault and no target geometries. Small probe and Hewlitt Packard generator.

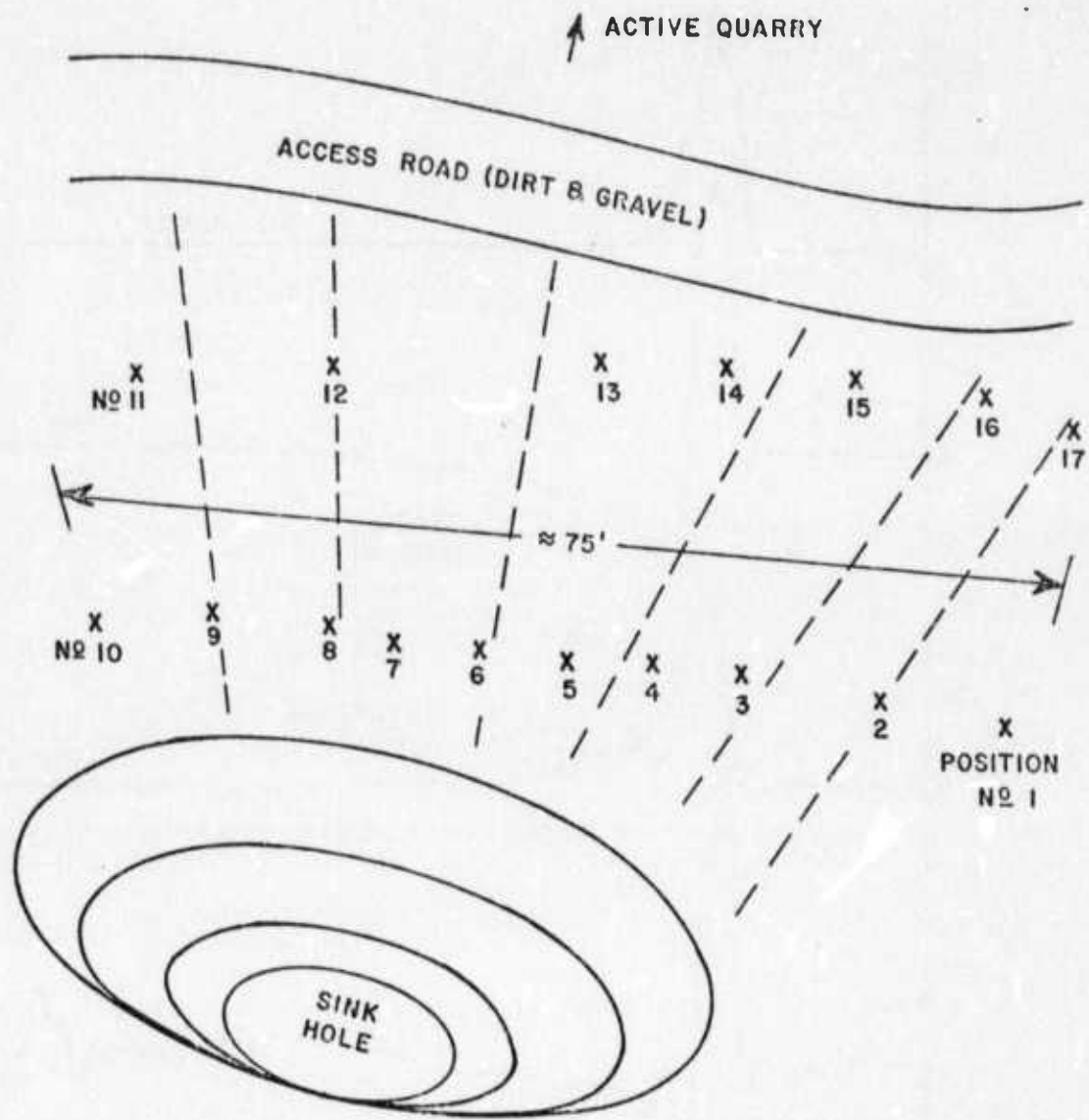


Fig. 24. Sketch of fault location measurement.

numbered X's marking the probe positions. As seen in the figure, two sweeps across the strip were made, using the small absorber covered probe and the Ikor pulser. The seemingly random spacing between measurements was necessary because of surface roughness, as it is always desirable to keep the probe as flat as possible on the surface of the rock. Figure 25 shows the time domain waveforms obtained at the 17 probe positions in Fig. 24 and an average of all 17 waveforms which is used as a no target reference.

Observe the large response in Fig. 25, positions 4, 5, 6, and 15. The response is delayed in time as the probe is moved away from position 4. This trend implies that the "target" under observation is very close to position 4. While some evidence of this "target" is apparent in positions 2 and 3, it is rather difficult to associate a similar correlation between the response and distance from target as in positions 4, 5, and 6 and Fig. 20. There were also a number of surface cracks in the vicinity, indicated by the dashed line in Fig. 24, which are probably responsible for all of the low magnitude responses in Fig. 25. The target in question here is also difficult to describe from a geometrical viewpoint. The fault line need not be perpendicular to the plane of the surface, in fact, it may be tilted at such an angle as to invoke a large response to the probe in position 4 and yet invoke only a minor response to position 3. Note that in the amplitude spectra of positions 4, 5, and 6, shown in Figs. 26 the characteristic low frequency fault response is observed, which is similar to those in Fig. 21. Position 15 contains the maximum response obtained in the second sweep across the fault. Again the amplitude spectrum of position 15 displays the same characteristics. The phase spectra are shown in Fig. 27. These data, and previous knowledge of the general direction of the fault lead to the conclusion that the fault under investigation follows a line that passes near positions 4 and 15. The precise location of the fault, however, cannot be verified. This section of the quarry has since been worked, and the head geologist generally agreed with our conclusions. However, he stated that so much fracturing occurred in this area that precise location was not possible.

Perhaps the most striking results obtained thus far is the response from a lithologic contrast at a depth of approximately 45 feet. Figure 28 shows the geometry of the measurement. The large (28' dipole) probe with the aluminum sheets is situated on a layer of rock about 45 feet above the quarry floor, and is operated in the orthogonal mode with the 50 volt 45 ns (HP) pulse generator. Both rock formations are dolomite, but the upper layer is an open porous reef-type material while the lower layer (quarry floor) is a dense material. Basically there is a large change in the specific gravity of the material, but the contrast is not sharp. The extent of this gradual transition is approximately 3 to 5 feet. On either side of the probe were joints running vertically from the surface near the probe to the quarry

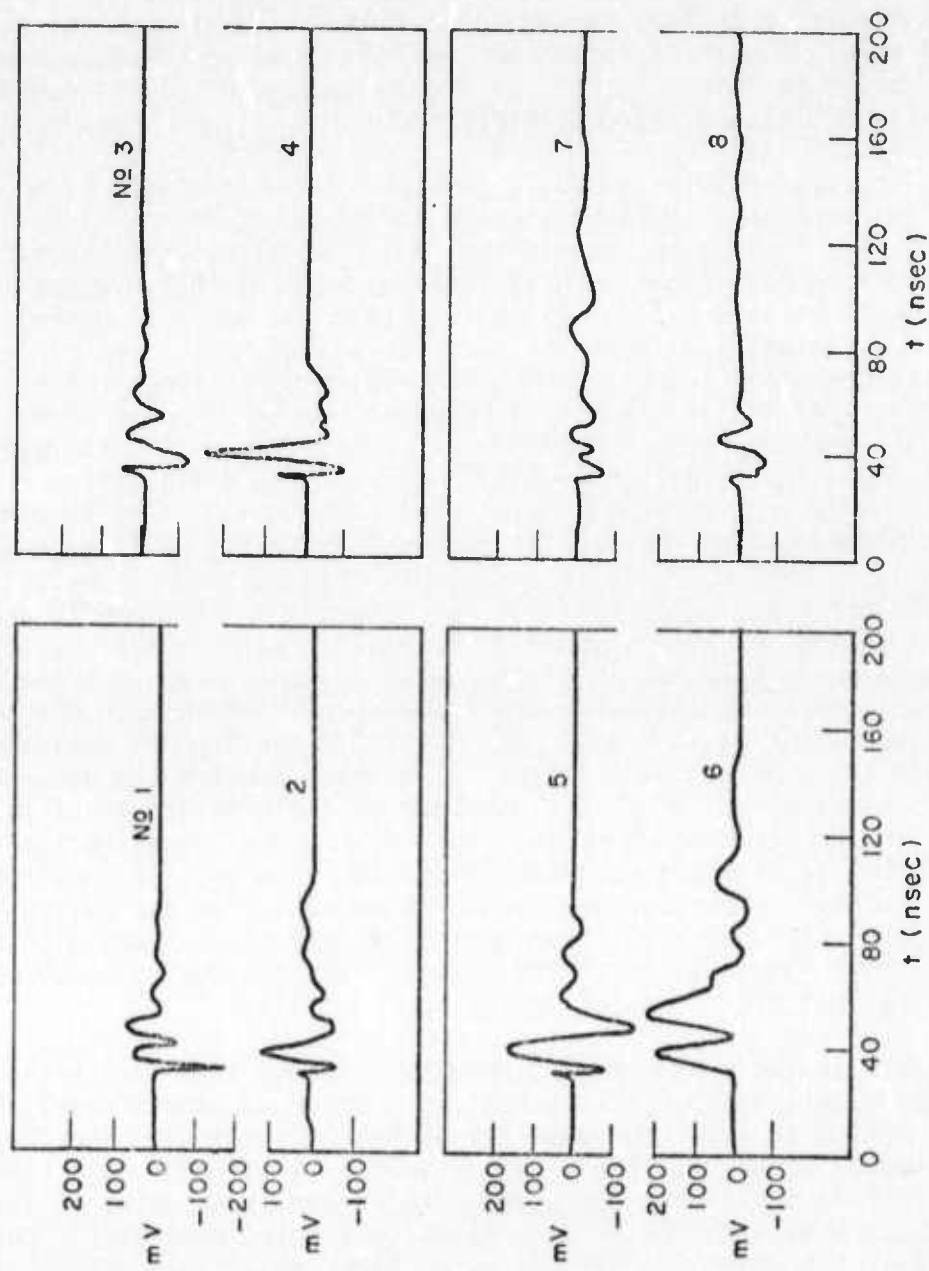


Fig. 25. Fault location measurements in dolomite.  
Small probe and Ikor generator.

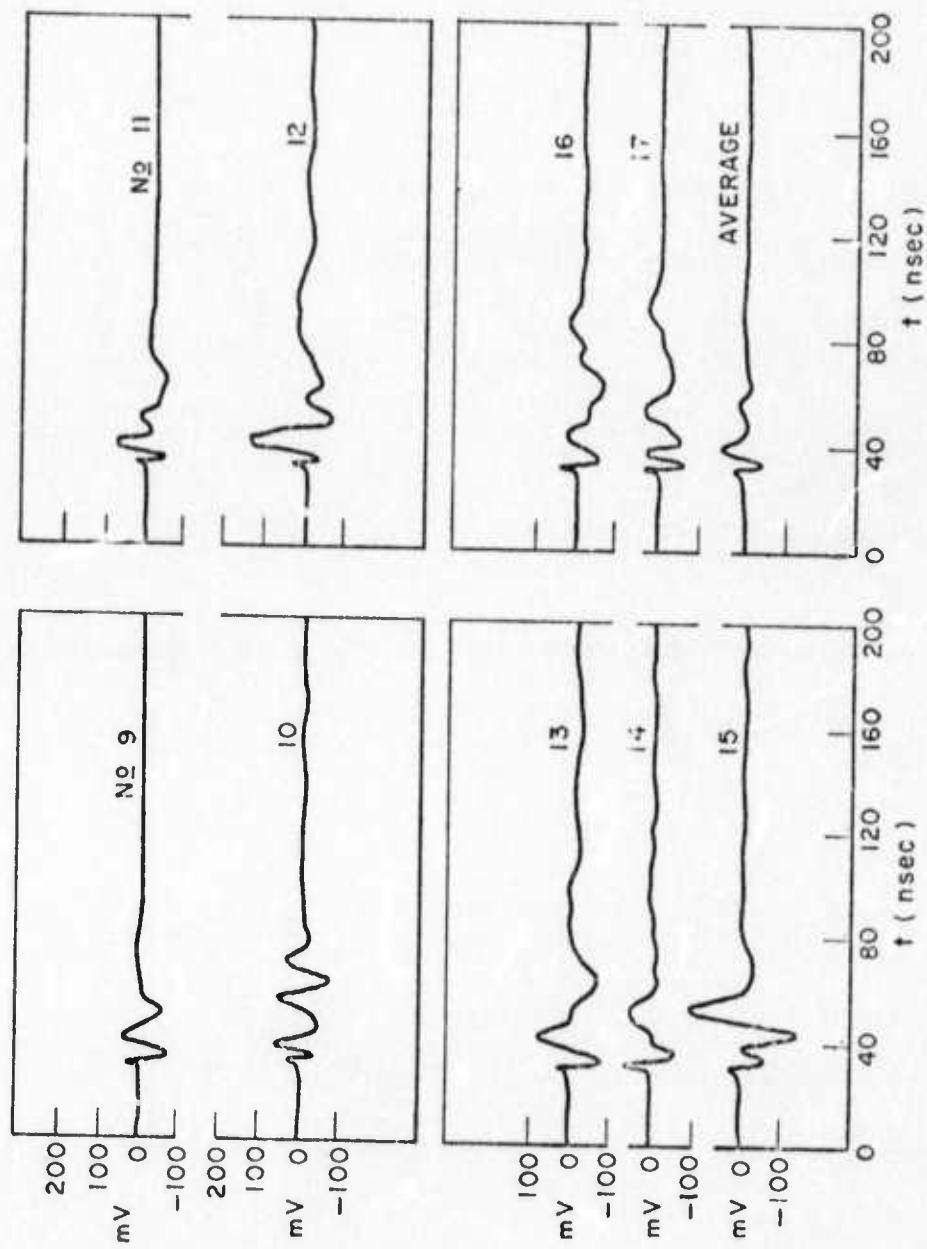


Fig. 25. (Contd)

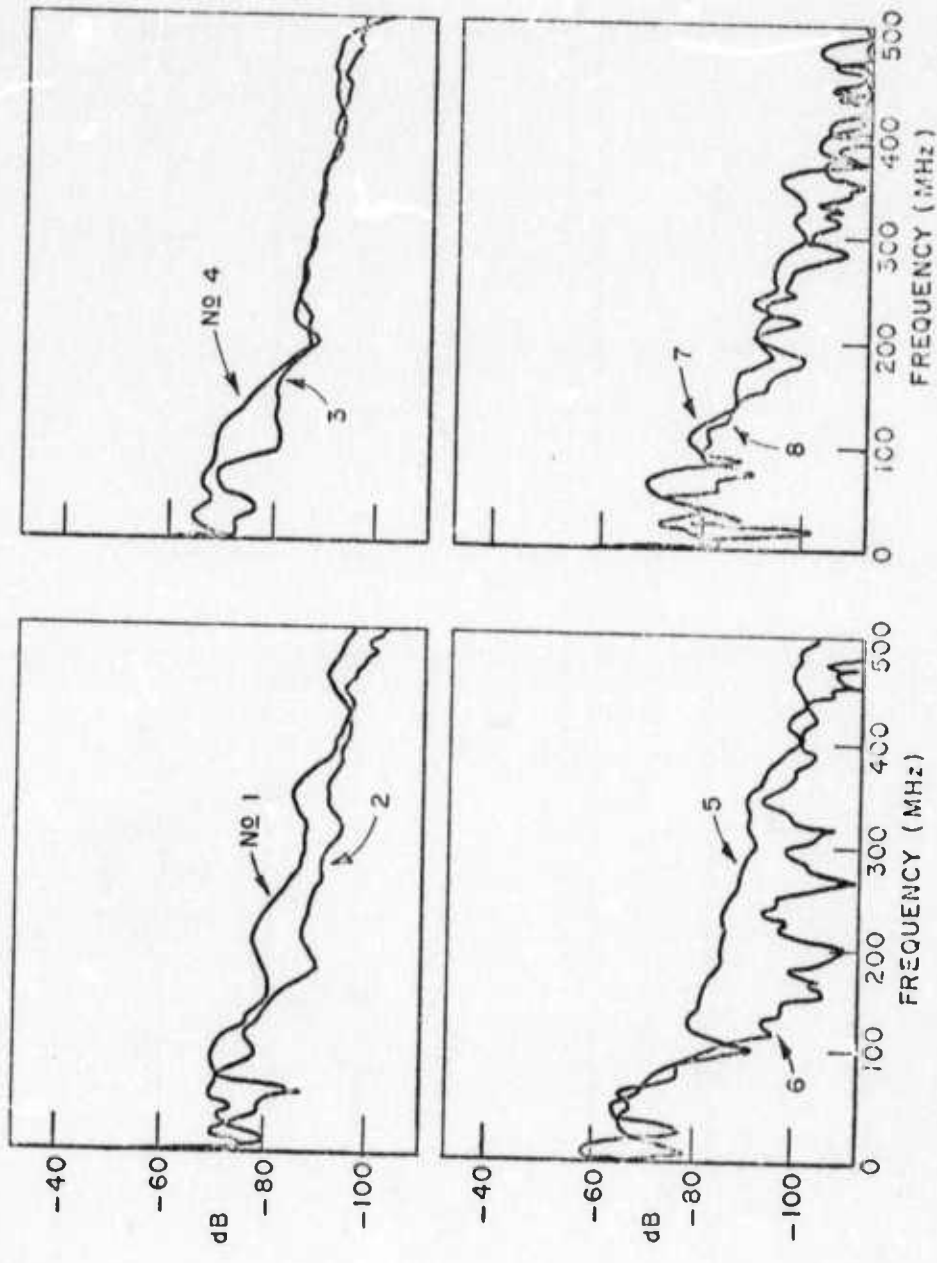


Fig. 26. Fault measurements in dolomite amplitude spectra.

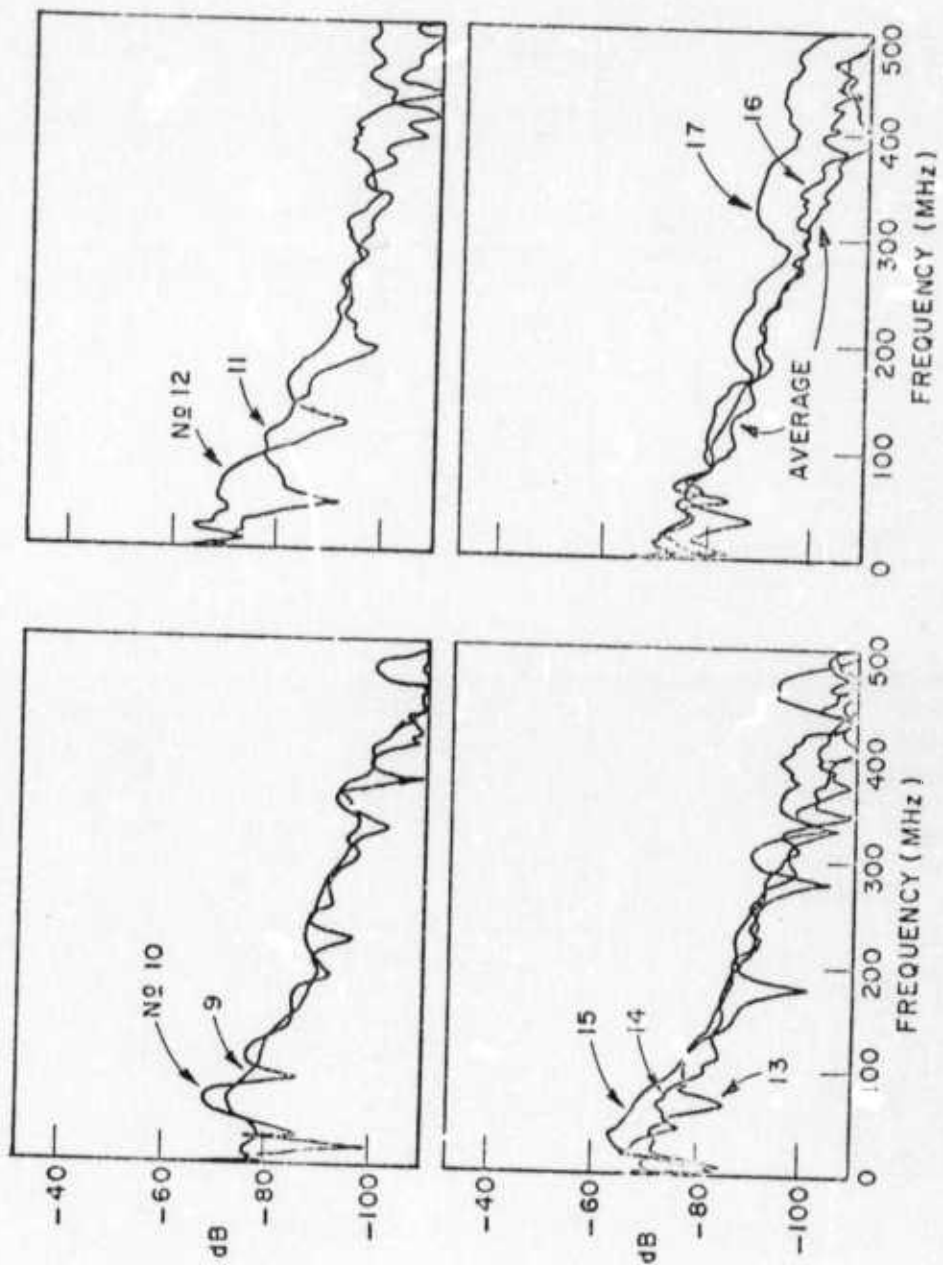


Fig. 26. (Contd.)

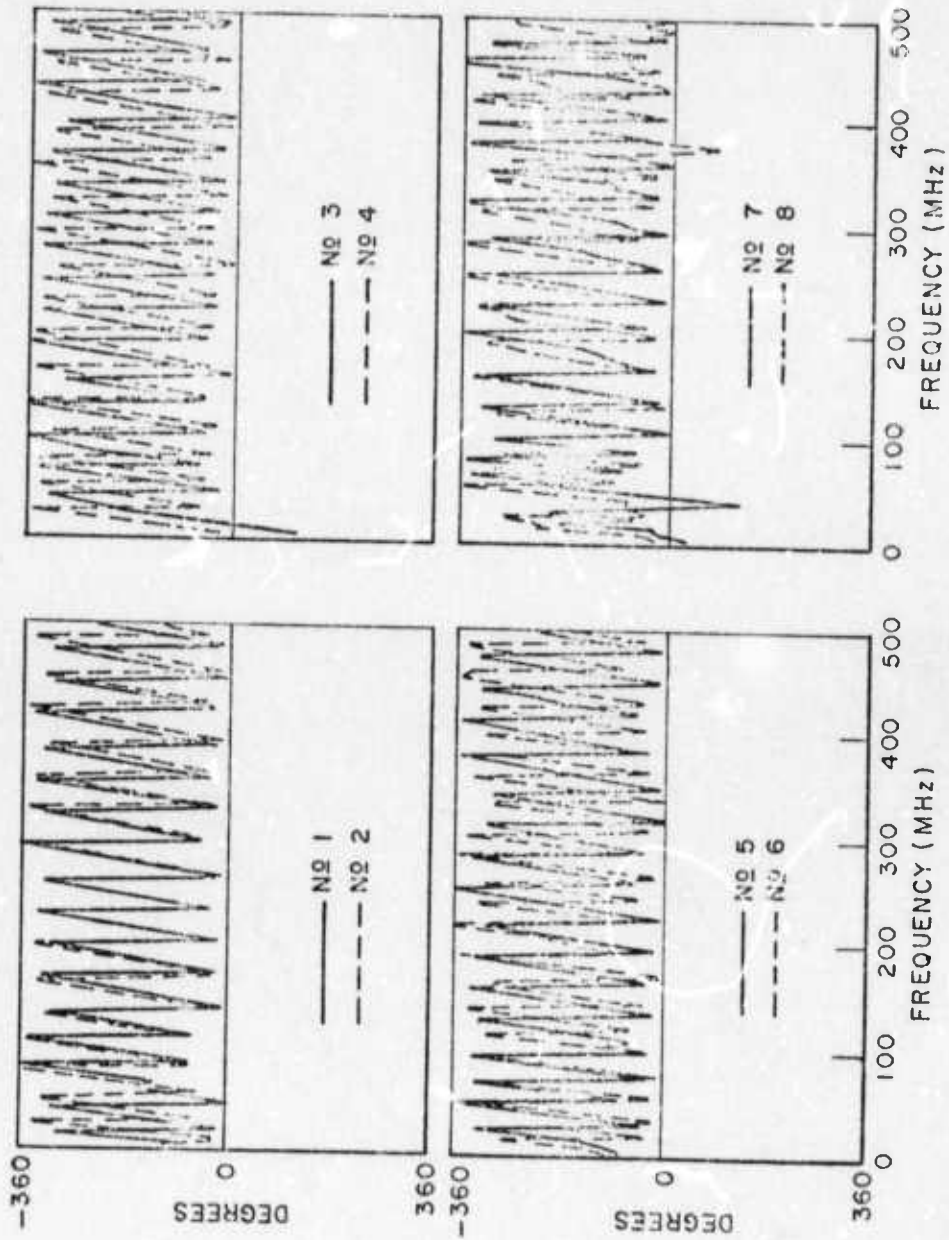


Fig. 27. Fault measurements on dolomite phase spectra.



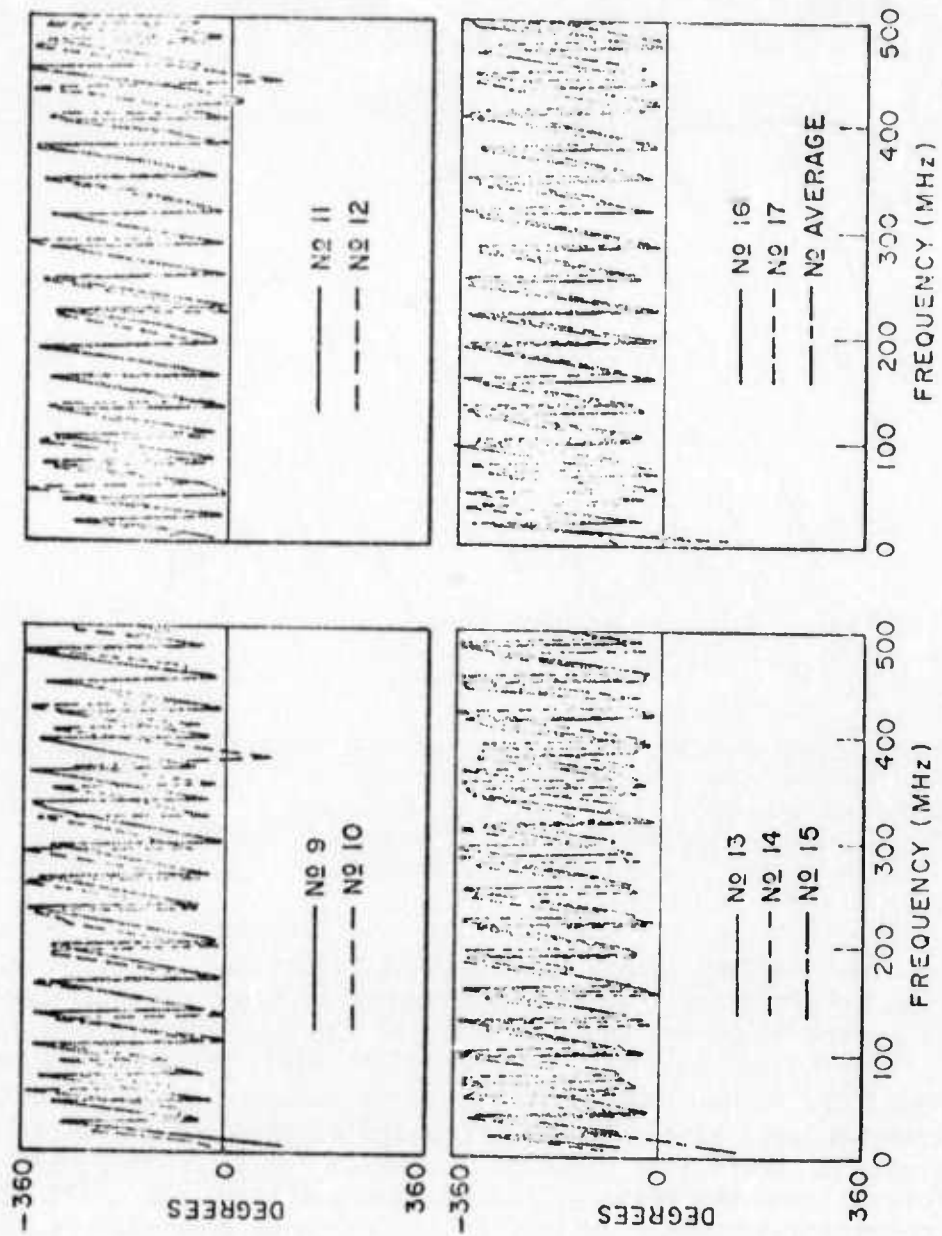


Fig. 27. (Contd)



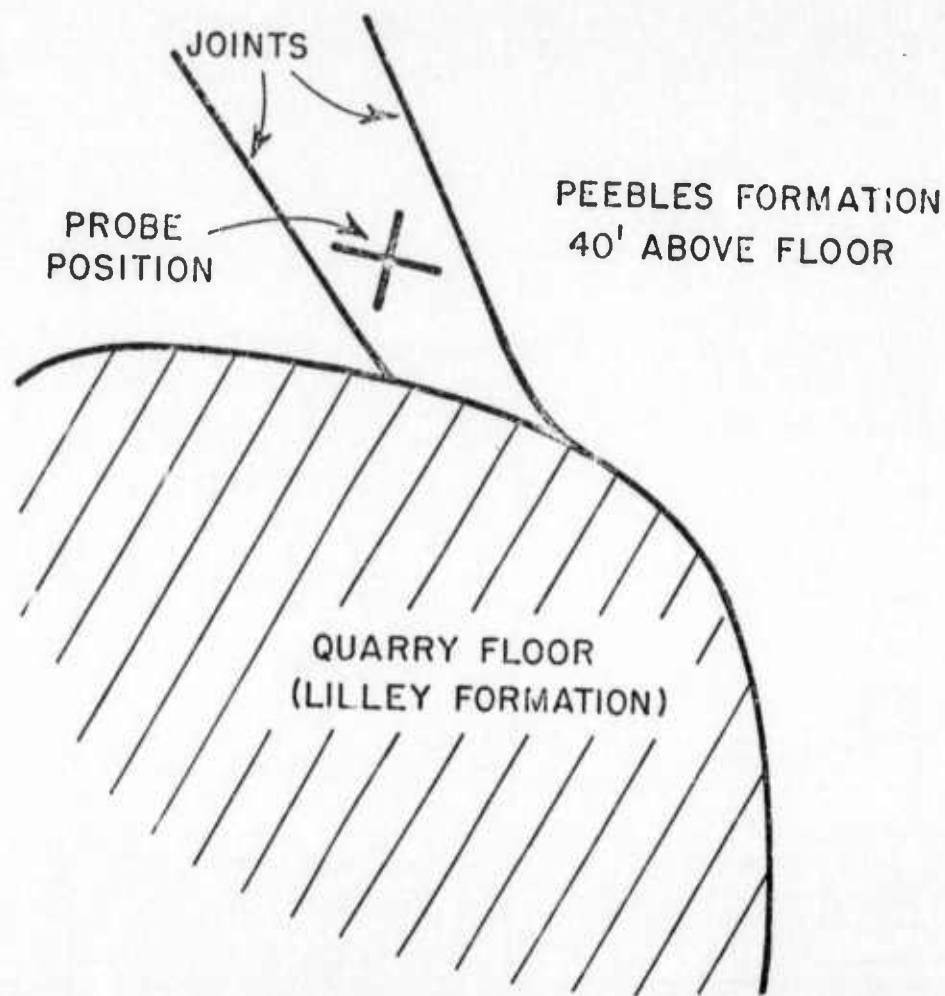
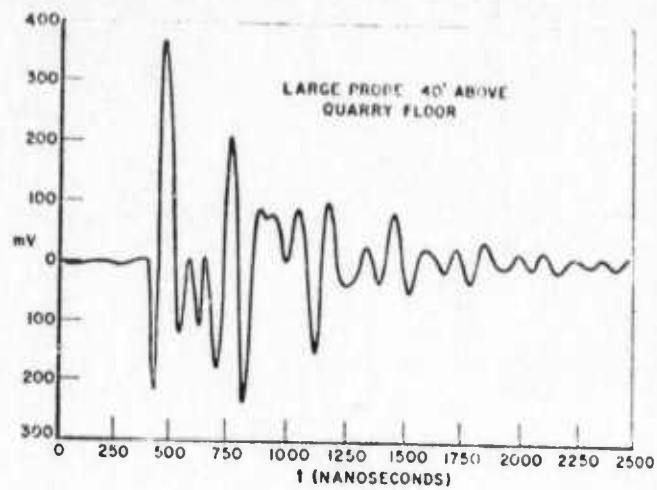
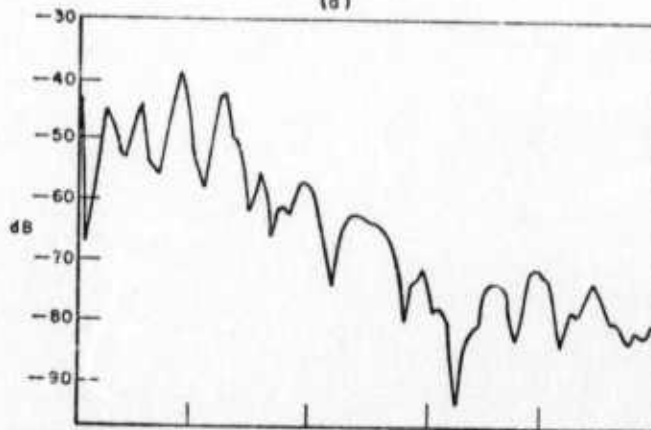


Fig. 29. Geometry of joint and lithologic contrast measurement.

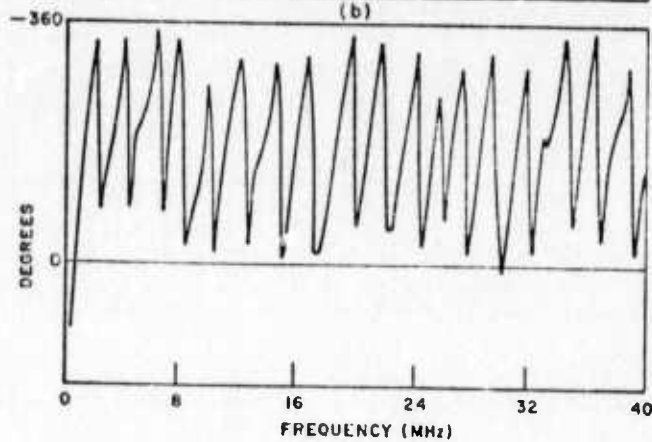
floor. The time and frequency domain waveforms for the probe in this position are shown in Fig. 29. Corresponding waveforms for the probe on the quarry floor are shown in Fig. 30 for comparison. From the measurement of the time delay (refractive index) during the transmission measurements, it was found that the large response at approximately 375 nsec measured from the direct coupled pulse corresponded to the lithologic contrast at a depth of 45 feet. The other responses are reflections from the vertical joints, and possibly, the cliff edge. The strong low-frequency content of the HP pulse generator is responsible for the duration of the ringing. Pulses are apparently being reflected back and forth in the cavity formed by the surface, the contrast, and the joints. The cable lengths were varied and it was established that the ringing shown was not due to reflections within the system.



(a)



(b)



(c)

Fig. 29. Joint and lithologic contrast measurement. Large probe and Hewlett Packard generator.  
 (a) time domain waveform  
 (b) amplitude spectrum  
 (c) phase spectrum

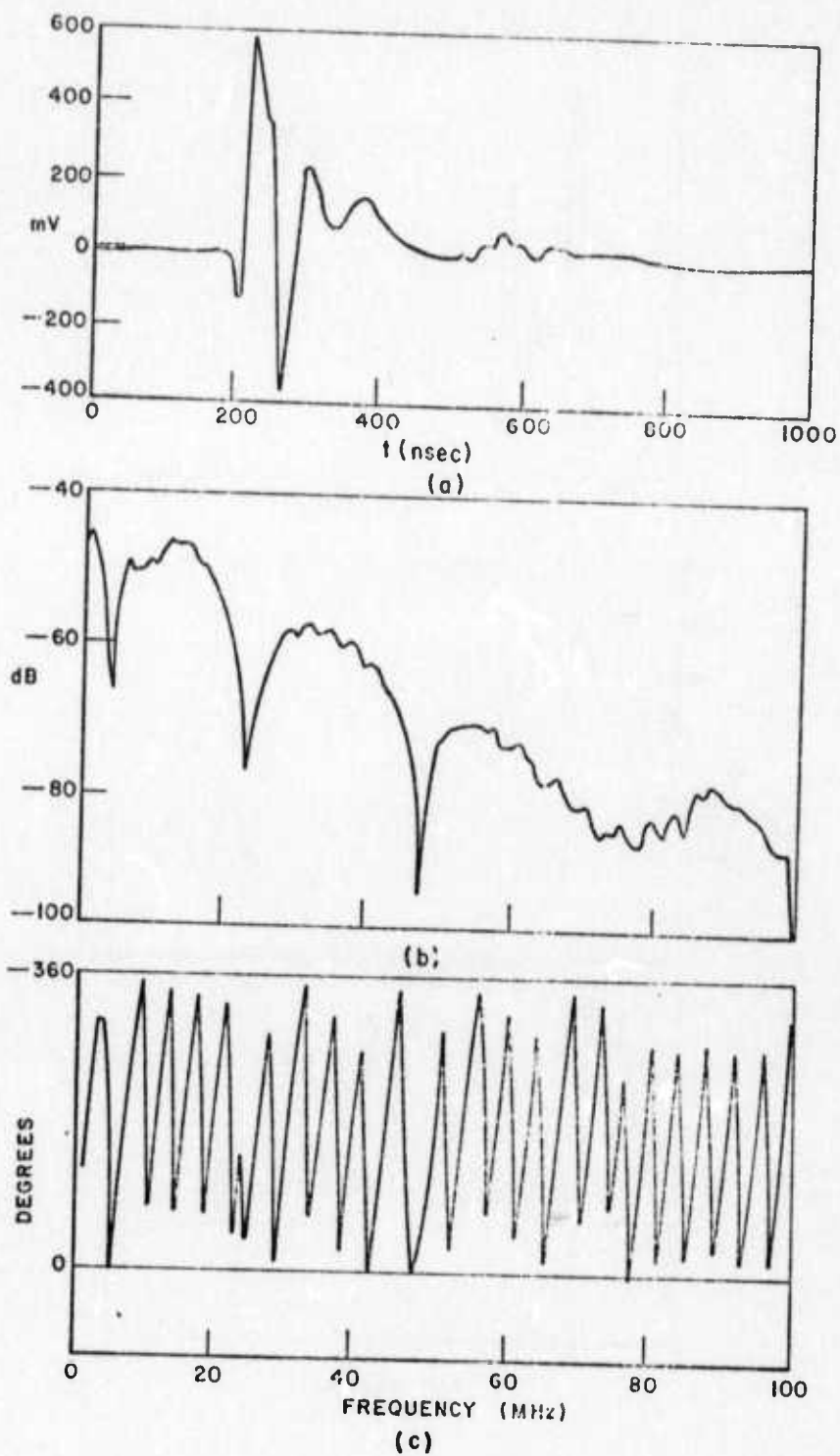


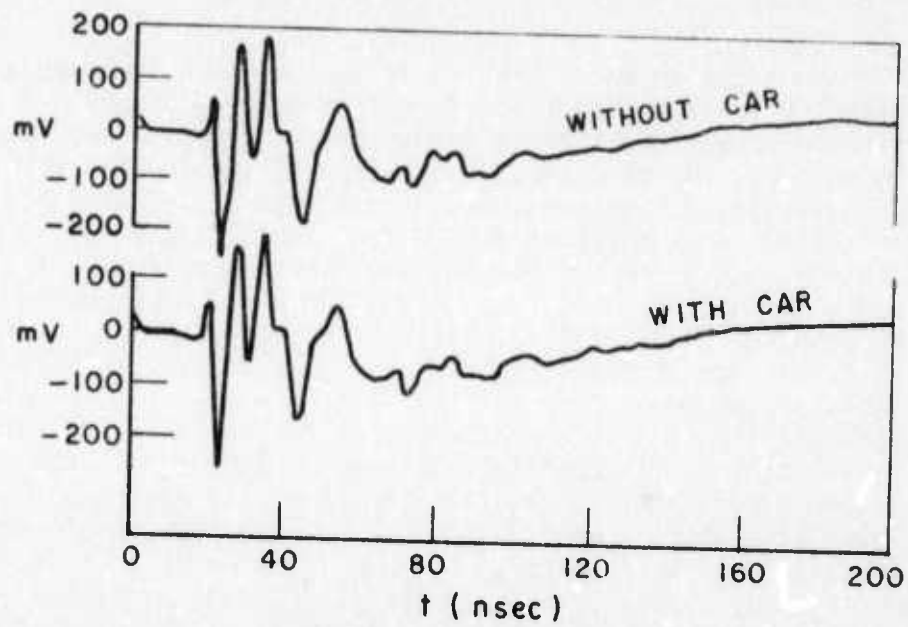
Fig. 30. Orthogonal Mode Measurement on quarry floor.  
 Large probe and Hewlett Packard generator.  
 (a) time domain waveform  
 (b) amplitude spectrum  
 (c) phase spectrum

The contrast shown in Fig. 28 is that between the Peebles formation (cliff) and the Lilley formation (quarry floor). A geological description of these formations is given in Reference [7]. Data to estimate the electrical properties of the Peebles formation (cliff) have not yet been obtained. Note that all of the data shown in this section were obtained during two visits to the quarry of one day duration each. Compare however the direct coupling in Fig. 29 for the cliff and that shown in Fig. 30 for the large probe using the HP generator on the quarry floor. With the large probe and the HP generator, the direct coupling is much less sensitive to minor variations in levelness than the small probe with the Ikor generator. Thus some significance can be attached to the change in direct coupling level - which basically confirms a change in electrical properties. Corings of both formations have been taken by the quarry personnel, but in any laboratory scheme for measuring electrical properties we now have, it would be necessary to shape the samples to existing equipment sizes. The quarry geologist is naturally reluctant to release core samples on this basis. Estimates of the electrical properties will be obtained via propagation measurements during the summer measurement period. There is possibly a second lithologic contrast shown in the quarry floor measurement in Fig. 29. The Lilley formation (quarry floor) changes to a shale type rock at a depth of roughly 40 feet below the quarry floor. The response in Fig. 30 occurring at approximately 350 ns roughly corresponds to this depth. Less confidence is felt in this response since the care taken to rule out internal reflections was not as extensive as those for the cliff measurement. Nevertheless the partial confirmation is distinctly encouraging.

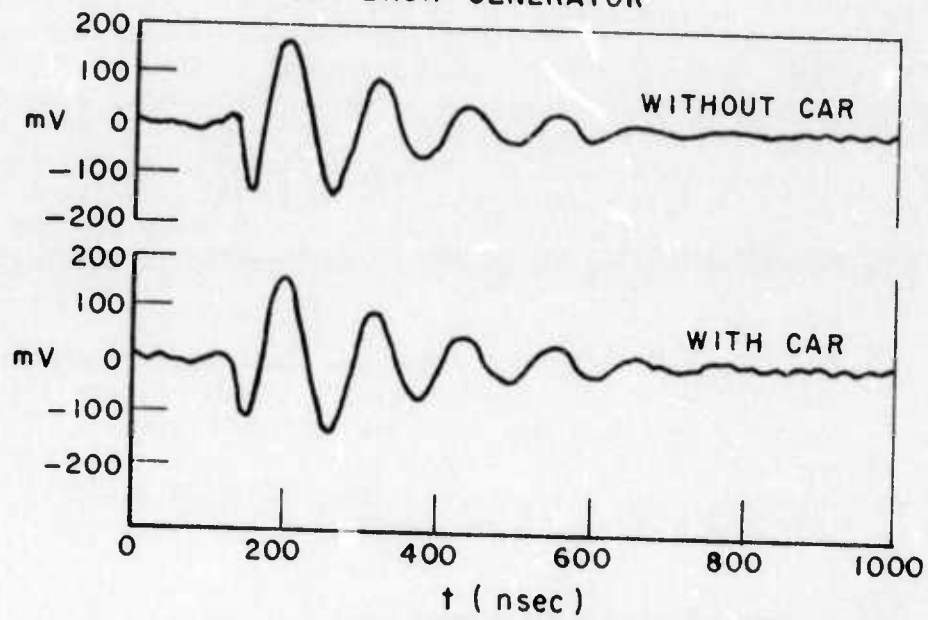
Finally, Fig. 31 shows the orthogonal mode waveforms with and without a car parked in one quadrant of the probe. Figure 31a corresponds to the Ikor pulser and Fig. 31b to the HP pulser. In both cases, there is essentially no change in the recorded waveform, again confirming the fact that the probe is insensitive to scatters on the surface, even when used over a rock medium.

## VII. PULSE PROPAGATION CALCULATIONS

Computer programs have been developed to completely analyze arbitrary wire antennas or arrays of antennas embedded in an infinite homogeneous medium[8]. Typical program output consists of self impedance, mutual impedance, current distribution, near zone fields and far zone patterns. Finite conductivity of the wire and insulating dielectric sleeves can also be taken into account. A piecewise sinusoidal expansion is assumed for the unknown current distribution on the antenna, and Galerkin's method is used to reduce the integral equation to a system of simultaneous linear equations. Although the



(a) IKOR GENERATOR



(b) H.P. GENERATOR

Fig. 31. Orthogonal measurements with and without surface obstacle.  
 (a) Ikor generator  
 (b) Hewlett Packard generator

program normally operates in the frequency domain, speed and accuracy are sufficient to permit a Fourier Transformation to the time domain. There is one program limitation that is determined by the amount of computer storage available. The antenna must be divided into a finite number of segments which is related to the number of terms in the piecewise continuous expansion for the current. In order to obtain sufficient accuracy, the length of each segment should be less than  $\lambda/4$ . At high frequencies, therefore, the number of elements could easily become too large for the computer to accommodate. The current limit of the Datacraft 6024 ElectroScience Laboratory computer is 50 elements. Larger computers such as the IBM 370 could accommodate perhaps 250 segments. The Fourier Transform modification has been added to the main program to allow conversion between the time and frequency domains. A time domain voltage pulse signal is applied to the terminals of the transmit antenna, shown in Fig. 32. This antenna is identical

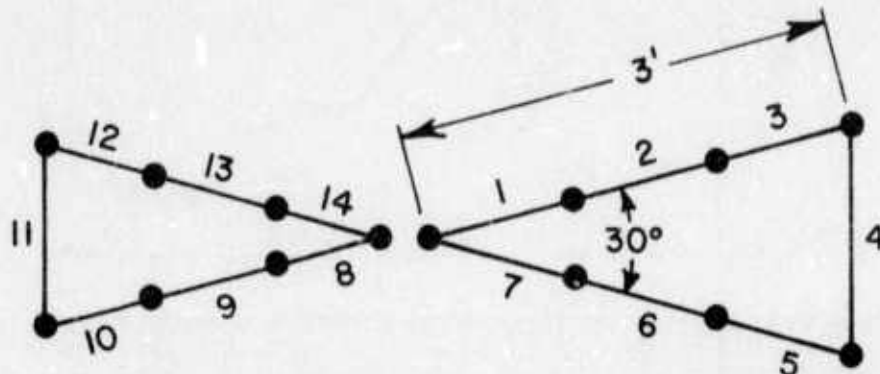


Fig. 32. Antenna structure used for propagation calculations.

to one of the dipoles in Fig. 1c. Note that Fig. 32 shows the antenna divided into 14 segments as needed for the calculation. The radius of the wires is  $3/8$ " and assumed to be perfect conductors. The input pulse is the 50 volt, 45 nsec (HP) pulse (Figs. 33a and 2b) after it has been passed through the cables, baluns, and twin lead. It can be seen from the amplitude spectrum of Fig. 33b that the most significant frequency content of the pulse is below 50 MHz, (above 50 MHz the amplitude spectra is down 40 dB) so the lengths of the segments in Fig. 32b had to be less than  $\lambda = \lambda/4 = c/4f\sqrt{\epsilon_r} = 4.45/\sqrt{\epsilon_r}$  feet, which they are for  $\epsilon_r < 20$ . The input time domain pulse (Fig. 33a) is Fourier transformed and the first 50 harmonics of the resulting complex spectrum (Fig. 33b) are applied to the terminals of the transmitting antenna. An induced voltage is calculated at the terminals of an identical receiving antenna a specified distance away at each of the fifty harmonics. The receiving antenna is terminated on a  $300\Omega$  load to agree with the  $300\Omega$  twin lead used in the pulse sounding system. This spectrum of received voltages is then inverse Fourier transformed to obtain the

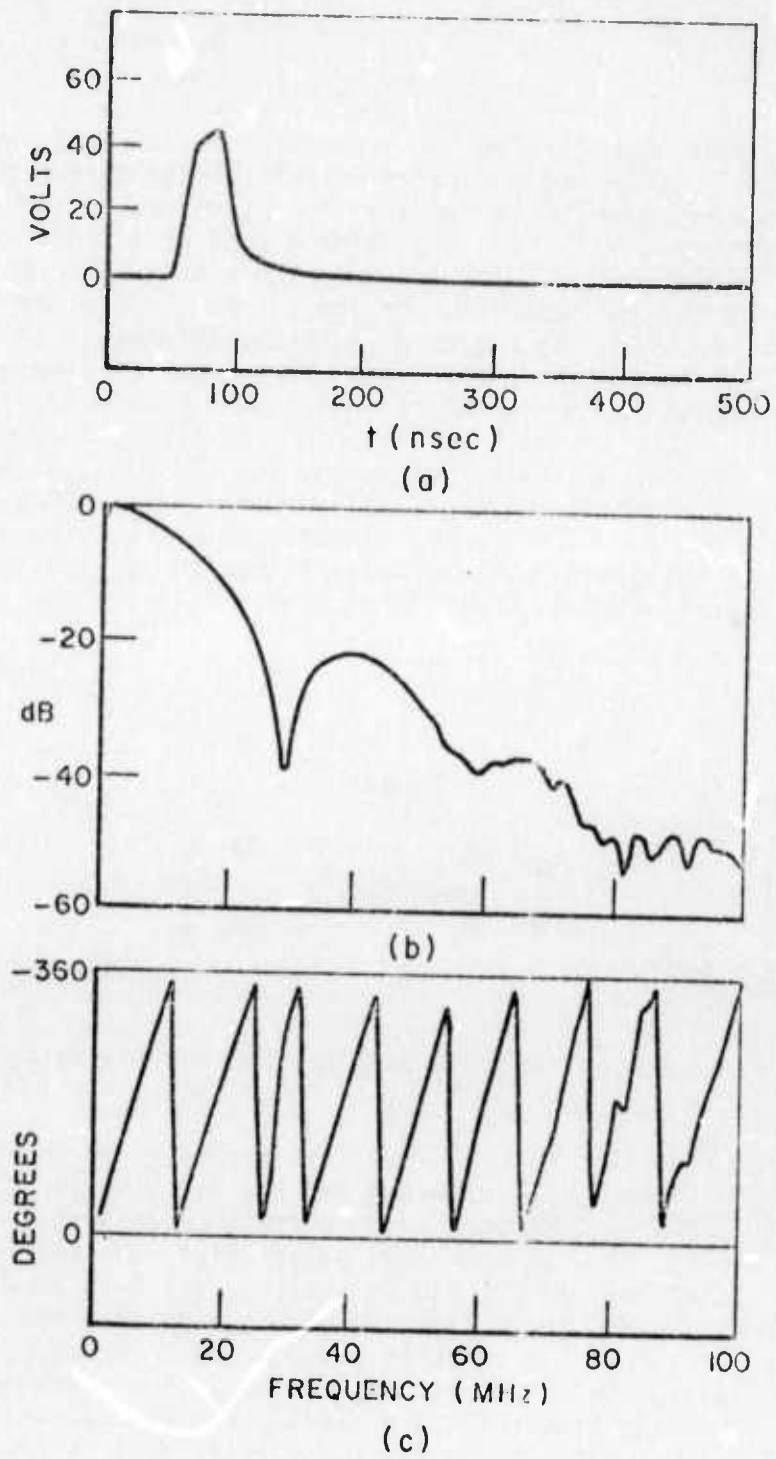


Fig. 33. Input pulse for propagation calculations.  
 (a) time domain waveform  
 (b) amplitude spectrum  
 (c) phase spectrum

received time domain waveform. These calculations have only been carried out with the 50 volt, 45 nsec, HP pulse, because the high frequency content of the 1000 volt, 250 psec pulse results in such a large number of segments that the present computer system cannot accommodate the program. The size of the large antenna with the aluminum sheets also presents a similar problem.

Figure 34 shows the effect of increasing conductivity on the transmitted pulse for a relative dielectric constant ( $\epsilon_r$ ) of 10 and a separation distance of 20 feet. As the conductivity is varied from  $\sigma = .001$  mho per meter to  $\sigma = .01$  mho per meter, the attenuation for plane wave propagation increases according to the relation

$$\alpha = \frac{\omega \sqrt{\mu_0 \epsilon_0 \epsilon_r}}{2} \left[ \sqrt{1 + \frac{\sigma^2}{\omega^2 \epsilon_0^2 \epsilon_r^2}} - 1 \right]^{1/2}$$

from .03774 to .16953. In dB per meter, this corresponds to roughly .3 dB/m and 1.5 dB/m. The changes in attenuation can best be seen by comparing the amplitude spectra of Fig. 34b. Note that for very low frequencies ( $< 2$  MHz), the received voltage increases with increasing conductivity, but for high frequencies, the received voltage decreases with increasing conductivity. Note also from the phase spectra of Fig. 34c, that the phase which is rotating in a counter clockwise direction, is further delayed by increasing conductivity. The upper waveform, calculated with  $\sigma = .001$  mho/m, is approaching the type of waveform expected for a hard rock medium. Typical values for the conductivity of a hard rock such as granite are less than .001 mho/m, so the magnitude of the transmitted pulse can be expected to increase. The ringing associated with the waveforms for low values of conductivity can be decreased by adjusting the load impedance of the receiving antenna.

Figure 35 demonstrates the effect of the relative dielectric constant,  $\epsilon_r$ , on the transmitted pulse. An increase in the value of the relative dielectric constant ( $\epsilon_r$ ) results in an increase in magnitude of the received waveform. Since the characteristic impedance  $\sqrt{\mu_0/\epsilon_0 \epsilon_r}$  is decreased by an increase in  $\epsilon_r$ , an increase in the magnitude of the received voltage is to be expected. Note that the start of the waveform for  $\epsilon_r = 20$  is delayed 30 nsec from the start of the  $\epsilon_r = 10$  waveform. The computer program is also accurately predicting the delay time of the transmitted signal,  $\tau = d\sqrt{\mu_0 \epsilon_r} = d\sqrt{\epsilon_r}/c$ , which obviously increases with increasing  $\epsilon_r$ . Figure 35b displays the effect of  $\epsilon_r$  on the amplitude spectra of the transmitted signals, and Fig. 35c shows the phase spectra. Note that the amplitude of the received voltage for  $\epsilon_r = 20$  is lower at high frequencies ( $> 50$  MHz) than the  $\epsilon_r = 10$  case. The phase is also delayed by increasing  $\epsilon_r$ .

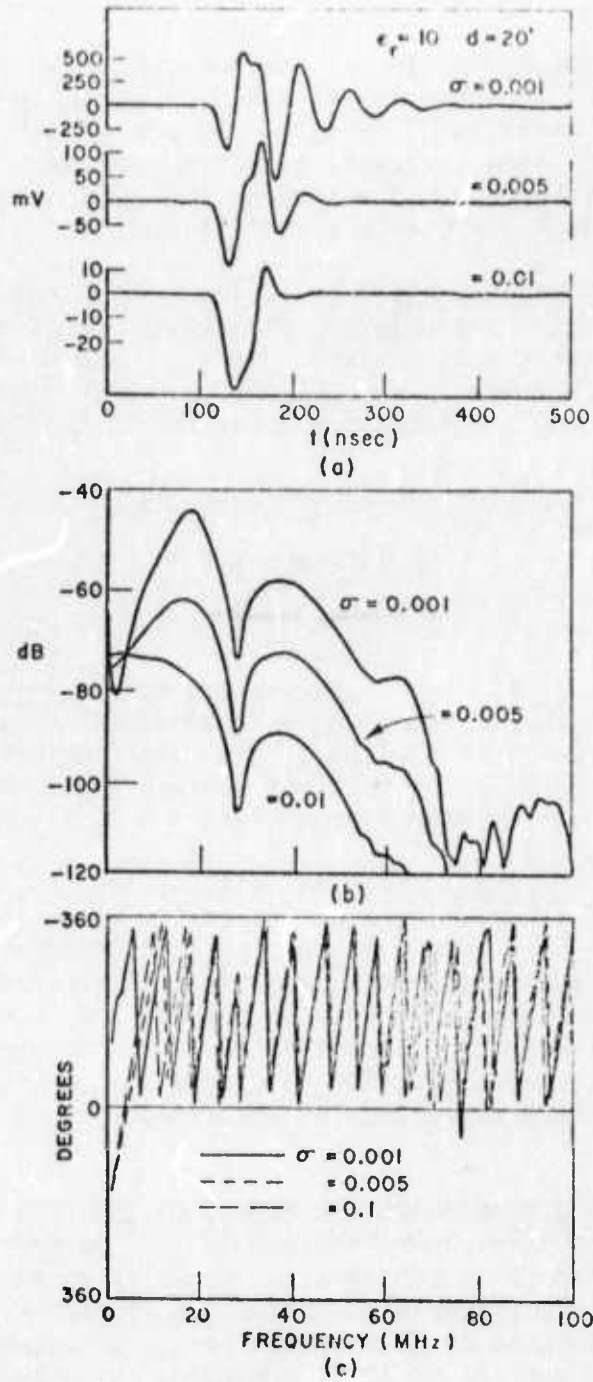
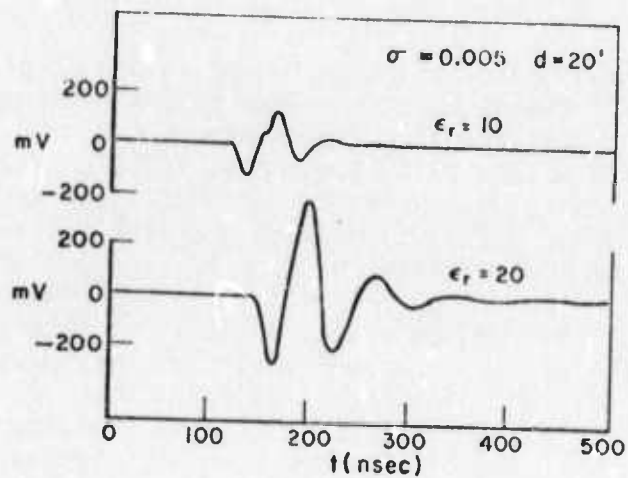
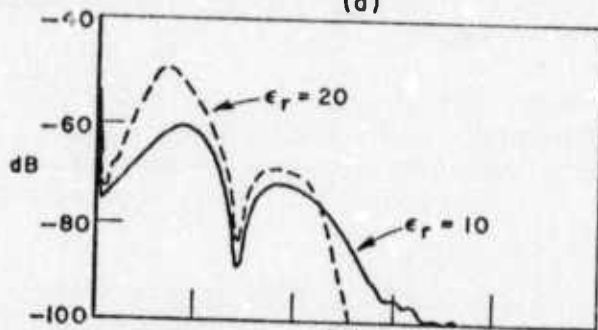


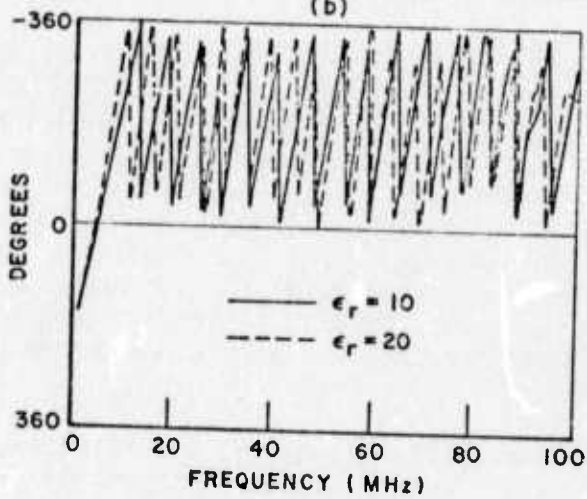
Fig. 34. Effect of conductivity on pulse propagation.  
 (a) time domain waveforms  
 (b) amplitude spectra  
 (c) phase spectra



(a)



(b)



(c)

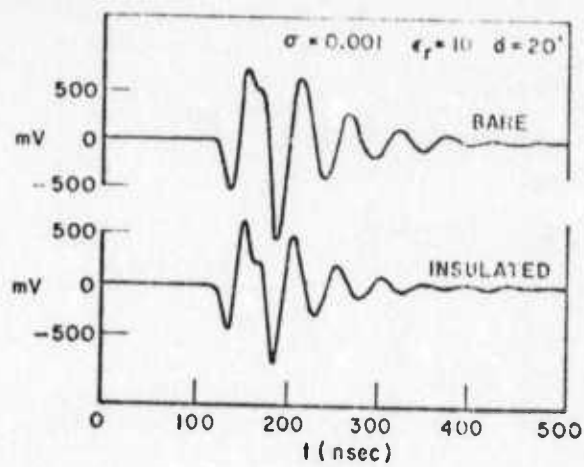
Fig. 35. Effect of dielectric constant on pulse propagation.  
 (a) time domain waveforms  
 (b) amplitude spectra  
 (c) phase spectra

The previous calculations were completed assuming a bare wire antenna, which is really not the case when the antenna is resting on the absorber. The effect of an insulating dielectric sleeve on the antenna of  $\epsilon_r = 1.0$ , and 1/16" thickness, is illustrated in Figs. 36 and 37. Figure 36 shows the transmitted pulse and spectra for  $\epsilon_r = 10$ ,  $\sigma = .001$  mho/m and  $d = 20$  feet without and with insulation, and Fig. 37 shows the measurements for  $\epsilon_r = 10$ ,  $\sigma = .01$  mho/m and  $d = 20$  feet, without and with insulation, respectively. Note the differences between the insulated and uninsulated cases for each conductivity, and compare the differences. Obviously, for low loss media, the effect of the insulation will not be as great as for a high loss medium. Figures 36 and 37 confirm this reasoning. It can be seen from the  $\sigma = .01$  case (Fig. 37b) that the coupling between the bare wire antennas is stronger at low frequencies while the coupling for the insulated antennas is stronger at higher frequencies.

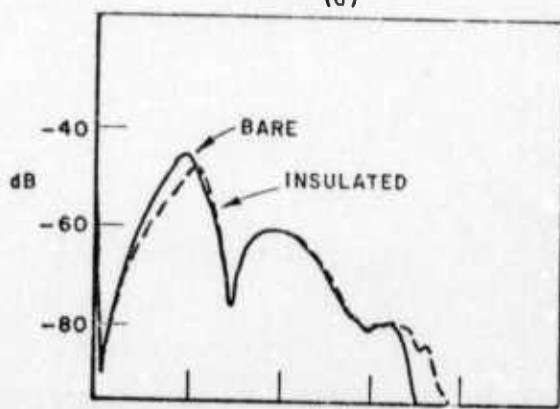
Figure 38 shows that for constant values of  $\epsilon_r$  and  $\sigma$ , the pulse shape does not change by increasing the path length. Only the magnitude of the waveform and amplitude spectrum is decreased. There is also a phase delay in the phase spectrum, which corresponds to a time delay in the time waveform.

Another important factor in determining the received waveform is the load impedance of the receiving antenna. To illustrate the dependence, Fig. 39 compares the differences between pulses transmitted on the same antennas in the same medium with load impedances of  $50\Omega$  and  $300\Omega$ . All previous waveforms were calculated with a  $300\Omega$  load to roughly correspond to the  $300\Omega$  twin lead of the measurement system. The impedance of the twin lead is really lower than  $300\Omega$  when it is lying on the interface between free space and the ground, but the actual value of the impedance changes with both frequency and the parameters of the medium. The ideal value of load impedance would naturally be a value that matches the impedance of the antenna. Note from Fig. 39 that a change in a purely resistive load only affects the magnitude of the received waveform and the amplitude spectrum. The phase spectrum remains the same.

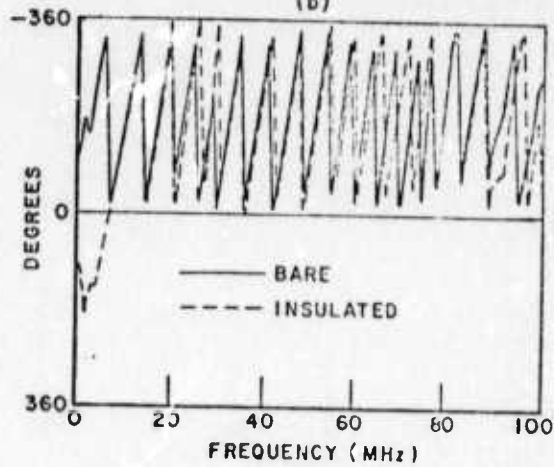
The relative dielectric constant and conductivity of a sub-surface medium are not constants but functions of frequency. The relative dielectric constant follows a general decreasing trend with increasing frequency, while the conductivity tends to increase with increasing frequency. Just what changes occur in the values is primarily determined by the moisture content of the medium. Figure 40 demonstrates the case of pulse transmission over two path lengths in a dispersive medium. The relative dielectric constant and conductivity were varied linearly over the 2 to 40 MHz range from 20 to 10 and .005 to .015 mho/m, respectively, and then held constant at  $\epsilon_r = 10$  and  $\sigma = .015$  from 40 MHz to 100 MHz. While this may not be a



(a)



(b)



(c)

Fig. 36. Effect of antenna insulation - low loss case.  
 (a) time domain waveforms  
 (b) amplitude spectra  
 (c) phase spectra

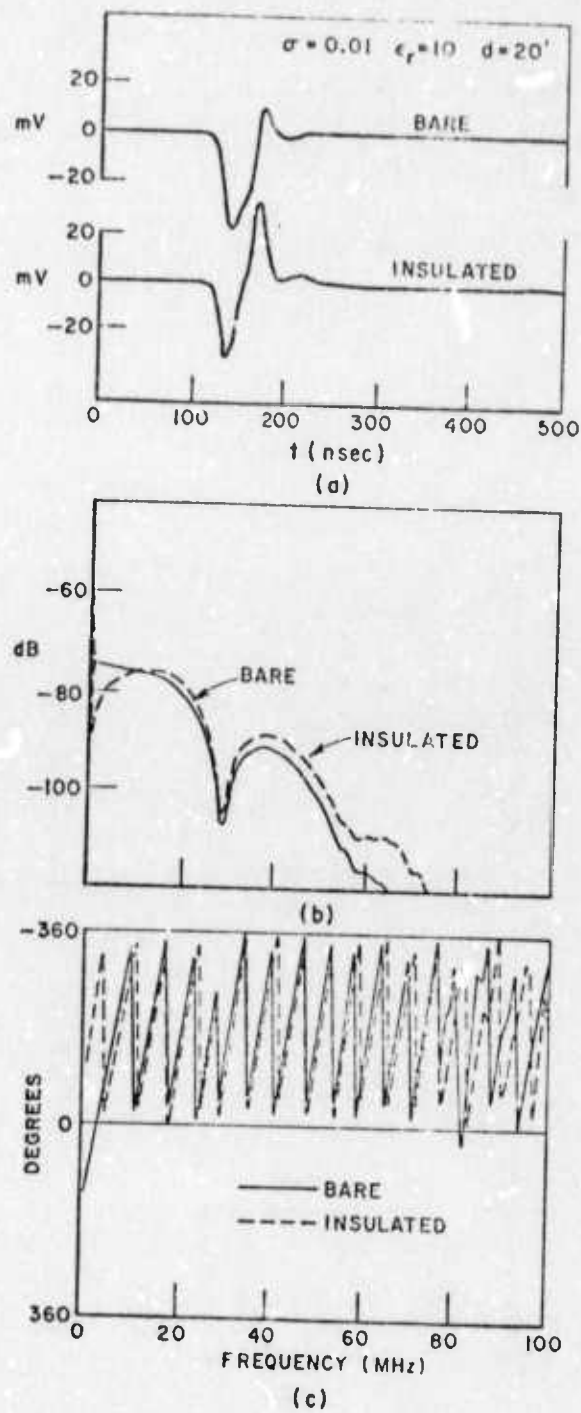


Fig. 37. Effect of antenna insulation - high loss case.  
 (a) time domain waveforms  
 (b) amplitude spectra  
 (c) phase spectra

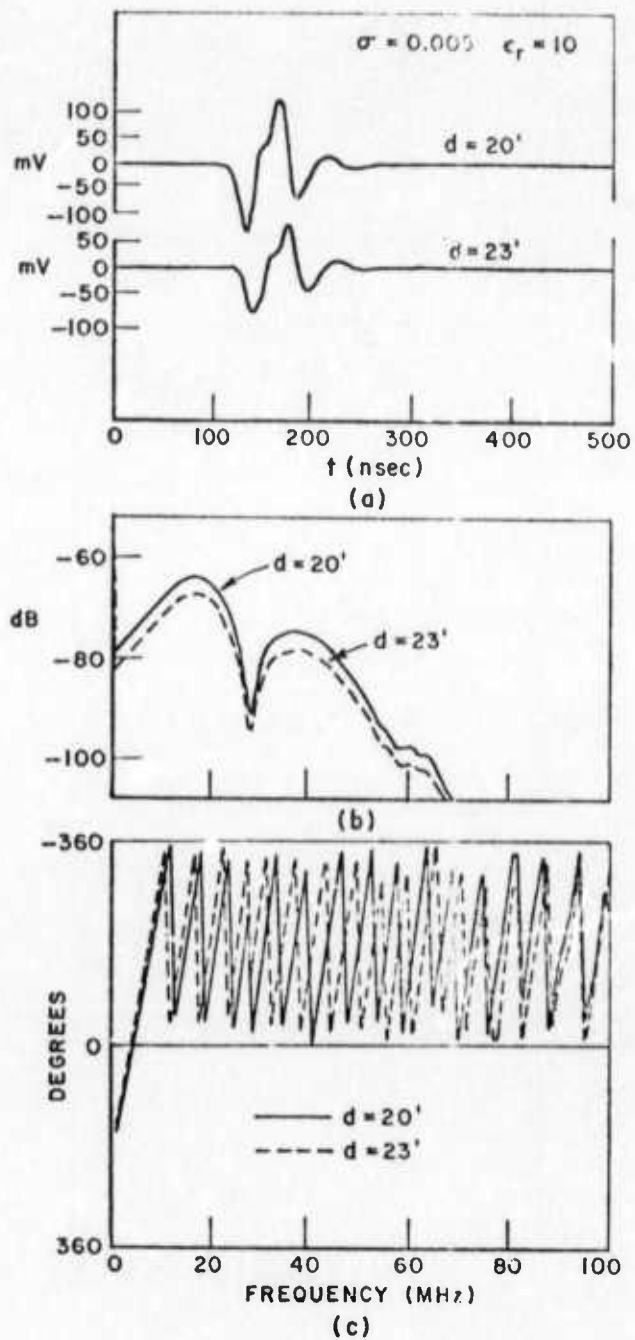


Fig. 38. Pulse propagation over two distances.  
 (a) time domain waveforms  
 (b) amplitude spectra  
 (c) phase spectra

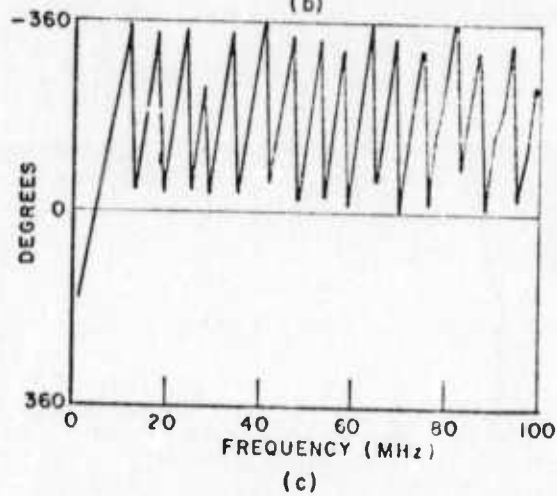
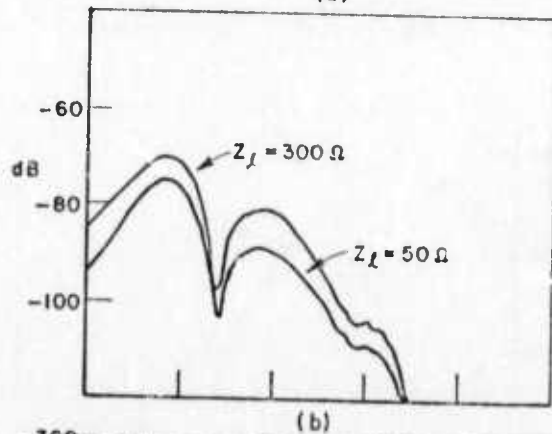
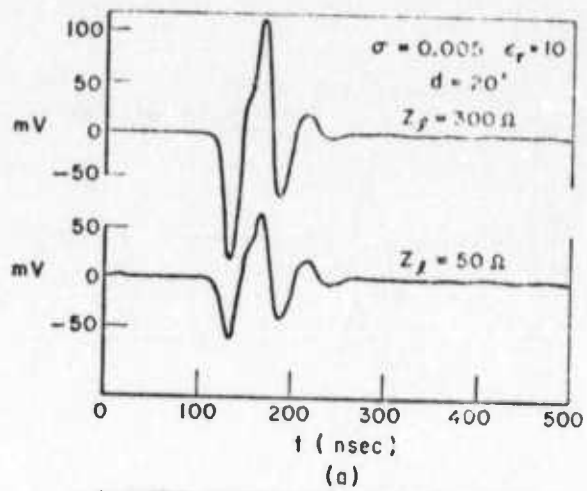


Fig. 39. Effect of receiving antenna load impedance.  
 (a) time domain waveforms  
 (b) amplitude spectra  
 (c) phase spectra

realistic frequency dependence, it is helpful simply to demonstrate the effects of dispersive constitutive parameters. From Fig. 40 it is evident that the base width of the time domain signals is greater than the base width of the constant parameter signals (Figs. 34-39). This spreading effect is one of the primary effects of dispersion. Note also that the waveform for the 25 foot path appears to be spread more than the 20 foot path waveform. The fact that the increased conductivity at higher frequencies causes an increase in attenuation of the higher frequencies accounts for the spreading effect.

Figure 41 compares a calculated waveform using parameters that were obtained from the propagation measurements through limestone to a measured pulse transmitted through 20 feet of limestone. Constant values of  $\epsilon_r = 10$  and  $\sigma = .005$  mho/m, which roughly corresponded to the data of Fig. 14, were used to obtain the calculated waveform. When compared to the measured transmitted pulse through 20 feet of limestone, which was recorded using the large dipole as transmitter and the small dipole as receiver, it is seen that the agreement is quite good. This data indicates that for transmission and reception directly below the antenna, the interface has little effect. Wait[9] has shown for an infinitesimal horizontal dipole source located on the interface that the horizontal component of the field directly below the dipole is essentially unchanged by the addition of the interface. For observation points not on the vertical axis centered on the dipole, however, the interface does significantly alter the fields.

As an additional test of the accuracy of the propagation methods (Section V) of determining  $\epsilon_r$  and  $\sigma$ , the method (Eq. (1)) was applied to the calculated waveforms of Fig. 38. The actual values of  $\epsilon_r$  and  $\sigma$  were 10 and .005 mho/m respectively. Fig. 42 shows the results. Above 15 MHz the values obtained for the dielectric constant are fairly accurate, but the conductivity is slightly inaccurate. For frequencies below 15 MHz, the conducting term of  $k^2 = \omega^2\mu\epsilon - j\omega\mu\sigma$  begins to dominate and causes the error in  $\epsilon_r$ . As the conductivity is increased, the inaccuracy of  $\epsilon_r$  spreads to frequencies slightly higher than 15 MHz, but the values of conductivity becomes more accurate.

## VIII. PROBE CALIBRATION

In an earlier section of this report (Section VII) the attenuation and dispersion effects of realistic rock media on the propagation of video pulse signals were demonstrated. Calculations were made using state-of-the-art analysis and computer programs for the complete analysis of arbitrary wire antennas in an arbitrary lossy medium. Programs were developed by Professor J.H. Richmond with principal support from another sponsor. A report detailing the analysis and computer programs is in preparation[8]. Note that this report is for the principal sponsor, and will not be distributed on this program. It will, of course,

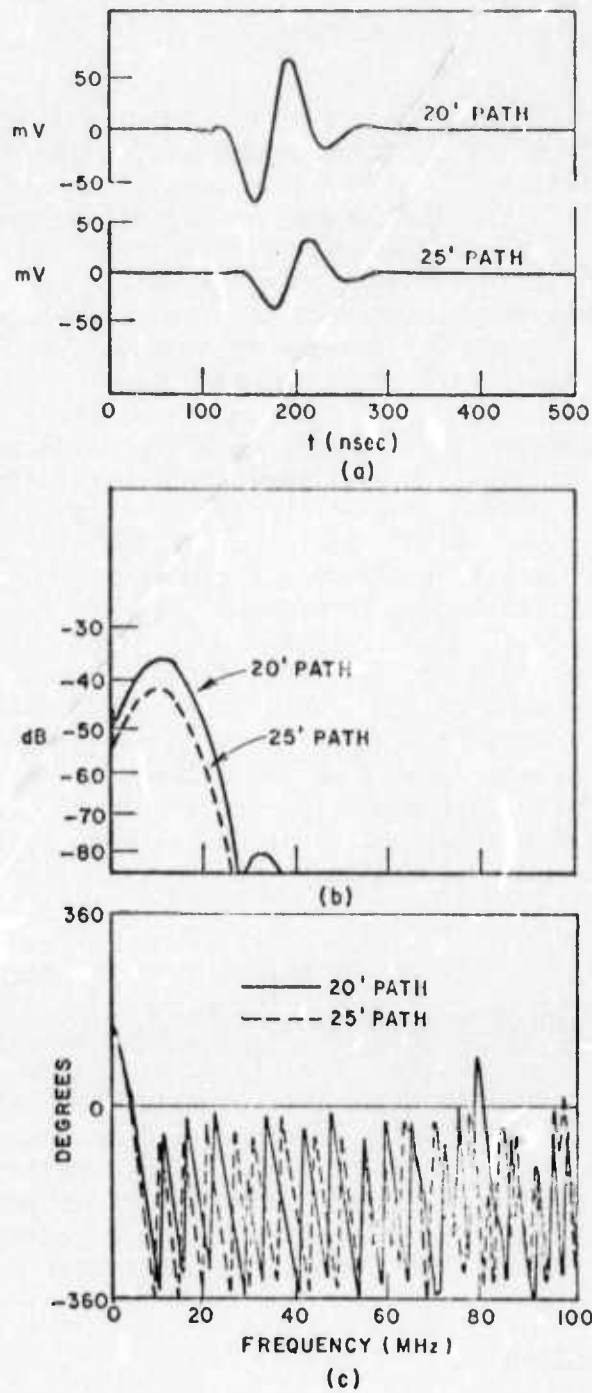


Fig. 40. Effect of dispersion on pulse propagation.  
 (a) time domain waveforms  
 (b) amplitude spectra  
 (c) phase spectra

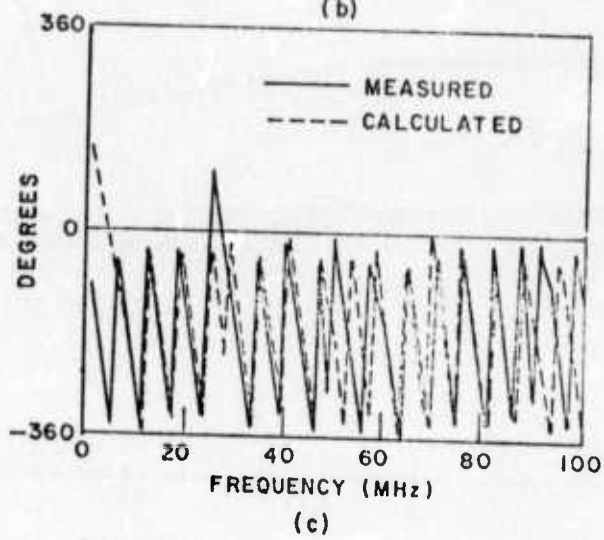
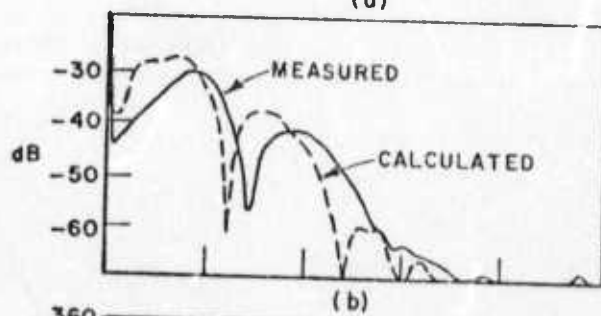
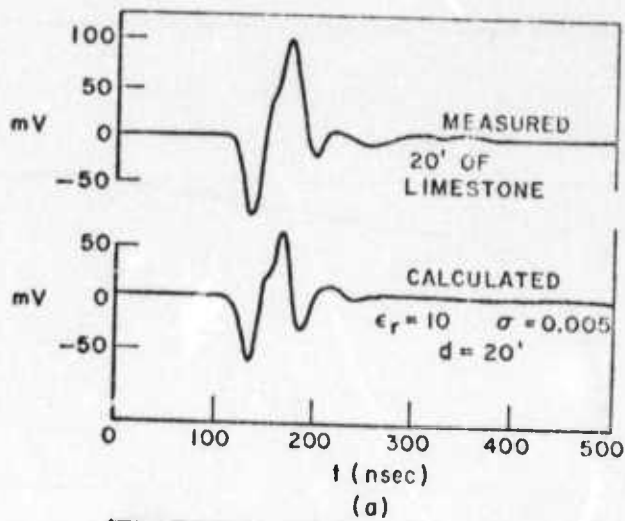


Fig. 41. Comparison of measured and calculated waveforms.

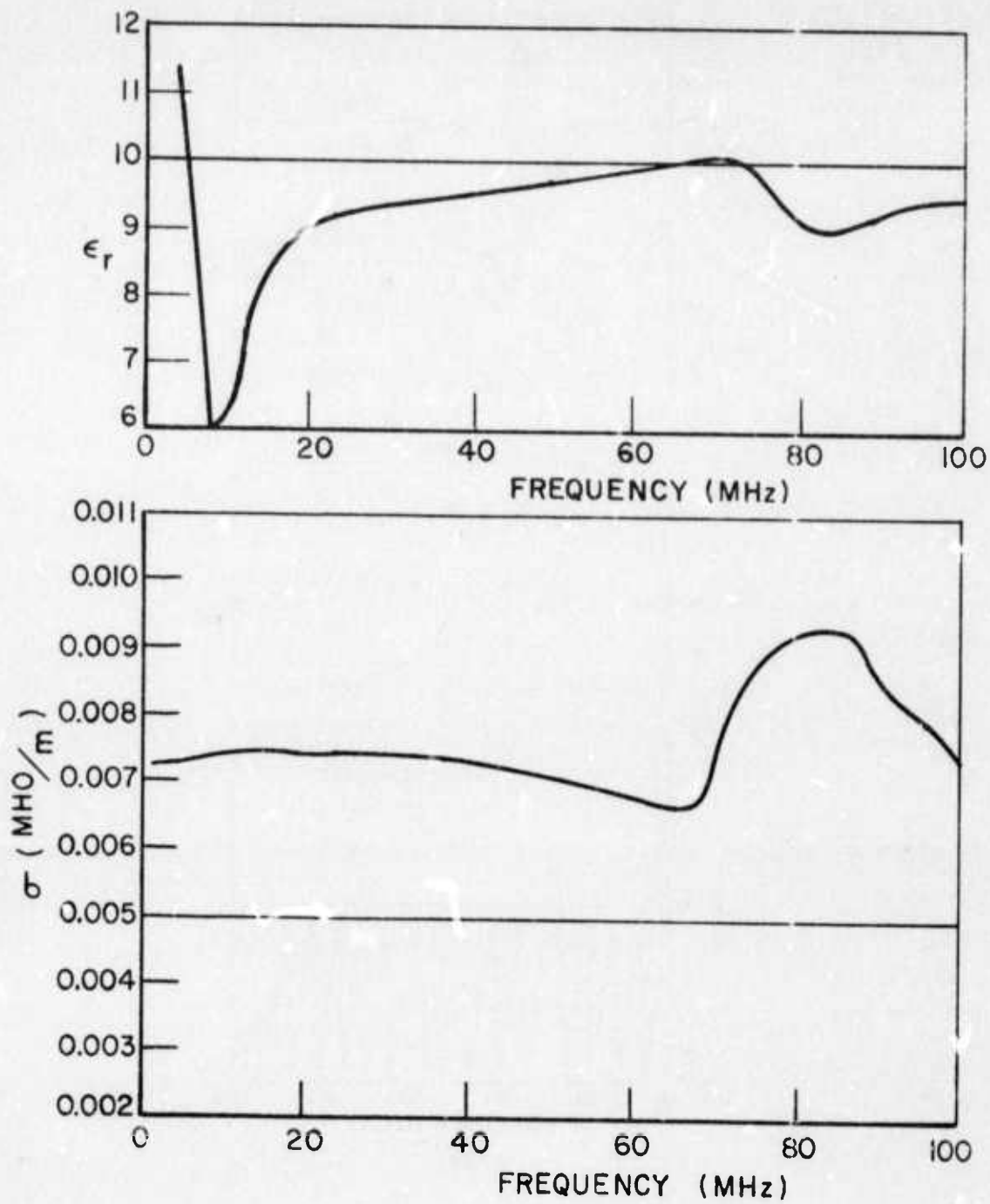


Fig. 42. Relative dielectric constant and conductivity derived from calculated waveforms.

be available from the National Technical Information Service. The programs have been made available for our use, and have provided computational advantages[1,2]. To complete a theoretical analysis capability for the pulse sounding probe, a correction of the programs to account for an air-rock interface is required. This correction, as will be seen, is neither obvious nor simple.

Consider first what is meant by probe calibration. Basically this means that the transfer function of the dipole antenna on the surface of the medium is known. Given this transfer function one can then calculate the spectral content of the signal actually incident on the subsurface target, assuming a homogeneous medium. Note that this last step requires a knowledge of the frequency-dependent constitutive parameters of the medium. Knowing the two-way effects of the antennas and the medium, the response waveform spectrum of an unknown target can then be normalized to obtain the spectrum of the target's impulse response and, via fast Fourier transform routines, the impulse response of the target. A simplified linear system analysis of the pulse sounding system was given in an earlier report[1]. The simplification involved was that the transfer function of the transmitting and receiving dipoles were assumed to be identical for the target and no target situations, as was the effects of the medium. Of course, in a strict sense the transfer function of the antennas cannot depend on the presence or absence of a subsurface target. However, the transfer function does have an angular dependence and in the no target measurement those fields which penetrate in the direction of the target are simply not obtained. Similarly, the medium effects will be somewhat different for the two cases because different portions of the medium are involved.

Under certain conditions which will not often be encountered in the field, it is possible to experimentally estimate the transfer function of the antenna from propagation measurements. The tunnel geometry in limestone described earlier provides such conditions. Lump the pulse spectrum and that of the cables, baluns and twin leads as  $G(s)$ , then if two identical antennas are used the received pulse spectrum is  $G(s) A_1^2(s) M(s)$ , where  $A_1(s)$  is the transfer function of the antenna in situ on the rock surface and  $M(s)$  is the transfer function of the medium. From earlier propagation measurements over two different path lengths  $M(s)$  is known. If  $R(s)$  is the received pulse spectrum then

$$A_1(s) = \left[ \frac{R(s)}{G(s)M(s)} \right]^{1/2}$$

The spectra of 1 of the 2 small dipoles shown in Fig. 1c are shown in Fig. 43. These data were obtained using the Ikor pulse generator.

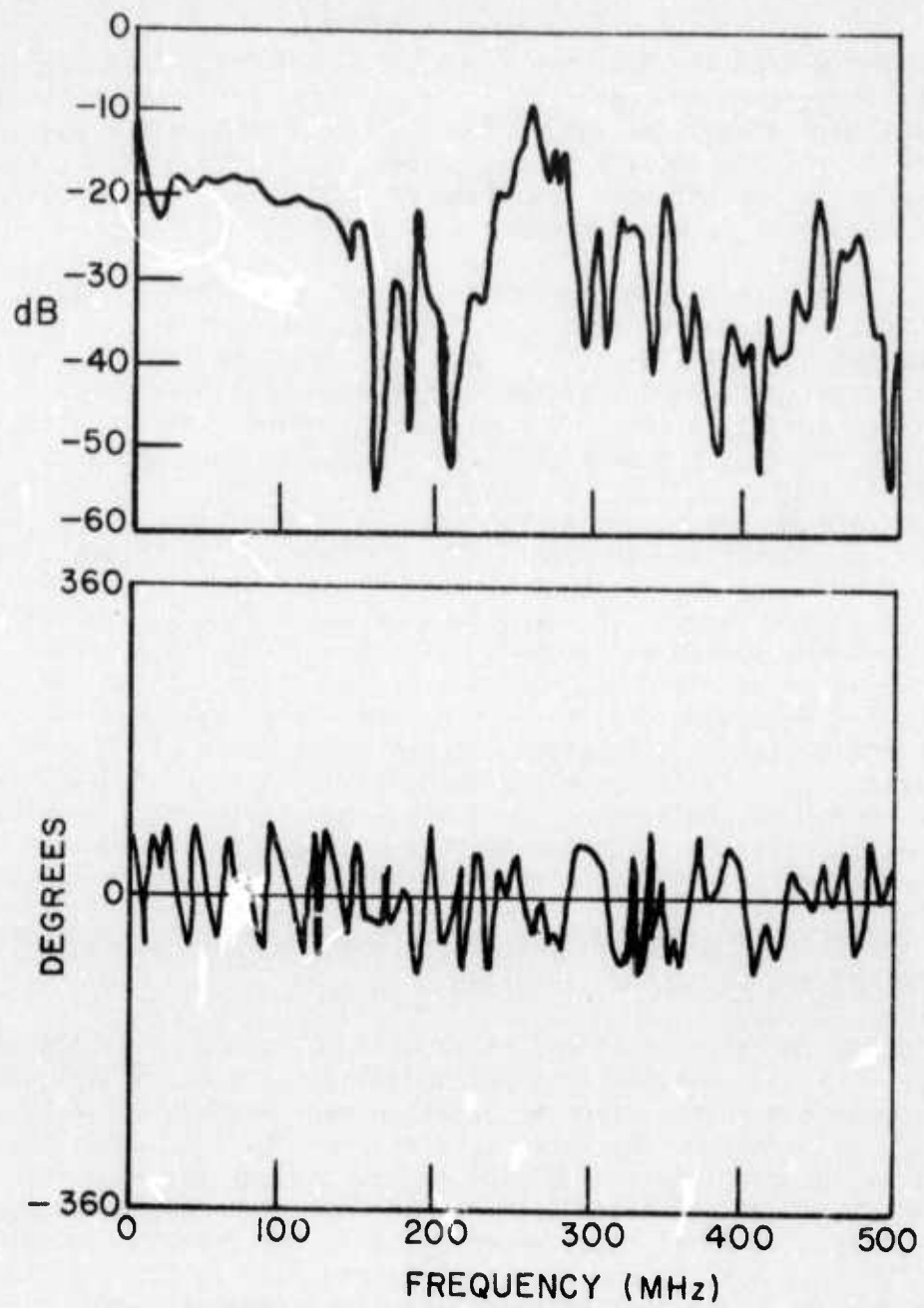


Fig. 43. Small antenna transfer function on limestone for broadside direction ( $\theta=90^\circ$ ), Ikor generator.

Note that the transfer function obtained is in the broadside direction from the dipole. An estimate of the actual pulse spectrum transmitted into the rock is then given by

$$P_T(s) = \sqrt{G(s) A_1(s)}$$

and

$$p_T(t) = F^{-1}(P_T(s))$$

is the time domain pulse signal. These are shown in Fig. 44b and Fig. 44a respectively. A similar measurement and processing with one of the large dipoles of Fig. 1a transmitting will yield the transfer function and the transmitted pulse for the large dipole. The tunnel roof is not sufficiently wide to accommodate the large dipole in the proper orientation but with  $A_1(s)$  known the small dipole can be used. These measurements have not been made as yet for the large dipole. Unfortunately, a tunnel or similar geometry does not exist in the dolomite quarry. Thus an experimental determination of the dipole transfer function does not appear to be feasible for that medium. Note however that the electrical properties of dolomite and limestone were quite similar. It is not unrealistic therefore to use the limestone results in processing data from the dolomite site.

A rigorous modification of the existing wire antenna programs to include the effects of an air-medium interface would essentially require a numerical evaluation of the appropriate Sommerfeld integrals. This is a formidable task and one which could have easily consumed the entire contract budget. Note that the numerous existing asymptotic evaluations of the integrals, as for example in Banos[10], are of limited utility because of the typical low conductivities of hard rock media and the broad spectral content of video pulse signals. As noted earlier, the rock medium is both a conductor and a dielectric within the spectral content of the same video pulse signal. For an idealized dielectric medium, i.e., lossless, an exact, closed form expression is easily obtained[11] for the transient fields produced by infinitesimal elements at the air-medium interface in the broadside direction. A numerical integration can extend these results to arbitrary observer locations, still however for an idealized dielectric medium the technique is essentially the same as was used for the infinite line source[1] lying on a dielectric half-space.

It is possible to formulate an approximate image-type correction for the lossy half-space where the total field at an arbitrary observation point within the lossy half-space is the sum of a direct contribution from a submerged wire antenna and a reflected (plane wave reflection coefficient) specular contribution from the lossy medium-air interface.

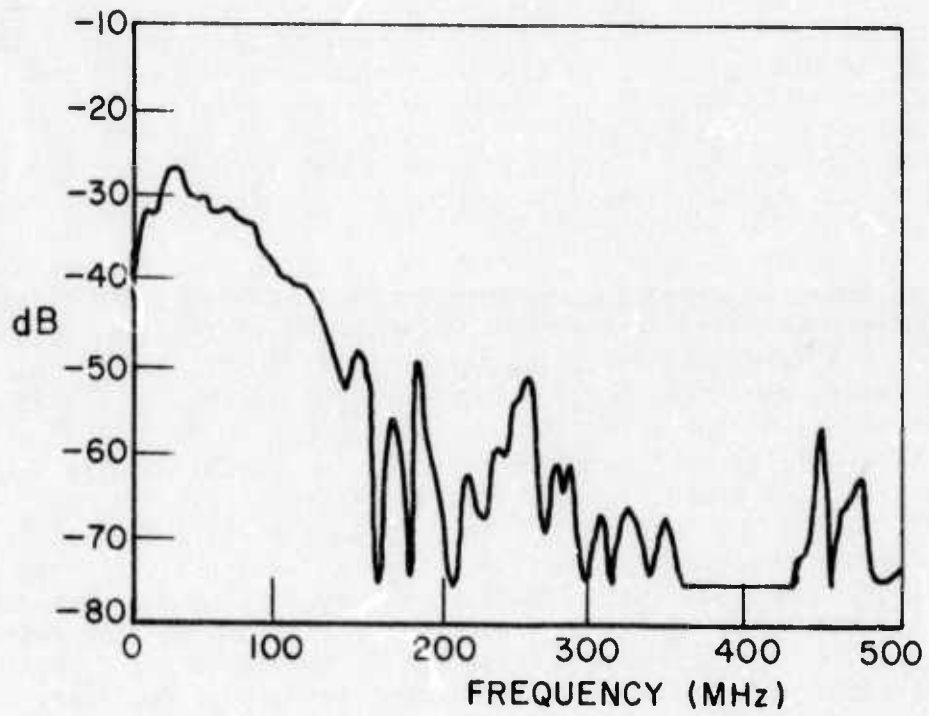
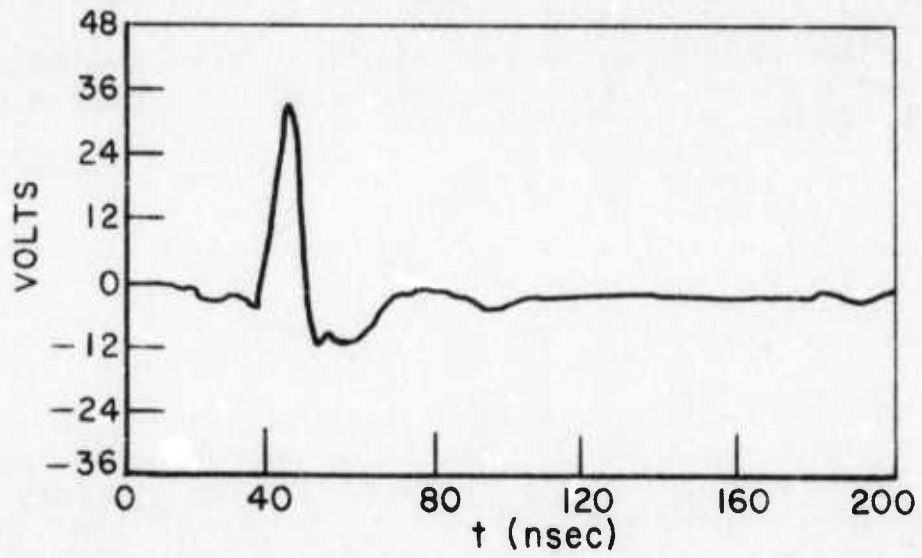


Fig. 44. Pulse transmitted into the limestone medium.

Note that the currents flowing on the antenna are the same as those when the antenna is immersed in an infinite lossy medium. As the antenna is brought to the medium-air interface, the image approximation is open to serious questions. However, one can modify the currents flowing on the wire antenna by assuming that the propagation factor for these currents is that for an infinite wire of very thin radius lying on the half-space. Wait[12] has shown that the first term of this propagation factor is simply the geometric mean of the propagation factors for air and the lossy medium. From these two modifications, i.e., image and current, estimates of the antenna input impedance and the subsurface fields can be obtained. Calculations of this type are in progress and will be compared to some experimental probing of the fields of the large probe to determine if the half-space corrections are reasonable.

#### IX. CONCLUSIONS

Significant progress has been made in the experimental development of an electromagnetic pulse sounding probe for use in hard rock media. A full scale version of the probe has been built and its effective matching into rock media (limestone) has been demonstrated experimentally. The matching does not require disturbance of the medium, i.e., the ground rods used for earlier overburden tests[1] have been eliminated. A limiter for protection of the sampling head used as a receiver in the system has been built and tested. The limiter will permit the probe to be used in the direct mode using full pulse power.

Using elements of the probe and 2 different pulse generators, propagation measurements through up to 28 feet of limestone have been made. From these data, methods for obtaining the frequency-dependent attenuation, relative dielectric constant and conductivity of the rock medium have been demonstrated. From these same data, a technique for obtaining the spectral and temporal transfer functions of the probe has been illustrated.

Full scale experimental measurements, using the probe in an orthogonal mode, have been made of fault, joint and lithologic contrasts targets occurring in a dolomite quarry. The maximum range was 45 feet for a lithologic contrast target. This is not necessarily the maximum range of the electromagnetic sounder, however, - present indications are that this range is somewhat less than 80 feet. As with any experimental measurement of an uncontrolled and inaccessible target, the interpretation given the measured data is always subject to qualification. It is maintained, however, that internal reflection mechanisms, i.e., multiple reflections on the cables etc., have been disproved and that the measured data fit the geological descriptions of the measured sites. Furthermore, none of the measured data are inconsistent with geological interpretations.

Theoretical advances have been modest because of the emphasis during the present contract period on experimental measurements. Realistic, pulse propagation calculations employing finite antenna elements in a lossy medium with frequency dependent constitutive parameters have been made. These are not quasi-static or idealized dielectric approximations, but numerical calculations where the substitution of assumed or measured frequency-dependent constitutive parameters for the medium are the only real approximation. Some progress has been made to extend these calculations to include an air-medium interface but the analyses are incomplete as yet. The problem is compounded by the fact that for realistic rock media, the media is both a conductor and dielectric for the video-type pulses of interest. Pulse propagation calculations which include an air-medium correction will be made during the present contract period. The validity of the air-medium correction, however, may not be fully explored.

It is felt that at this time the electromagnetic pulse sounding probe is fully ready for testing in an actual hard rock tunnel site. The system at present is a laboratory instrument, i.e., components are not necessarily field-hardened, but permit measurements in the field. Successful measurements reported here fully justify testing of the pulse sounding probe in an actual tunnel geometry. A fully calibrated probe and system would not be necessary at present. Formal testing of the electromagnetic pulse sounding probe is recommended to provide a realistic comparison with current acoustic and seismic techniques.

#### X. FUTURE PLANS

During the second interim of the contract it is intended to concentrate on 2 primary objectives: Refinement of the antenna analysis to permit half-space corrections to be made for an arbitrarily shaped wire antenna, and a second measurement program at the Plum Run Quarry site. The new measurements will include direct as well as orthogonal mode responses using peak pulse outputs. In addition, the original intention of interrogating joint and fault targets with the probe on vertical rock faces will be completed. This will permit the joint and fault targets to be viewed with orientations with respect to the probe which are more likely to be encountered in an actual tunneling operation.

The refinement of the antenna analysis will permit calibration of the probe and via this calibration an improved processing of the target responses. In addition, a design capability for theoretically matching the antenna geometry to an arbitrary medium will be obtained.

#### ACKNOWLEDGMENT

The authors are indebted to Mr. Max Warner of Marblecliff Quarry and Dr. Richard Bowman of Plum Run Stone Division, both for access to the respective quarries and for numerous explanations of geological features. Appreciation is also expressed to Professor Charles Summerson of the Ohio State University Geology Department for his advice concerning measurement site locations.

#### REFERENCES

1. Moffatt, D.L., "Electromagnetic Pulse Sounding for Geological Surveying with Application in Rock Mechanics and Rapid Excavation Program," Report 3190-1, 18 October 1971, The Ohio State University ElectroScience Laboratory, Department of Electrical Engineering; prepared under Contract H0210042 for Bureau of Mines, Dept. Interior (ARPA).
2. Peters, L., Jr. and Moffatt, D.L. "Electromagnetic Pulse Sounding for Geological Surveying with Application in Rock Mechanics and Rapid Excavation Program," Report 3190-2, September 1972, The Ohio State University ElectroScience Laboratory, Department of Electrical Engineering; prepared under Contract H0210042 for Bureau of Mines, Dept. Interior (ARPA).
3. Electromagnetic Probing in Geophysics, J.R. Wait, Editor, The Golem Press, 1971.
4. Parkhomenko, E.I., Electrical Properties of Rocks, Plenum Press, 1967.
5. Wait, J.R. and Fuller, J.A., "E.M. Coupling of Coaxial and Coplanar Loops in Uniform Dissipative Media," Proceedings of the IEEE, (Correspondence), August 1972.
6. Wait, J.R. and Spies, K.P., "Note on Determining Electrical Ground Constants from the Mutual Impedance of Small Coplanar Loops," Journal of Applied Physics (Correspondence), Vol. 43, No. 4, March 1972.
7. Guidebook for Field Trips, The Geological Society of America, Cincinnati Meeting, 1961.
8. Richmond, J.H., "Radiation and Scattering by Wire Structures in Active and Passive Media," Report 2902-9, The Ohio State University ElectroScience Laboratory, Department of Electrical Engineering; (in process).
9. Wait, James R., "Propagation of Electromagnetic Pulses in a Homogeneous Conducting Earth," Applied Science Research, Sec. B, Vol. 8.

10. Ban̄os, A, Dipole Radiation in the Presence of a Conducting Half-Space, Pergamon Press, 1966.
11. Schaffer, R., "Transient Currents on a Perfectly Conducting Cylinder Illuminated by Unit-Step and Impulsive Plane Waves," Report 2415-2, 3 May 1968, The Ohio State University Electro-Science Laboratory, Department of Electrical Engineering; prepared under Contract F19628-67-C-0239 for Air Force Cambridge Research Laboratories. (AFCRL-67-0691) (AD 668 536)
12. Wait, J.R., "Theory of Wave Propagation along a Thin Wire Parallel to an Interface," Radio Science, Vol. 7, No. 6, June 1972, pp. 675-679.